Renal Cancer Resistance to VEGF Receptor Tyrosine Kinase Inhibitors

Kevin Sharpe

February, 2014

Submitted in partial fulfilment of the requirements of the Degree of Doctor of Philosophy

I, Kevin Sharpe, confirm that the research included within this thesis is my own work or that where it has been carried out in collaboration with, or supported by others, that this is duly acknowledged below and my contribution indicated. Previously published material is also acknowledged below.

I attest that I have exercised reasonable care to ensure that the work is original, and does not to the best of my knowledge break any UK law, infringe any third party's copyright or other Intellectual Property Right, or contain any confidential material.

I accept that the College has the right to use plagiarism detection software to check the electronic version of the thesis.

I confirm that this thesis has not been previously submitted for the award of a degree by this or any other university.

Signature:
Date:

Abstract

Aim: To investigates the molecular changes that occur in response to VEGFr TKI therapy to better understand the acquired resistance process. A further goal is to investigate the potential of SRC inhibitors to slow or prevent VEGFr TKI resistance.

Methods: Work was conducted in *in vitro* assays (MTS assays, scratch and transwell migration assays), a preclinical *in vivo* model of resistance (786-O xenografts) and IHC was conducted in sequential RCC patient tissue taken before and after 12-16 weeks of VEGFr TKI therapy.

Findings: 100% (n=15) of 786-O xenografts developed a resistant phenotype when continually exposed to VEGFr-TKI treatment. PCR with species-specific probes showed VEGFr-TKI induced significant up-regulation of several pro-angiogenic factors in both the tumour and host compartments. These factors included VEGF ligand, FGF-2, HGF, and MET receptor. In addition, genes associated with epithelial mesenchymal transition were up-regulated in treated xenografts. Interestingly, the pro-angiogenic factor PGF and the pro-metastatic gene s100a4 were up-regulated with time, independently of treatment. Gene pathway analysis suggested VEGFr-TKI treatment induced a process resembling fibrosis or wound healing. Furthermore, collagen was increased in treated xenografts.

IHC in RCC patient tissue verified that some of the above pathways were affected in the clinical setting. VEGFr-TKI treatment caused a significant reduction in vessel density (CD31), and up-regulation of FGF-2 ligand and vessel-bound MET receptor. Collagen was also increased in VEGFr-TKI treated clinical samples.

In vitro assays demonstrated that VHL gene mutation promoted resistance to SRC TKIs. Adding a SRC TKI to VEGFr-TKI therapy had a synergistic anti-tumour effect on 786-O xenografts. However, the combination could not prevent growth in tumours that had acquired a VEGFr TKI resistant phenotype. There was no evidence that the addition of a SRC TKI affected genes implicated in the resistance process.

Interpretation: VEGFr-TKI treatment is associated with dynamic molecular changes to several relevant biomarkers. Targeting any one pathway in isolation may have an incremental anti-tumour effect, but because multiple pathways are affected, it is perhaps unlikely to result in a sustained improvement in tumour response. Heterogeneity of protein expression adds further complication to a targeted approach.

Collagen deposition increases with VEGFr TKI therapy. Collagen has been shown to promote angiogenesis and metastasis. Further investigation is warranted to understand whether the addition of anti-fibrotic agents to anti-angiogenic therapy could have an incremental benefit on patient outcome.

CONTENTS

Table of Figures:

List of Tables:

Chapter 1:

Introduction

1.1 Cancer cells and the tumour microenvironment

Cancer can be thought of as a multistep process in which normal cells evolve progressively to a neoplastic state [1]. Often this involves malignant cells acquiring the 'hallmarks of cancer'. In their seminal work, Hanahan and Weinberg identified six 'hallmarks' that drive malignancy [2] including an enhanced ability to survive and proliferate.

More recently, a better understanding of the tumour microenvironment has allowed us to recognize the importance of non-malignant cells in tumourgenesis [3] [4]. For example, myeloid cells and cancer associated fibroblasts have been shown to help promote angiogenesis and escape immune surveillance [5] [6].

Because angiogenesis and metastasis are thought to be key pillars of VEGF-TKI (vascular endothelial growth factor-tyrosine kinase inhibitors) resistance, these two 'hallmarks of cancer' are reviewed in more detail.

1.2 Angiogenesis

Angiogenesis is the formation of a network of blood vessels consisting of a thin layer of endothelial cells supported by pericytes and smooth muscle cells. Tumour-associated angiogenesis is the formation of vessels that can penetrate deep into the malignant tissue helping to supply tumours with oxygen and nutrients required for growth and survival [7]. The angiogenic process requires the production of pro-angiogenic factors at the tumour site, which recruit key components of the blood vessels, such as endothelial cells, in addition to promoting proliferation and survival of these component cells once at the tumour site [7].

The Von Hippel Lindau (VHL) / Hypoxia-Inducible Factor (HIF) pathway plays a key role in regulating the expression of several pro-angiogenic factors. Under normoxic conditions functional VHL labels HIF transcription factors for proteasomal degradation. Under hypoxic conditions, or through loss of functional VHL, HIF-alpha is allowed to stabilise, resulting in the constitutive up-regulation of pro-angiogenic genes [8].

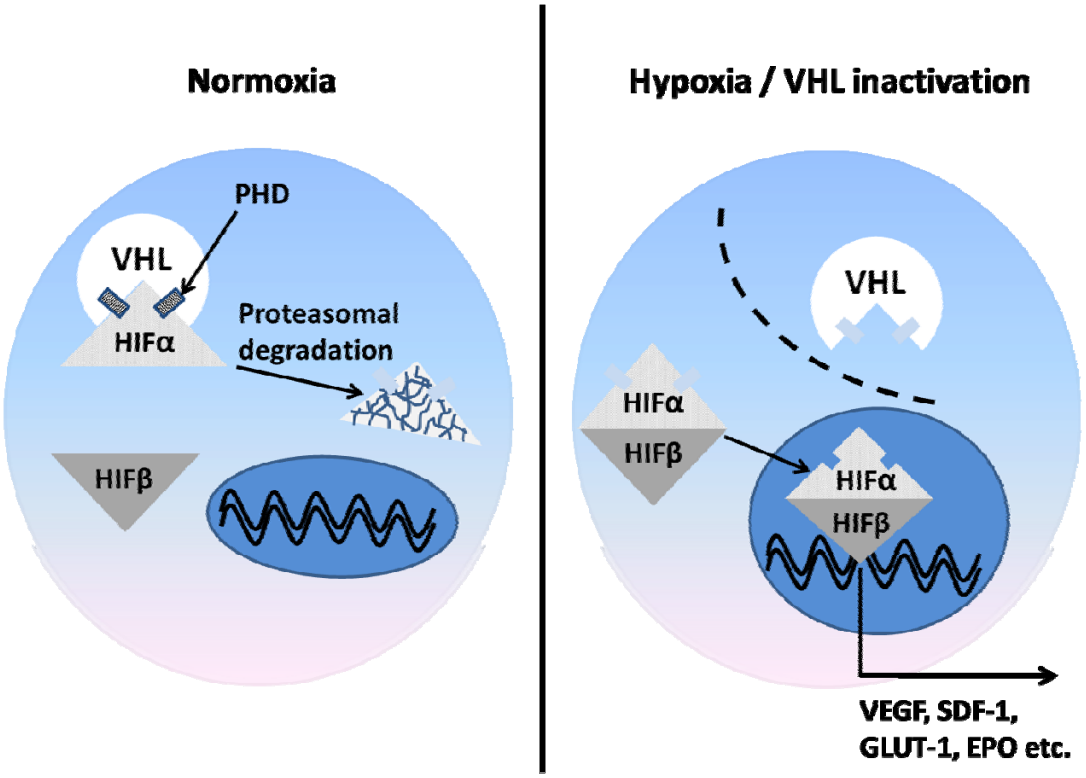

Figure 1.1: VHL mediates expression of pro-angiogenic genes

Perhaps the most notable pro-angiogenic factor produced by tumours is VEGF, a family of signal proteins that initiate cellular responses by binding to tyrosine kinase receptors (VEGFRs) located on the cell surface of endothelial cells [9]. Tumour-associated angiogenesis is thought to be primarily driven by VEGF-A (also sometimes referred to simply as VEGF), which binds to VEGFR-1 and VEGFR-2 [9]. VEGFR-2 is believed to be the key mediator of endothelial cell response, although VEGFR-1 is thought to play an important role in recruiting bone marrow-progenitors [10]. VEGFR-1 may also be important for the recruitment of pro-angiogenic myeloid cells to the tumour site [10].

In addition to VEGF, FGF-2 (fibroblast growth factor-2) and HGF (hepatocyte growth factor) represent two important alternative pro-angiogenic ligands. These two alternative pro-angiogenics factors are thought to promote vessel formation through direct interaction with their corresponding receptors which are present on endothelial cells (FGFR1-4 and MET receptor respectively) [11] [12].

While the above mentioned ligands interact directly with endothelial cell receptors, other pro-angiogenic factors are thought to promote angiogenesis through interactions myeloid cells. A good example is interleukin-8 (IL-8). IL-8 targets the CXCR1 and CXCR2 receptors, which are thought to be present on some endothelial cells. However IL-8 is thought to have a stronger chemotactic effect on neutrophils and monocytes [13]. Consequently, tumour derived IL-8 could potentially promote angiogenesis through direct interaction with endothelial cells, but may be more influential through its recruitment of pro-angiogenic myeloid cells.

Finally, some molecules can promote angiogenesis without having any direct effect on endothelial cells. Cytokines such as GM-CSF or M-CSF, for example, can promote angiogenesis through an indirect, pro-inflammatory mechanism, but are not thought to have any direct effect on endothelial cell signalling [14]. Proteinases such as the matrix metalloproteinase family (MMPs) provide another good example of this pro-angiogenic concept. MMPs are capable of degrading the extracellular matrix (ECM). In this way cell can more easily move through the ECM, which could help the recruitment of endothelial cells to the tumour site [15]. MMPs may also release latent pro-angiogenic factors, such as VEGF, which are stored in the ECM.

1.3 Metastasis and epithelial-mesenchymal-transition

The process of metastasis involves several significant steps; the metastatic cell must reduce cell-to-cell and cell-to-matrix adhesion, increase motility, acquire enough invasive capability to migrate through the extracellular matrix and, if migrating though vessels or the lymphatic system, the cell must be capable of intravasation and subsequent extravasation. Finally, the cell must be capable of survival and proliferation at a distant site.

By undergoing epithelial-mesenchymal transition (EMT) cells initially anchored at the primary site may accomplish many of the processes described above. EMT is biological process thought that is thought to be activated during embryogenesis and play a physiological role in wound healing and fibrosis.

As the name suggests, a molecular hallmark of cells undergoing EMT is the down-regulation of epithelial markers such as e-cadherin and the up-regulation of mesenchymal markers such as n-cadherin and vimentin. Phenotypically this process is thought to promote a less adhesive, more motile cell capable of penetrating through local tissue.

Several signaling pathways are thought to promote EMT. Some of these pathways include TGF-β, Wnt, Notch, and Hedgehog [16] [17] [17] [18]. These pathways can converge on the transcription factors Snail, Slug and Twist to promote EMT [19]. Importantly, these EMT-inducing transcription factors have been shown to be effected by hypoxia, providing a potential direct link between anti-angiogenic therapy and EMT [20] [21].

1.4 Renal cell carcinoma

Renal cell carcinoma (RCC) accounts for approximately 90% of all cancers of the kidney [22] and these represent approximately 2% of all cancers reported [23]. RCC is thought to derive from proximal tubule cells [24]. Like much of the adult kidney, proximal tubule cells derive from the mesoderm during development through a process of mesenchymal-epithelial transition [25].

Inactivation of the von-hippel landau (VHL) gene is by far the most common genetic alteration found in renal carcinoma. Deletion or mutation occurs in approximately 60% of cases [26], with silencing by promoter methylation present in about another 20% of cases [27]. VHL is the master regulator of multiple pro-angiogenic factors. Consequently, RCC patients tend to present with highly vascular tumours.

Clear Cell RCC represents the majority of renal carcinomas. Histologically Clear Cell tumors can be identified by clusters of malignant cells, with a clear cytoplasm, surrounded by a dense endothelial network. Clear Cell RCC provides the focus of this thesis, and the main target of anti-angiogenic therapy. Other less common subtypes, such as Papillary Carcinoma and Chromophobe RCC, are not susceptible to VHL mutation. Anti-angiogenic therapy does not provide standard of care for these subtypes.

1.4.1 RCC treatment options

As with other cancers, patients presenting with a small localised tumour have a significantly better prognosis than more advanced cases. According to data from the US National Cancer Data Base, 5 year-survival for patients presenting with localised disease is approximately 80%, but this falls to less than 10% for patients presenting with metastatic disease. In localised cases, nephrectomy is an effective treatment. However, because renal-cell carcinoma is characterised by a lack of early-warning signs, a high proportion of patients present with metastases [28]. Common sites of metastasis include lung, bone, liver and brain.

The poor prognosis for patients presenting with metastatic disease can be explained, in part, by the lack of effective therapy beyond surgical resection. In general, RCC is considered resistant to both chemotherapy and radiotherapy. Until the recent emergence of tyrosine kinase inhibitors, immunotherapy, in the form of interferon-α or interleukin-2 (Il-2), provided the mainstay of treatment. FDA approval of cytokine therapy was based on as series of clinical trials that demonstrated response rates of 5-20% and complete response rates of approximately 5% [29-31]. Complete responses generated by cytokine therapy are often durable. These durable responses, albeit in a small proportion of patients, provided much of the impetus that led to regulatory approval. Cytokine therapy, particularly high dose IL-2 is associated with significant treatment-related toxicities including fever, chills, flu like symptoms, myalgia and fatigue. Studies investigating high-dose IL-2 required patients to be highly selected with excellent performance status. Similar considerations are needed when selecting patients suitable for this treatment option in the clinical setting.

An improved understanding of the genetics and pathogenesis of RCC has led to the emergence of targeted therapy. VHL function is impaired in 60- 70% of RCC tumours [26, 27]. The regulatory approval of VEGF-TKI therapy for metastatic RCC patients has revolutionised treatment strategies and these drugs now provide first line standard of care [32].

1.5 Targeting angiogenesis in renal carcinoma

The development of the first multi-tyrosine kinase inhibitors (TKIs) [32] caused a paradigm shift in the treatment of metastatic RCC. Since 2005, the US regulatory authorities have approved four anti-angiogenic tyrosine kinase inhibitors for the treatment of metastatic RCC; sunitinib, sorafenib, pazopanib and axitinib. In addition, the monoclonal antibody, bevacizumab, which targets the VEGF-A ligand, received regulatory approval for use in combination with interferon-α. Table 1.2 below provides an overview of the key clinical studies investigating anti-angiogenic therapies that provided the basis for their adoption as standard of care in RCC.

Drug / drug combination	Previous treatment	Comparator	Study size	Primary endpoint	Endpoint met	PFS in months (active / comparator)	Publication
First line treatment							
Sorafenib	None	Interferon	189	PFS	No	5.7 / 5.6	Escudier et al - J Clin Oncol 2009;27:1280-9
Sunitinib	None	Interferon	750	PFS	Yes	11.0 / 5.0	Rini et al - Lancet 2012;378:1931-9
Pazopanib	None	Sunitinib	1110	PFS*	Yes	8.4 / 9.5	Motzer et al - N Engl J Med 2013;369:722-31
Axitinib	None	Sorafenib	288	PFS	No	10.1 / 6.5	Hutzon et al - Lancet Oncol 2013;14:1287-94
Bevacizumab + interferon	None	Interferon	732	PFS	Yes	8.5 / 5.2	Rini et al - J Clin Oncol 2008;26:5422-8
Bevacizumab + interferon	None	Interferon	649	PFS	Yes	10.2 / 5.4	Motzer et al - N Engl J Med 2007;356:115-24
Second line treatment							
Axitinib	TKI or cytokines	Sorafenib	723	PFS	Yes	6.7 / 4.7	Huang et al - Cancer Res 2010;70:1053-62
Sorafenib	Cytokines	Placebo	903	PFS	Yes	5.5 / 2.8	Motzer et al - Lancet 2008;372:449-56
Pazopanib	Cytokines or none	Placebo	415	PFS	Yes	9.2 / 4.2	McTigue et al - PNAS 2012;109:18281-9
PFS = progression free survival, OS = overall survival, * non-inferiority design, TKI = Sorafenib, sunitinib or pazopanib							

Since VEGFR2 is thought to be the key mediator of endothelial cell response to VEGF, the TKIs have been designed, primarily, to inhibit activation of VEGFR-2, but all four approved drugs also inhibit VEGFR1 and VEGFR3, to some extent. Additional TKIs targeting anti-VEGFR2 are in clinical trials including cediranib and tivozanib.

Further to inhibiting VEGF receptors, the TKIs are known to inhibit other tyrosine kinases, which may also contribute towards the observed clinical benefit. For example, sunitinib inhibits PDGF alpha and beta receptors [33], present on pericytes and endothelial cells. Sunitinib also affects receptors, such as the c-Kit receptor [33], which are present on myeloid and lymphoid progenitors and play a role in their recruitment to the tumour site.

1.6 Resistance to anti-VEGF therapy

An early hope of anti-VEGF therapy was that by targeting the tumour vasculature, rather than unstable tumour cells, drug resistance would be less likely to occur [34]. This early hope has not translated into clinical reality. In addition to patients presenting with intrinsic (or pre-existing) resistance to therapy, tumours can develop resistance after initially responding to therapy (acquired resistance). Acquired resistance is the main problem in the RCC setting. The majority of RCC patients enjoy an initial response to therapy, but ultimately acquired resistance emerges and tumour progress. Data from the pivotal trial leading to the approval of sunitinib in mRCC shows that while approximately 50% of patients were deemed as complete or partial responders (defined as at least a 30% reduction in the sum of the target lesions), and a further 40% experienced stable disease, more than 90% of patients had progressive disease within 14 months of starting therapy [32]. As yet, no predictive biomarkers for VEGF-targeted therapy have been firmly established. However, observations from clinical and pre-clinical studies have generated several hypotheses as to how tumours are capable of developing the 'acquired resistance phenotype':

Pre-clinical and clinical studies have revealed a significant increase in circulating VEGF levels in patients receiving VEGFR TKI or bevacizumab, an anti-VEGF monoclonal antibody [35]. Whether this feedback loop contributes to acquired resistance is not fully understood. It is, perhaps, less likely to play an important role in RCC tumours lacking functional VHL than some other tumour types, since VHL null RCC tumours already generate high levels of VEGF prior to treatment onset.

In addition to the potential contribution from increased VEGF production, two key resistance mechanisms have been proposed; 1) a switch to alternative angiogenic pathways 2) increased metastatic potential as a result of treatment.

1.6.1 A switch to alternative angiogenic pathways

Placental growth factor (PGF) is another member of the VEGF family members that has shown to be increased in patients receiving anti-VEGF therapy. PGF binds to VEGFR-1. Consequently, VEGFR-2 focused TKIs may be less capable of counteracting the effects of PGF (although the approved TKIs mentioned are thought to inhibit VEGFR-1 to some extent). The impact of PGF on resistance remains controversial, but PGF has been shown to act synergistically with available VEGF ligand [36].

Several anti-VEGF studies have associated increased expression of fibroblast growth factor (FGF) family members with tumour rebound and renewed angiogenesis. For example, Casanovas et al showed both a correlation of increased FGF with renewed angiogenesis and further demonstrated that the application of an 'FGF-trap', which targets several FGF isoforms could prevent this mechanism of vascular relapse [37]. More recently, Welti et al demonstrated FGF1 and FGF2 were capable of inducing resistance to the VEGFR-2 TKI, sunitinib, *in vitro* [38]. Furthermore, the same authors use a 74 patient tissue micro-array to demonstrate the presence of FGF2 in both RCC tumour cells and the associated endothelium.

Another pro-angiogenic factor suggested as a possible resistance mediator in RCC is interleukin-8 (IL-8). Huang et al used 3 different RCC xenograft models to show an association between IL-8 levels and tumour rebound during sunitinib treatment [39]. Furthermore, in one xenograft, using 786-O cells, the authors showed that an anti-IL-8 antibody provided a therapeutic benefit in tumours displaying an anti-VEGF-resistant phenotype.

1.6.2 Promotion of a 'metastatic phenotype'

Recent work suggests that anti-angiogenic therapy may promote metastasis, potentially undermining any survival benefit conferred by slowing growth of the existing tumour [40] [41]. Metastasis, not the primary tumour kills cancer patients, in most cases, yet most anti-VEGF preclinical work has traditionally focused on the

effect on the primary tumour, ignoring any impact on metastatic potential [42]. But two recent papers showed that while anti-VEGF treatment retarded primary tumour growth, invasion and metastatic potential were enhanced [40, 41]. Furthermore, in these pre-clinical studies anti-VEGF treatment was associated with shortened survival.

Treatment-induced hypoxia provides one plausible trigger to explain these observations. As a consequence of anti-angiogenic therapy, tumour cells may respond by activating pro-invasive, pro-metastatic pathways in order to escape their hypoxic microenvironment [43]. Furthermore, anti-VEGF treatment may select for more malignant cells, with higher metastatic potential, which are better equipped to survive the hypoxic environment.

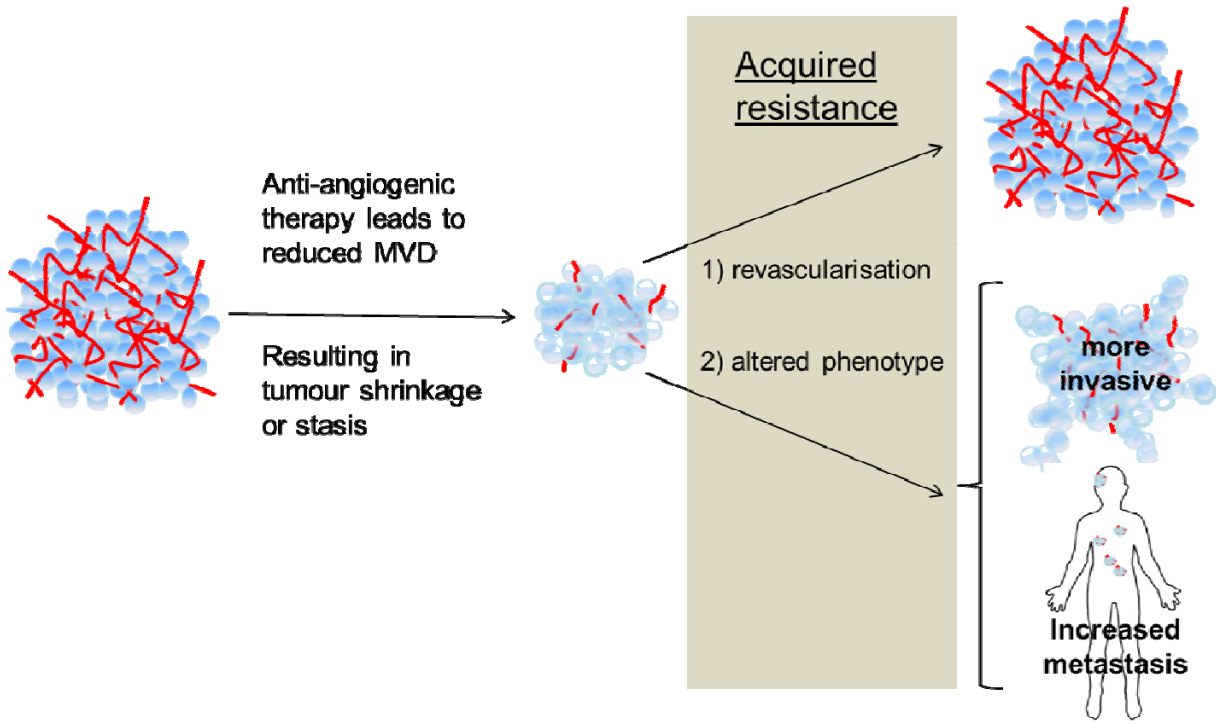

Figure 1.2: Proposed mechanisms of resistance to VEGF-TKIs

MVD = Microvessel Density

1.6.3 Recruitment of bone marrow derived cells and vasculogenesis

An accumulating body of evidence suggests that non-maligant cells, particularly bone marrow derived cells (BMDC) could be involved in anti-VEGF resistance. At least three separate mechanisms have been proposed to explain how BMDC recruitment can contribute to tumour progression; the latter two are more closely linked to potential escape mechanisms:

Firstly, a subgroup of BMDCs, known as myeloid derived suppressor cells, may help the tumour escape from a cell mediated immune response [44] [45] [46].

Secondly, infiltrating BMDCs could promote re-vascularisation by producing members of the FGF family, IL-8 and other alternative pro-angiogenic factors.

The third potential mechanism is promotion of vasculogenesis. Vasculogenesis can be defined as the de novo production of vessels *in situ* from circulating endothelial progenitor cells. This differs from angiogenesis, which can be defined as the sprouting of new vessels from pre-existing ones. Vasculogenesis was initially thought to be confined to embryonic development, but recent evidence suggests a role in tumour vascularisation, and potentially, anti-angiogenesis therapy resistance. For example, Bolontrade et al provided evidence that migration of BMDC into Ewing's sarcoma tumours and their subsequent differentiation into endothelial cells can contribute to tumour growth [47].

So in addition to helping the tumour evade the immune system BMDCs could provide two different mechanisms, one direct and one indirect, to help re-vascularise the tumour to allow tumour progression despite anti-VEGF treatment.

1.6.4 Metabolic change

Clinical observations using FDG-PET and preliminary animal studies suggest that changes in tumour metabolism may play a role in undermining anti-VEGF therapy. At this stage, this work is hypothesis-generating and needs further validation. Nevertheless work carried out by the author of this thesis in collaboration with others (but not included in the results section of this thesis) aimed to explore this hypothesis [48].

1.7 The potential of SRC inhibitors in renal cancer

Some of the ongoing work to establish important anti-VEGF resistance mechanisms has been highlighted. None of these potential mechanisms have been firmly established and more work is needed to validate which pathways are important in the different cancer types. Increased knowledge could lead to improved patient outcome through both improved initial patient selection and a more durable therapeutic response in treated patients. One potential therapeutic strategy would be to combine a SRC inhibitor with the existing anti-VEGF therapies. A background to SRC is given to better understand the rationale for this combination:

1.7.1 SRC background

In 1911, Peyton Rous described a virus that appeared to induce tumours in chickens [49]. This hypothesis remained controversial until 1955 when v-Src, a rous sarcoma virus gene was shown to be capable of inducing tumours [50].

v-Src and its human cellular counterpart c-Src encode a non-receptor tyrosine kinase, SRC. SRC proteins contain four src homology domains SH1-SH4 [51], with SH1 containing the kinase domain. Full activation requires auto-phosphorylation of a tyrosine residue (Tyr419 in human c-Src). Inactivation can occur through phosphorylation of Tyr530, which causes the c-terminal domain to bind back to its SH2 domain, locking the protein in a closed structure with the kinase domain inaccessible.

SRC protein is one of 9 members of the SRC kinase family. The other SRC kinase proteins are FYN, YES, BLK, YRK, FGR, HCK, LCK and LYN [52]. SRC is the protein most often implicated in cancers [52] but the potential for SRC inhibitors to impact other family members should be noted. By inhibiting other SRC family members, particularly FGR, HCK and LYN, SRC inhibitors may impact the myeloid compartment in addition to tumour cells [53].

Over-expression of SRC protein and / or an increase in its activity has been observed in numerous cancer types [54]. For example, colorectal cancer shows a

progressive increase in c-SRC activity as the tumour stage advances. Colorectal metastatic lesions often have the highest levels of c-SRC activity, indicating a potential role for c-SRC in mediating tumour progression and metastasis [55]. Preclinical models have shown SRC can impact tumour cell proliferation, survival, metastasis and angiogenesis:

Perhaps most notable is SRC's apparent ability to effect motility and adhesion, which is mediated in a large part through its interaction with the proteins that make up the focal adhesion complex. Focal adhesions form next to the cell membrane and allow integrins to link the actin cytoskeleton to extracellular-matrix (ECM) proteins. SRC interacts directly with the focal adhesion kinase, FAK. The SRC-FAK complex interacts with several other substrates, including CAS, paxillin and p190Rho [56]. These cytoskeletal proteins assemble into supramolecule structures, associate with stress fibers such as actin, and, dynamically regulate the shape and motility of the cell. In addition to the focal adhesion complex, adheren junctions can also regulate adhesion and motility. Again SRC is a principle player in the formation of these subcellular structures. Adheren junctions regulate cell-to-cell adhesion (rather than cell-to-ECM controlled by focal adhesion). c-SRC can disrupt adheren junctions by preventing E-cadherin localisation and important contact points. Further to their role in cell–matrix adhesion, SRC and member of the focal adhesion complex, participate in a two way cell-signaling process that can influence survival, proliferation and gene transcription [57]. For example, evidence suggests that SRC-FAK signaling to c-JUN can promote the expression of matrix metalloproteinases such as MMP2 and MMP9 [52]. These proteases help degrade the ECM facilitating and cell migration. In this way, SRC can increase metastatic potential at multiple stages of the metastatic process; firstly by reducing adhesion and promoting cells release both from the ECM and other cells and secondly by up-regulating proteases to facilitate invasion and movement to distant sites.

While, SRC has consistently demonstrated the ability to promote cell migration across in a wide range of cell lines, its ability to influence proliferation and survival is much less consistent. Several mechanisms have been proposed to explain how SRC activation can promote proliferation including the abrogation of MYC requirement at G0/G1 and decreased b-catenin binding to cyclin D1 [52].

However, evidence from studies using SRC inhibitors seems to indicate that the effect on proliferation is cell line specific.

Angiogenesis is regulated by multiple cytokines that creating a cascade that favours endothelial cell migration and proliferation in the tumour microenvironment. SRC has been associated with increased expression of the pro-angiogenic factors IL-8 and VEGF, the latter is thought to be mediated through STAT3 activation [52]. Furthermore, SRC inhibition may reduce endothelial migration to the tumour site through mechanisms described above including, reduced motility of endothelial cells and reduced expression of MMP2 and MMP9 [52, 58].

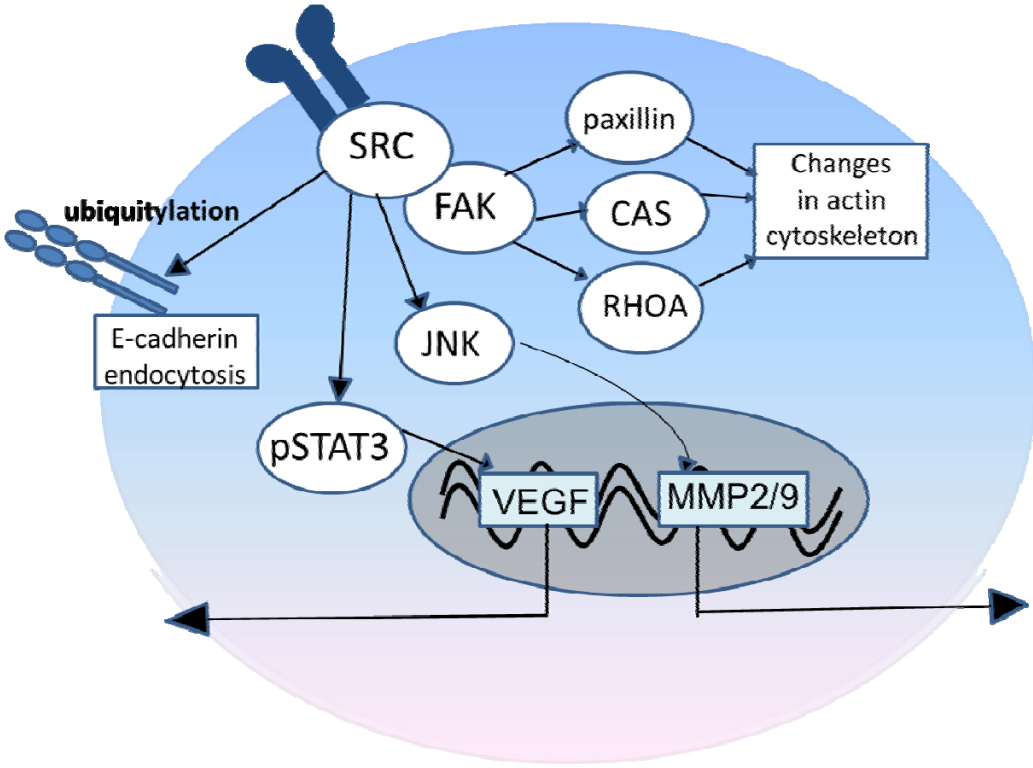

Figure 1.3: SRC mediates molecular pathways involved in angiogenesis and metastasis

1.7.2 SRC inhibition and VEGFr-TKIs; the rationale for combination

The EMT process potentially provides a direct link between VEGF-TKIs and metastasis. Perhaps the most obvious mechanism by which SRC inhibitors may synergistic combination with VEGF-TKIs is to counteract this potential promotion of a metastatic phenotype. SRC inhibitors could increase adhesion, reduce motility and regulate production of pro-metastatic factors such as the MMPs.

Tumour re-vascularisation is thought to promote resistance to VEGF-TKIs. SRC inhibitors could help counteract this process through several mechanisms. SRC has been proposed to regulate VEGF through the STAT3 pathway and also through VHL stabilisation. SRC inhibitors may also directly effect endothelial cells reducing their ability to survive, proliferate and migrate to the tumour site [58]. Finally, SRC has been suggested to regulate MMP production [52, 58]. Finally, MMPs are not only important in metastasis. By down-regulating MMP production, SRC inhibitors could limit endothelial recruitment and reduce the release of latent pro-angiogenic factors, such as VEGF.

The recruitment of BMDCs may help promote resistance. SRC inhibitors could also limit BMDC recruitment [58] both the motility of these cells or by impacting their production in the bone marrow [59].

Finally, IL-8 has been implicated in RCC resistance [39]. SRC has been proposed as an important regulator of this gene [60]. Reduced IL-8 production through SRC inhibition could counteract this proposed mechanism of resistance.

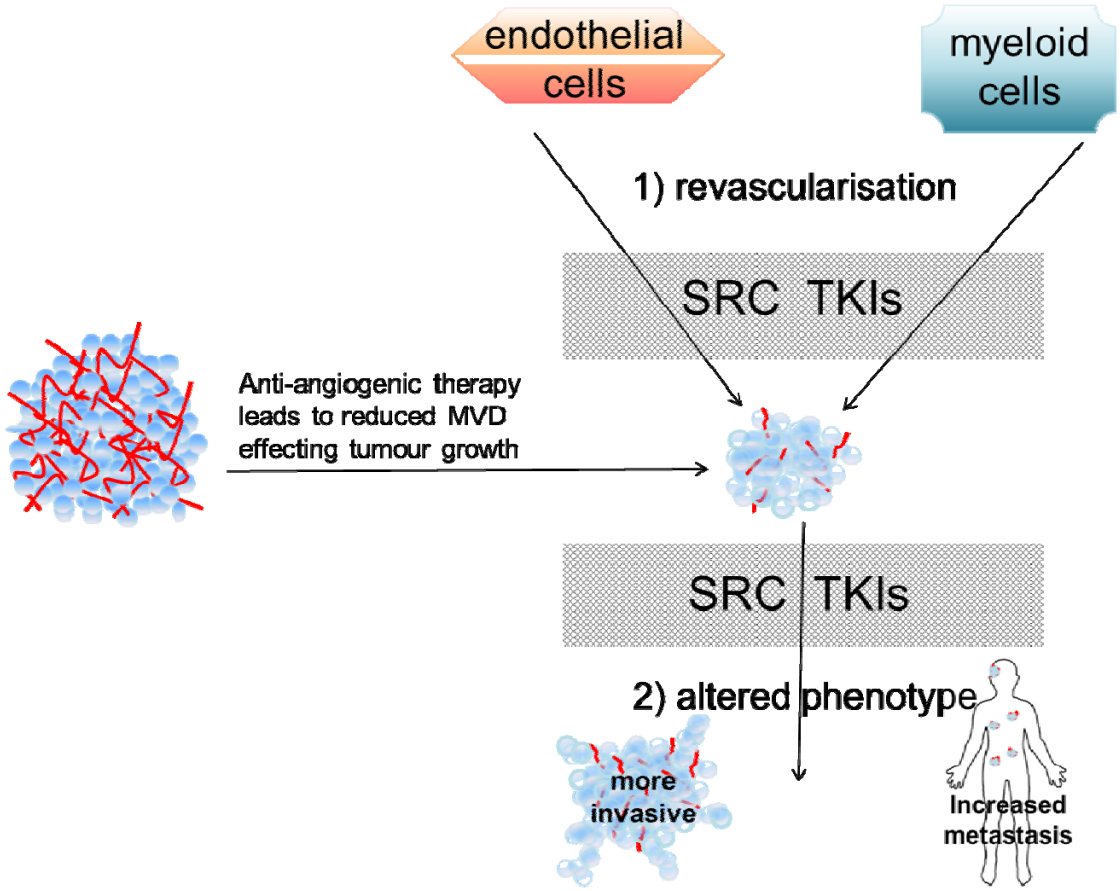

Figure 1.4: Potential mechanisms of action for SRC TKIs targeting VEGF-TKI resistance

1.8 Aims and objectives

The primary aim of this project is to further investigate the molecular pathways driving resistance to VEGF-TKI therapy and determine whether SRC inhibitors can help counteract the onset of resistance. Our hypothesis that SRC inhibitors may provide a synergistic combination with anti-VEGF therapy in this setting is based on an extensive body of work (albeit in non-renal models) that suggests SRC is capable of enhancing metastatic potential in addition to regulating molecules associated with angiogenesis. The principal objectives of this thesis are to:

1. Develop a preclinical model of 'evasive resistance'.

2. Investigate the molecular pathways driving resistance in this preclinical model.

3. Using RCC patient tissue, determine whether the preclinical model is representative of the clinical resistance process.

4. Use the preclinical model of resistance to investigate whether SRC inhibitors can be effective in this setting.

5. Determine whether there are subgroups of RCC patients that are more likely to respond to SRC therapy.

The preclinical work carried out for this PhD complements an ongoing 130 patient, phase II clinical study comparing the effect of combined SRC inhibitor (AZD0530) and VEGF inhibition (cediranib) to VEGF inhibition alone in Sunitinib refractory patients (Principal Investigator; Dr Tom Powles, Barts and the London).

Chapter 2:

Materials and Methods

2.1 Cell culture:

In vitro experiments and xenogaft studies were performed with RCC cell lines ACHN, Caki-1, 786-O and A-498 originally obtained from American Type Culture Collection (Manassas, VA).

Cell lines	Origin	VHL status	HIF-1a status
ACHN	Metastatic (pleural effusion) lesion of a 22 year old, male, caucasion patient	Wild-type	Wild-type
786-O	Primary lesion of a 58 year old, male, caucasion patient	VHL null	HIF-1a null
CAKI-1	Metastatic (skin) lesion of a 49 year old, male, caucasion patient	Wild-type	Wild-type
A498	Taken from a lesion of a 52 year old, female, caucasion patient	VHL null	HIF-1a null

RCC4-vector and RCC4-VHL were obtained from the European Collection of Cell Cultures (London, UK). DNA fingerprinting was carried out to avoid contamination or misidentification.

Between experiments, cells were stored in 10% Dimethyl Sulfoxide (DMSO), 30% heat-inactivated fetal calf serum, 60% RPMI 1640 in liquid nitrogen. For *in vitro* assays, cells were thawed and maintained in RPMI 1640 media supplemented with 10% heat-inactivated fetal calf serum (PAA) and 1% streptomycin (PAA) at 37°C in a humidified atmosphere of 10% CO_2, 21% O_2. For HIF-stabilizing experiments that required hypoxic conditions, cells were transferred to a humidified atmosphere with 10% CO_2, 1% O_2.

2.2 Reagents for *in vitro* assays:

Dasatinib (LC laboratories) and Saracatinib (AZD0530, AstraZeneca) were dissolved in 20mg/ml DMSO (stock) and desired dose levels were achieved by serially diluting the stock by adding medium prior to conducting *in vitro* assays. Appropriate DMSO-only controls were utilized as required. For HIF-stabilizing assays, dimethyloxalylglycine (Sigma) was dissolved in distilled water at 20 mg/ml before diluting in RPMI media to required concentrations.

Kinase	Mean IC50, nM/L, mean
Src	2.7
Lck	< 4
Yes	4
EGFR L861Q	4
Lyn	5
EGFR L858R	5
Fyn	10
Fgr	10
Blk	11
Abl	30
EGFR	66
Kit	200
EphA2	236
Csk	>1000

Table 2.1: Inhibitory activity of AZD0530 on isolated tyrosine kinases. Adapted from Green et al [61].

Kinase	IC50 nM/L), mean
Lck	0.4
Src	0.5
Yes	0.5
Abl	<1
c-kit	5
PDGFR-beta	28
p38	100
EGFR	180
HER2	780
MEK	>1000

Table 2.2: Inhibitory activity of dasatinib on isolated tyrosine kinases. Adapted from Lombardo et al [62].

Kinase	IC50 nM/L), mean
VEGFR family	
KDR (VEGFR-2)	<1
Flt-1 (VEGFR-1)	5
Flt-4 (VEGFR-3)	3
PDGFR family	
c-Kit	2
PDGFR-h	5
PDGFR-a	36
CSF-1R	11
Flt-3 >1	
Representatives from other kinase families	
FGFR1	26
Src	13
Abl	26

Table 2.3: Cediranib (AZD2171) inhibition of VEGF receptor tyrosine kinase activity and selectivity profile. Adapted from Wedge et al [63].

Kinase	IC50 (nM/L), mean
VEGFR family	
VEGFR2	38
VEGFR1	15
VEGFR3	30
PDGFR family	
c-Kit	<10
PDGFR-beta	55
PDGFR-alpha	69
CSF-1R	35
Flt-3	21
Representatives from other kinase families	
FGFR1	675
Src	1000
Abl	610

Table 2.4: Sunitinib (SU-11248) inhibition of VEGF receptor tyrosine kinase activity and selectivity profile. Adapted from Roskoski et al [33].

2.3 Cell viability assays:

To measure cell proliferation or cytotoxicity a colorimetric assay (Promega) was used. This assay uses a tetrazolium compound (MTS) to assess cell viability. For MTS assays, cells were seeded at 3-6 x 10^3 cells per well on 96-well plates and cultured in 100ul of RPMI-media overnight. After 24 hours, 100ul of dasatinib or saracatinib was added to achieve a range of final concentration between 0 and 2.5uM.

Cell viability was determined at 24-72 hours following the manufacturer's protocol (Promega); briefly, after 24 or 72 hours, media was removed by shaking the 96 well plate. 100ul of MTS reagent was added and plates were incubated between 2-4 hours or until controls measured had an optimetric density (OD) value of 1.5-1.8 using an ELISA multi-plate reader set to an absorbance of 490nm.

2.4 Migration assays:

Scratch assays were performed in 6-well plates. In general, 7.5 x 10^4 cells per well were plated and incubated for 24-48 hours until cells formed a confluent monolayer. A cross was scratched into the monolayer using the tip of a 1ml pipette, cells were washed in PBS and 2ml of RPMI + 10% FCS media was added, which contained between 0nM, 10nM, 50nM or 250nM dasatinib. An image was taken immediately after media was added and cells were incubated for 18 hours. A further imaged was taken after 18 hours and dynamic changes in cell migration were observed by comparing the size of the scratch at the two time points. This assay was performed in triplicate for each drug concentration.

For transwell migration assays, cells were trypsinised, spun down, re-suspended in serum-free media and counted using a haemocytometer. 2.5 x 10^5 cells were added to each transwell and incubated for 3 hours to allow cells to adhere to the transwell membrane. All media was removed before 200ul of serum-free media containing 0nM, 10nM, 50nM or 250ul of dasatinib was added to the upper chamber of the transwell. The lower chamber contained 500ul of media with the

identical drug concentration, but with the addition of 5% fetal calf serum, which served as a chemoattractant. Cells were incubated at 37C for 18 hours before cells that had migrated through the membrane were fixed, stained with haematoxylin and counted.

2.5 Western blots:

Cell lysates were harvested in PBS containing 1% triton and 1% protease inhibitor. A Bradford assay (Bio-Rad) was used to quantify protein levels. For immuno-blotting, 30µg of protein was resolved in 10% SDS polyacrylamide gel at 100V for 120 minutes. Protein was transferred to nitrocellulose membrane (Bio-Rad) at 0.2A for 90 minutes. Membranes were blocked in 1% BSA for 60 minutes before incubation overnight with the primary antibody. Membranes were washed in 1% TBS Tween for 5 minutes three times and incubated with the appropriate secondary antibody for 60 minutes. Membranes were washed in 1% TBS Tween for 5 minutes three times before proteins were revealed using chemiluminescent HRP substrate (Millipore). Membranes were re-incubated with a primary antibody targeting alpha smooth muscle actin to provide a loading control.

2.6 *In vivo* studies:

2.6.1 ACHN pilot study

ACHN xenografts were established in 6-8 week old female SCID mice (Charles River) by s.c. injection of 5×10^6 tumour cells in 200 ul PBS into the animals right flank. To test the effect of dasatinib on tumour growth, animals were randomised (1:1) 7 days post inoculation into two treatment groups (n=5); daily dasatinib 10mg/kg body weight by oral gavage or vehicle control. Dasatinib was prepared freshly each week in 50:50 propylene glycol/water, which also served as the vehicle.

ACHN cells were luciferase-tagged to allow tumour measurement by IVIS imaging (Caliper Life Sciences). Twice a week mice underwent intraperitoneal injection with 150 mg/kg D-luciferin. Mice were anaesthetized by isofluorane and tumours imaged 8 minutes after luciferin injection. Bioluminesence was quantified using Living Image software (Caliper Life Sciences).

2.6.2 Tolerability studies:

Prior to 786-O or A498 xenograft anti-tumour studies, a tolerability study was undertaken to confirm the planned drug dose levels were well tolerated in 6-8 week old female SCID mice (AstraZeneca). Tumour-free mice (n=2) were treated with sunitinib (40mg/kg) and a combination of cediranib and saracatinib (3mg/kg + 25mg/kg) and body weight was measured daily. The dose level of sunitinib (40mg/kg) in both the tolerability studies and subsequent anti-tumor studies was chosen to match the protocol used by Huang et al [39]. Cediranib and saracatinib dose levels were selected based on previous work conducted by AstraZeneca. Specifically, for saracatinib, the 25mg/kg dose is believed to be the minimal dose that achieves complete SRC inhibition in mice. The 3mg/kg dose for cediranib was based on previous pharmacokinetic work that suggested this dose best represented the dose level used in the clinic.

2.6.3 786-O pharmacodynamic xenograft studies (PD studies):

A PD study was undertaken to assess the pharmacodynamic effect of sunitinib, cediranib and saracatinib on mice harbouring 786-O tumours. 786-O xenografts were established in 6-8 week old female SCID mice (AstraZeneca) by s.c. injection of 5×10^6 tumour cells in 200 ul 50:50 PBS/Matrigel (Becton Dickinson). 30 days post inoculation (tumour volumes 0.2-0.8 cm^3) tumours were left for 30 days until animals were randomised into treatment groups (n = 7 for the vehicle group and n= 5 for all other treatment groups). Animals were underwent short-term chronic dosing with saracatinib (25mg/kg), cediranib (3mg/kg), sunitinib (40mg/kg) or vehicle (1% polysorbate 80), which involved administration once daily by oral gavage for 4 days and necropsies took place 2 hours after the final dose. Tumour tissue was taken for pharmacodynamic analysis; tumours were cut into half with one half frozen in liquid nitrogen (used later for RNA analysis) and the other half was paraffin-embedded for IHC analysis. Bone marrow samples were harvested for flow cytometric measurement of myelosuppression. Plasma was taken and stored at -80C for subsequent cytokine analysis.

2.6.4 786-O and A498 anti-tumour studies:

To measure the effect of saracatinib, cediranib and sunitinib on mice harbouring 786-O tumours, xenografts were established in 6-8 week old female SCID mice (AstraZeneca) by s.c. injection of 5×10^6 tumour cells in 200 ul 50:50 PBS/Matrigel (Becton Dickinson) mix into the animal's flank. Tumours were measured twice weekly with calipers and tumour volumes calculated taking length to be the tumour's longest diameter and width to be the corresponding perpendicular diameter using the following formula:

$$\text{tumour volume} = \sqrt{(\text{length}) \times (\text{width}) \times (\pi / 6)}$$

To compare treatment groups, the geometric mean of each cohort was calculated. Data were log transformed to take account of any size dependency before statistical analysis.

For anti-tumour studies, animals were randomised into treatment groups (n = 12-15 per group) when tumours were deemed to have reached a defined palpable size; this took place 30 days post inoculation when tumour volumes

were 0.2-0.8 cm^3. Saracatinib (25mg/kg), cediranib (3mg/kg) and sunitinib (40mg/kg) were prepared freshly each week in 1% polysorbate 80, which also served as the vehicle control. All drugs and vehicle were administered once daily by oral gavage and necropsies took place 2 hours after the final dose was administered.

A similar protocol was followed to assess the anti-tumour affect of sunitinib on A498 xenografts.

2.7 *Ex-vivo* flow cytometric quantification of myeloid cells:

At the termination of both PD and anti-tumour studies, a single femur from each animal was removed and bone marrow was flushed with a syringe filled with 1ml of 50% PBS/50% FCS. Samples were stored on ice until the completion of animal termination and then spun at 1600rpm for 5mins. Supernatant was poured off and the pellet re-suspended in 2 ml of PBS. Flow cytometry was performed for a total of 50,000 events per sample. Forward scatter and side scatter were analysed using previously determined values to gate cells into 4 cell types; monocytes, granulocytes, lymphocytes and red blood cells.

2.8 Immunohistochemistry:

A tissue microrarray (TMA) was constructed from biopsy and nephrectomy tissue samples from three separate Phase 2 trials. For xenograft derived tissue, freshly resected xenograft tumours were fixed in 4% w/v formalin overnight and whole sections were embedded in paraffin.

The following primary antibodies were used to assess protein expression; CD31 (1:600, AstraZeneca), FGF-2 (1:100, Peprotech), MET receptor (1:200, Invitrogen), CD3 (1:100, Novocastra), CD45 (1:100, Novocastra), Ki67 (1:100, Dako), s100a4 (1:150, Cell Signalling). Isotype controls were employed.

MET receptor and FGF-2 protein levels in the RCC patient derived TMAs were analysed by the author and a trained histopathologist (Colan Ho-yen and Rukma

Doshi respectively). Both the author and histopathologists were blinded at the time of scoring. When the score given by the author and histopathologist diverged further discussion took place until a consensus was reached. If necessary, a 3rd opinion was sought. Scores accounted for the strength of protein expression (scored 0 to 3) and the percent of tissue stained. Ki67 scores from patient derived TMAs were independently assessed by a trained pathologist (Dan Berney). Vessel density (CD31), CD45 or CD3+ve immune cells, were quantified using a computerised image analysis system (ARIOL, Applied Imaging, Genetix) using visually-trained parameters. Xenograft tissue protein expression of S100A4 and Ki67 were quantified using the ARIOL system.

Antigen retrieval conditions, both pH and time, were optimized for the primary antibody under investigation. In the majority of cases this optimisation work had already taken place prior to the work contained in this PhD. In general, sections were de-waxed through graded alcohols to distilled water and immersed in a sealed vessel containing 250ml of antigen retrieval buffer (Dako) with a pH of between 6 and 9.9 depending on the antibody of interest. Sections were heated to a temperature of 110°C in a microwave histoprocessor (RHS) for between 2-5 minutes. Sections were then allowed to cool in running water for approximately 15 minutes. For s100a4, MET receptor and Ki67 staining of RCC patient tissue, antigen retrieval took place in a pressure cooker; sections or TMAs were left for 7 minutes once the antigen retrieval buffer had boiled and then allowed to cool in running water.

EnVision (Dako) or ABC (Thermo Scientific) kits were used depending on the primary antibody used. Sections were incubated with peroxidase blocking solution (EnVision) for 10 minutes. If the ABC kit was being used endogenous Avidin / Biotin was also blocked at this stage. Sections are incubated with 5% Normal Goat Serum for 20 minutes before the primary antibody was added and sections were incubated for a further 60 minutes. Sections were rinsed twice in 0.05% TBS Tween and then incubated with an appropriate secondary antibody from either the ABC kit (Thermo Scientific) or EnVision ready-to-use (Dako). Slides were rinsed twice in 0.05% TBS Tween and incubated with DAB solution for 10 minutes. Sections were rinsed in distilled water, counterstained with haematoxylin and dehydrated through graded alcohols to xylene before cover slips were attached.

2.9 RNA extraction and cDNA synthesis of tumour samples for gene expression analysis:

At necropsy tumour samples cut in half with one half snap frozen transferred to a -80°C freezer for gene expression analysis. For RNA extraction, 30-50 mg of tumour samples was taken and placed in 2ml round bottom tubes containing a ball bearing. 600ul of RLT lysis buffer (qiagen) containing β-mercaptoethanol was added to each sample before tissue was homogenised. 600ul of homogenate was transferred to a new tube and spun down before supernatant was transferred to a fresh tube.

Total RNA was extracted using a QIAcube (Qiagen) following the manufacturer's protocol. RNA concentrations were quantified on a NanoDrop and normalised to 250ng/ul by adding RNase-free water (Qiagen). RNA was assessed using for quality control purposes (Agilent's 2100 Bioanalyser Instrument with Nano Chip Assay). For gene expression analysis an RNA integrity number value (RIN value) of 6–10 was considered acceptable.

First strand cDNA samples from 61 different xenograft tumours were selected for gene expression analysis (n=6 for treatment groups and n=7 or 8 for the vehicle groups). Selection was based on the RIN value and tumour size. For treatment groups the 6 samples with acceptable RIN values closest to the mean tumour volume in that treatment group were selected for gene expression analysis. cDNA synthesis was carried out using the Applied Biosystems High Capacity cDNA Reverse Transcription Kit on a thermal cycler as per the manufacturer's instructions.

2.10 Gene expression analysis:

Pre-amplification of cDNA samples was performed using the TaqMan PreAmp Master Mix using 1.25µL of cDNA in a 5 µL reaction. After 14 cycles pre-amplified cDNA was stored at −20°C until needed. Pre-amplified cDNA was added to the 2x TaqMan Universal Master Mix and loaded into a 24x24 dynamic array chips (Fluidigm). Primer probes were also loaded into the array chips and the chip was primed in a NanoFlex Controller (Fluidigm). High throughput RT-PCR analysis was carried out using a BioMark Real-Time PCR System (Fluidigm). The cycling program consisted of 10min at 95°C followed by 40 cycles of 95°C for 15 sec and 1 min at 60°C.

The following human and mouse-specific probes were used to examine the effect of drug treatment on the tumour compartment and the host compartment. Human-specific and mouse-specific probes were validated by AstraZeneca prior to the onset of the work contained in this thesis using human and murine cell lines.

Human-specific probes

Gene Symbol	Assay ID
ACVR1	Hs01090689_m1
ACVR1B	Hs03676620_s1
ACVR1C	Hs00377065_m1
ACVRL1	Hs00163543_m1
ANGPT1	Hs00375823_m1
ANGPT2	Hs01048043_m1
AXL	Hs01064436_m1
BMP10	Hs03676570_m1
BMP2	Hs00154192_m1
BMP4	Hs03676628_s1
BMP6	Hs01099596_m1
BMPR1A	Hs01034913_g1
BMPR1B	Hs01010965_m1
BMPR2	Hs00176148_m1
BSG	Hs00936295_m1
CACNA1G	Hs00367969_m1
CACNA1H	Hs01103523_m1
CACNA1I	Hs01096205_m1
CCL17	Hs00171074_m1
CCL2	Hs00234140_m1

Mouse-specific probes

Gene Symbol	Assay ID
Acta2	Mm00725412_s1
Acvr1b	Mm03053291_s1
Acvr1c	Mm01331057_m1
Acvrl1	Mm01300353_g1
Angpt1	Mm00456498_m1
Angpt2	Mm00545822_m1
Axl	Mm00437221_m1
Bmp10	Mm01183889_m1
Bmp2	Mm01340178_m1
Bmp4	Mm03676636_s1
Bmp6	Mm01332882_m1
Bmpr1a	Mm01208758_m1
Bmpr1b	Mm03053312_s1
Bmpr2	Mm00432129_m1
Bsg	Mm00814798_m1
Cacna1g	Mm00486572_m1
Cacna1h	Mm00445382_m1
Cacna1i	Mm01299026_m1
Ccl12	Mm01617100_m1
Ccl17	Mm00516136_m1

CCL22	Hs01574247_m1
CCL3	Hs00234142_m1
CCL4	Hs00237011_m1
CCL5	Hs00982282_m1
CCL7	Hs00171147_m1
CD82	Hs00356310_m1
CDH1	Hs01013953_m1
CDH11	Hs00901475_m1
CDH12	Hs00362037_m1
CDH3	Hs00354998_m1
CDH6	Hs00191832_m1
CDH8	Hs01031173_m1
CHRNA3	Hs01088199_m1
CHRNA5	Hs00181248_m1
CHRNA7	Hs01063372_m1
CHRNB4	Hs00609520_m1
CSF1R	Hs00234622_m1
CSF3	Hs00236884_m1
CSF3	Hs00738431_g1
CSF3	Hs99999083_m1
CST3	Hs00264679_m1
CSTA	Hs00193257_m1
CSTB	Hs00164368_m1
CTSB	Hs00947439_m1
CTSD	Hs00157201_m1
CTSK	Hs01080388_m1
CTSL1	Hs00266474_m1
CTSL2	Hs00822401_m1
CTSS	Hs00175403_m1
CX3CL1	Hs00171086_m1
CXCL1	Hs00236937_m1
CXCL10	Hs00171042_m1
CXCL12	Hs00930455_m1
CXCL5	Hs00171085_m1
CXCR4	Hs00237052_m1
CXCR7	Hs00664172_s1
CYTL1	Hs01573280_m1
DKK3	Hs00951303_m1
DLL4	Hs01117333_m1
EDG1	Hs00173499_m1
EDG3	Hs00245464_s1
EFNB2	Hs00970627_m1
ENG	Hs00164438_m1
ENPP2	Hs00905125_m1
ENTPD1	Hs00169946_m1
EPHB4	Hs01119118_g1

Ccl2	Mm00441242_m1
Ccl22	Mm00436439_m1
Ccl3	Mm00441258_m1
Ccl4	Mm00443112_m1
Ccl5	Mm01302428_m1
Ccl7	Mm00443113_m1
Cd82	Mm00492061_m1
Cdh1	Mm00486906_m1
Cdh11	Mm00515466_m1
Cdh12	Mm01165359_m1
Cdh2	Mm00483213_m1
Cdh3	Mm01249215_m1
Cdh6	Mm01310024_m1
Cdh8	Mm01242096_m1
Chrna3	Mm00520145_m1
Chrna5	Mm00616329_m1
Chrna7	Mm01312230_m1
Chrnb4	Mm00804952_m1
Csf1r	Mm00432689_m1
Csf3	Mm00438335_g1
Cst3	Mm00438347_m1
Csta	Mm01344699_g1
Cstb	Mm00432769_m1
Ctsb	Mm01310506_m1
Ctsd	Mm00515586_m1
Ctsk	Mm00484036_m1
Ctsl	Mm00515597_m1
Ctss	Mm00457902_m1
Cx3cl1	Mm00436454_m1
Cxcl1	Mm00433859_m1
Cxcl10	Mm00445235_m1
Cxcl12	Mm00445552_m1
Cxcl2	Mm00436450_m1
Cxcl5	Mm00436451_g1
Cxcr4	Mm01292123_m1
Cxcr7	Mm00432610_m1
Cytl1	Mm01217841_m1
Dkk3	Mm00443800_m1
Dll4	Mm01338020_m1
Efnb2	Mm01215897_m1
Eng	Mm00468256_m1
Enpp2	Mm00516572_m1
Entpd1	Mm00515447_m1
Ephb4	Mm01201157_m1
F2r	Mm00438851_m1
F2rl1	Mm00433160_m1

F2R	Hs00169258_m1
F2RL1	Hs00173741_m1
F2RL3	Hs01006385_g1
FGF1	Hs00361126_m1
FGF17	Hs03676568_gH
FGF18	Hs03676581_s1
FGF19	Hs00391591_m1
FGF2	Hs00266645_m1
FGF5	Hs03676587_s1
FGF6	Hs00907866_m1
FGF8	Hs01097227_g1
FGF8	Hs03676619_s1
FGF9	Hs03676566_mH
FLT1	Hs01052936_m1
FLT3	Hs00975659_m1
FLT4	Hs01047679_m1
FZD4	Hs03986777_s1
FZD5	Hs00361869_g1
GAS6	Hs00181323_m1
GDF2	Hs00211913_m1
HDGF	Hs00610315_gH
HEY1	Hs01114113_m1
HGF	Hs00300159_m1
HIF1A	Hs00936368_m1
HSPA5	Hs00946084_g1
ID1	Hs00704053_s1
ID1	Hs03676575_s1
ID2	Hs00747379_m1
ID3	Hs00171409_m1
ID4	Hs02912975_g1
IFI44L	Hs00199115_m1
IFIT1	Hs01911452_s1
IL1A	Hs99999028_m1
IL1B	Hs99999029_m1
IL1R1	Hs00991010_m1
IL1RN	Hs00893626_m1
IL6	Hs99999032_m1
IL6R	Hs00169842_m1
IL6R	Hs00794121_m1
IL8	Hs00174103_m1
IL8RA	Hs00174146_m1
IL8RB	Hs00174304_m1
ITGA5	Hs00233743_m1
ITGAV	Hs00233808_m1
KCNH1	Hs00924320_m1
KCNK9	Hs00363153_m1

F2rl3	Mm00433161_g1
Fgf1	Mm01258325_m1
Fgf15	Mm00433278_m1
Fgf17	Mm00433281_g1
Fgf18	Mm03676637_s1
Fgf2	Mm01289199_m1
Fgf5	Mm03053745_s1
Fgf6	Mm01183111_m1
Fgf8	Mm03676635_mH
Fgf9	Mm01319105_m1
Flt1	Mm00438980_m1
Flt3	Mm00438996_m1
Flt4	Mm00433337_m1
Fzd4	Mm03053556_s1
Fzd5	Mm00445623_s1
Gas6	Mm00490378_m1
Gdf2	Mm00807340_m1
Gpr116	Mm01269030_m1
H28	Mm00518988_m1
Hdgf	Mm00725733_s1
Hgf	Mm01135184_m1
Hif1a	Mm00468875_m1
Hpse	Mm00461768_m1
Hspa5	AIAAC6K
Id1	Mm03676649_s1
Id2	Mm00711781_m1
Id3	Mm01188138_g1
Id4	Mm00499701_m1
Ifit1	Mm00515153_m1
Il1a	Mm99999060_m1
Il1b	Mm01336189_m1
Il1r1	Mm00434237_m1
Il1rn	Mm01337566_m1
Il6	Mm99999064_m1
Il6ra	Mm00439653_m1
Il8rb	Mm00438258_m1
Itga5	Mm00439797_m1
Itgam	Mm00434455_m1
Itgav	Mm00434506_m1
Kcnh1	Mm01316769_m1
Kcnk2	Mm01323942_m1
Kcnk9	Mm02014295_s1
Kdr	Mm01222419_m1
Kiss1	Mm03058560_m1
Kit	Mm00445212_m1
Lpar1	Mm00439144_m1

KDR	Hs00176676_m1
KISS1	Hs00158486_m1
KIT	Hs00174029_m1
LPAR1	Hs00954504_m1
LPAR1	Hs03986771_m1
LPAR3	Hs00173857_m1
MERTK	Hs00179024_m1
MET	Hs00179845_m1
MGP	Hs00969490_m1
MMP13	Hs00233992_m1
MMP2	Hs00234422_m1
MMP7	Hs01042796_m1
MMP9	Hs00957555_m1
MST1	Hs00360684_m1
MST1R	Hs00899925_m1
NOTCH1	Hs00413187_m1
NOTCH3	Hs01128541_m1
NRP1	Hs00826128_m1
NRP2	Hs00187290_m1
NT5E	Hs01573922_m1
PDGFA	Hs00236997_m1
PDGFB	Hs00966526_m1
PDGFC	Hs00211916_m1
PDGFD	Hs00937332_m1
PDGFRA	Hs00183486_m1
PDGFRB	Hs00182163_m1
PGF	Hs01119262_m1
PLAT	Hs00263492_m1
PLAU	Hs01547054_m1
PLAUR	Hs00182181_m1
PLG	Hs00264877_m1
PRKCE	Hs00942878_m1
PROK2	Hs01587689_m1
PTPRJ	Hs01119326_m1
RALBP1	Hs00799096_s1
RHOA	Hs01051295_m1
RHOB	Hs03676562_s1
RHOC	Hs00747110_s1
RPSA;RPSAP	Hs00347791_s1
S100A4	Hs01569256_m1
SERPINB2	Hs00234032_m1
SERPINB5	Hs00985285_m1
SERPINE1	Hs01126604_m1
SGK1	Hs00178612_m1
SGK2	Hs00367639_m1
SGK3	Hs00179430_m1

Lpar1	Mm03986786_m1
Lpar3	Mm01312593_m1
Mertk	Mm01336149_m1
Met	Mm00434924_m1
Mgp	Mm00485009_m1
Mmp13	Mm01168713_m1
Mmp2	Mm03928978_m1
Mmp7	Mm01168420_m1
Mmp9	Mm00442991_m1
Mst1	Mm01229834_m1
Mst1r	Mm00436365_m1
Notch1	Mm00435249_m1
Notch3	Mm00435270_m1
Nrp1	Mm00435372_m1
Nrp2	Mm01254530_m1
Nt5e	Mm01144394_m1
Pdgfa	Mm01205760_m1
Pdgfb	Mm01298578_m1
Pdgfc	Mm00480205_m1
Pdgfd	Mm00546829_m1
Pdgfra	Mm01211694_m1
Pdgfrb	Mm00435546_m1
Pecam1	Mm00476702_m1
Pgf	Mm00435613_m1
Plat	Mm00476931_m1
Plau	Mm00447054_m1
Plaur	Mm01149438_m1
Plg	Mm01312967_m1
Prkce	Mm00440894_m1
Prkd1	Mm00435790_m1
Prkd2	Mm01264603_m1
Prok2	Mm01182451_m1
Ptprj	Mm01327824_m1
Ralbp1	Mm00485718_m1
Rhoa	Mm01228062_g1
Rhob	Mm03676631_s1
Rhoc	Mm03928976_mH
Rpsa	Mm00726662_s1
S100a4	Mm00803371_m1
S1pr1	Mm00514644_m1
S1pr3	Mm00515669_m1
Serpinb2	Mm00440905_m1
Serpinb5	Mm00436763_m1
Serpine1	Mm00435860_m1
Serpine2	Mm00436753_m1
Shh	Mm03053649_s1

SHH	Hs00179843_m1
SNAI1	Hs00195591_m1
SPHK1	Hs00184211_m1
SPHK2	Hs00219999_m1
SPP1	Hs00167093_m1
SPP1	Hs00960641_m1
TEK	Hs00176096_m1
TGFB1	Hs00171257_m1
TGFBR1	Hs00610318_m1
THBS1	Hs00962914_m1
TIE1	Hs00178500_m1
TIMP1	Hs99999139_m1
TIMP3	Hs00165951_g1
TRPC6	Hs00395102_m1
TRPM8	Hs00375481_m1
TRPV2	Hs00901640_m1
TRPV4	Hs01099348_m1
TWIST2	Hs03986784_s1
TYRO3	Hs03986773_m1
VEGFA	Hs00900054_m1
VEGFB	Hs00957980_g1
VEGFC	Hs00153458_m1
VIM	Hs00958112_g1
WNT1	Hs03986774_s1

Snai1	Mm00441533_g1
Snrk	Mm00505255_m1
Sphk1	Mm01252544_m1
Sphk2	Mm00445021_m1
Tek	Mm01256892_m1
Tgfb1	Mm00441724_m1
Tgfbr1	Mm00436964_m1
Thbs1	Mm01335418_m1
Tie1	Mm00441786_m1
Timp1	Mm00441818_m1
Timp3	Mm01224941_m1
Trpc1	Mm00441975_m1
Trpc6	Mm01176083_m1
Trpm8	Mm01299593_m1
Trpv2	Mm00449223_m1
Twist2	Mm00492147_m1
Tyro3	Mm00444547_m1
Vegfa	Mm00437304_m1
Vegfb	Mm00442102_m1
Vegfc	Mm01202432_m1
Vim	Mm01333430_m1
Wnt1	Mm00810320_s1

Delta Ct values for each gene were calculated with reference to human/murine-specific 18s probes (AstraZeneca). A computer script using the R programming language was written to display Delta Ct values as a heatmap.

Principal component analysis was carried out for quality control purposes.

2.11 ELISA (Enzyme-Linked ImmunoSorbent Assay)

The affect of drug treatment of serum levels of human PGF were investigated by ELISA (Human Quantikine ELISA, R&D systems). Serum was collected at study termination and stored at -80C. Samples were thawed on ice and 100µl of serum was added to each well of the 96-well plate. Samples were incubated for 2 hours at room temperature before being washed as per the manufacturer's instructions. 200µl of conjugate was added and incubated for a further 2 hours before another round of washing. 200µl substrate was added and the plate incubated for 20 minutes before 50µl of stop solution was added. Samples were transferred to a multi-plate reader (570nm absorbance) and levels of PGF quantified with reference to the manufacturer's standard. Tumour-derived PGF levels were normalised with reference to tumour size at study termination.

2.12 Collagen staining

To determine collagen content in both xenograft and RCC patient tissue, whole sections were dewaxed and hydrated through graded alcohols to distilled water. Slides were incubated in sirius-red for one hour before washing in acidified water (acetic acid diluted to 1/200 with distilled water). Slides were rinsed twice in 0.05% TBS Tween and incubated with DAB solution for 10 minutes. Sections were rinsed in distilled water and dehydrated through graded alcohols to xylene before cover slips were attached. Collagen was quantified with the ARIOL system using visually trained parameters.

2.13 Statistics

A Student's two-tailed t-test was used to investigate the affect of drug treatment versus control. A p-value of <0.05 was considered to be statistically significant.

Chapter 3:

Investigating the effect of VEGFR-TKI therapy on matched pairs of RCC patient tissue

3. 1 Introduction

The advent of VEGF receptor tyrosine kinase inhibitors (VEGFR TKIs) has revolutionised the treatment of metastatic renal cell carcinoma (mRCC). The TKIs sunitinib and pazopanib are now established as first line therapy. Both these drugs are thought to act primarily as anti-angiogenic agents, targeting VEGF receptors located on tumour vessels. Direct anti-tumour effects and the ability to enhance immune response may also contribute to the observed clinical efficacy [64] [46] [65].

An initial hope of anti-angiogenic therapy was that targeting tumour vessels, rather than inherently unstable tumour cells, could help prevent drug resistance occurring. Clinical experience has been very different [66]. Intrinsic resistance, although less common in mRCC than other tumour types, occurs in approximately 20% of cases [67]. Patients that do benefit from an initial response invariably progress at some stage. Numerous resistance mechanisms have been proposed. Perhaps most prominent is the hypothesis that tumours can compensate for VEGF inhibition by switching to alternative angiogenic factors such as fibroblast growth factor-2 (FGF-2) [68] [69] or the HGF/MET receptor pathway [70] [71].

3.2 Aim of chapter

A better understanding of the resistance mechanisms underlying tumour progression has been hampered by; (1) lack of access to treated patient tissue and (2) the lack of a representative preclinical model. In this chapter we try to address both issues.

As a result of three recent clinical trials, we gained access to VEGFR-TKI-treated tissue samples [72] [73] [74]. Pre-treatment biopsies were taken prior to onset of sunitinib or pazopanib therapy and then nephrectomies were performed after approximately 3 months of treatment. Using TMAs constructed from this tissue we investigated important questions including the following:

- Do VEGFR-TKI's result in decreased vessel density? What is the degree of this reduction and does it correlate with patient outcome?

- Are alternative (non-VEGF) pro-angiogenic factors up-regulated at the tumour site? Do either the baseline levels of pro-angiogenic factors or the degree of increase predict patient outcome?

In the final section of this chapter we aim to address the lack of a representative preclinical model. We attempt to replicate published work in which the authors developed a preclinical model of 'sunitinib resistance'. This preclinical model of resistance provides the backbone for the *in vivo* work included in the next two chapters.

3.3 Results

3.3.1 Tissue origin and patient characteristics

Human tissue used in this chapter derives from patients enrolled in 3 independent single arm phase II studies with very similar inclusion criteri. Two of these trials used the VEGFR-TKI sunitinib (50mg PO OD – 4 weeks on 2 weeks off) while the other trial used the VEGFR-TKI, pazopanib (800mg PO OD) [72 73 74].

Renal carcinoma was confirmed by biopsy prior to inclusion in the studies and these biopsies were later used for IHC analysis. Unlike standard of care, which involves nephrectomy prior to treatment onset, all 3 studies investigated the use of VEGFR-TKI therapy prior to planned nephrectomy. Nephrectomy was performed as soon as practicably possible after stopping VEGFR-TKI treatment.

In total 98 patients were enrolled in these studies, but 36 patients were ineligible for analysis of matched tissue for various reasons; disease progression prior to planned surgery (n=20), co-morbidity (n=2), patient choice not to undergo surgery (n=9) and patients not recommencing VEGF TKI therapy within 6 weeks (n=5). The primary analysis focuses on the prognostic significance of the observed changes to biomarkers on matched patient tissue i.e. tissue taken from the same patient pre- and post- treatment. 62 of the original 98 patients were eligible for this analysis. These patients restarted the same TKI therapy post nephrectomy with no evidence of progression of disease during pre-nephrectomy systemic therapy. Patient characteristics for eligible patients are shown below. The author of this thesis played no role in measuring these clinical parameters. Author contribution was restricted to data collection and analysis.

	All patients	Patients eligible for primary analysis
Number of patients	98	62
Age	59 (range: 37-78)	57 (range: 38-82)
Gender		
male	75	45
female	23	17
MSKCC prognostic risk		
intermediate	70	51
poor	28	11
Number of metastatic sites		
1	30	25
2	39	22
3+	29	15
Treatment		
Pazopanib	34	22
Sunitinib	64	40
Reason for not having surgery and restarting TKI		
PD	20	NA
Patient choice	9	
Unfit for surgery	2	
No TKI post surgery	5	
Total	36	
Platelet count	300 (76-857)	294 (76-857)
Neutrophil count	5.8 (2.3-15.5)	5.35 (2.3-13.3)
Best response to treatment		
PD	20	0
SD	62	47
PR/CR	16	15
T stage at nephrectomy		
T1	NA	9
T2		18
T3		29
T4		6
PS at baseline		
0	11	8
1	67	43
2	20	11
Clear cell grade at surgery		
1	NA	3
2		19
3		31
4		6
NA		3

Table 3.1 Patient characteristics

3.3.2 The effect of VEGFR-TKI treatment on vessel density

VEGFR-TKIs are thought to act primarily through their impact of the tumour vasculature. To determine the impact of therapy on microvessel density (MVD), matched pairs of pre- (initial biopsies) and post-treated tumours (nephrectomies) were examined by IHC.

Vessels were detected by IHC staining for CD31 protein. Vessel density (MVD), defined as total area stained positive for CD31 / total area of tissue core, was quantified using a computerised image analysis system (Ariol, Applied Imaging, Genetix) using visually-trained parameters. In patients where more than one scorable tissue core was available the mean score was calculated.

In the matched patient samples MVD was significantly decreased with therapy (median fall 49.2%. $p<0.01$) [Figure 3.1]. Treatment reduced MVD in 35 out of 41 patients where scorable tissue was available. The prognostic significance of the change in MVD was calculated using multivariate Cox regression analysis. Factors in the multivariate model included gender, grade, necrosis, MSKCC prognostic score, TKI treatment (sunitinib or pazopanib), initial response to TKI therapy, sites of disease. Individuals with a greater reduction in tumor vasculature (CD31 fall above median) had a better survival (HR3.07: 1.12-8.42 $p<0.05$) [Figure 3.2].

(a) CD31 – example of nephrectomy tissue with high vessel density

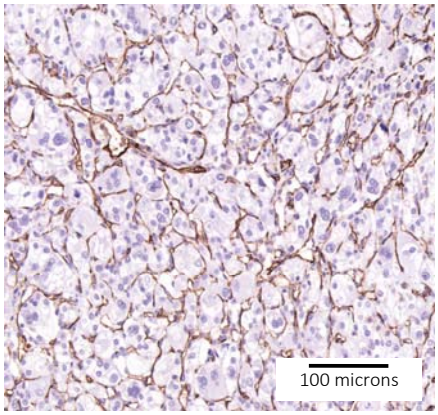

(b) CD31 - example of nephrectomy tissue with low vessel density

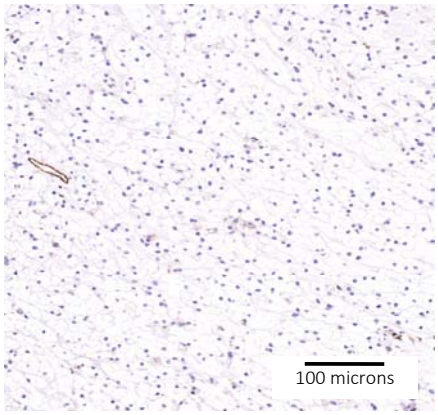

(c) MVD – matched pairs

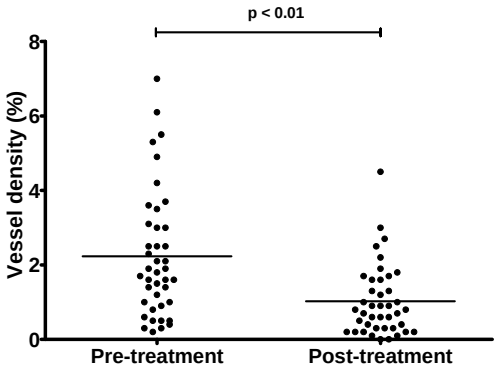

(d) MVD – all tissue samples

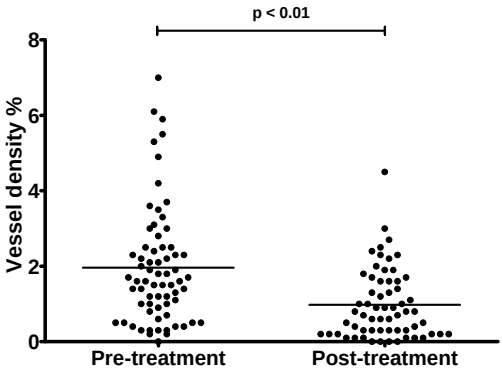

Figure 3.1: The effect of VEGFR-TKI therapy on vessel density in human RCC samples. Panels (a) and (b) shows examples of CD31 staining in a highly vascular nephrectomy core and a nechrectomy core with low vessel density respectively. Panel (c) shows the impact on vessel density as measured by CD31 in patient-matched pairs (n=48). Vessels stained for CD31 were quantified using a computerised image analysis system (Ariol, Applied Imaging, Genetix) using visually-trained parameters. Microvessel density was defined as 'area stained positive for CD31 / total tissue area'. Panel (d) shows CD31 scores from matched samples and also includes data from unmatched biopsies and nephrectomies (biopsies n=68, nephrectomies n=62).

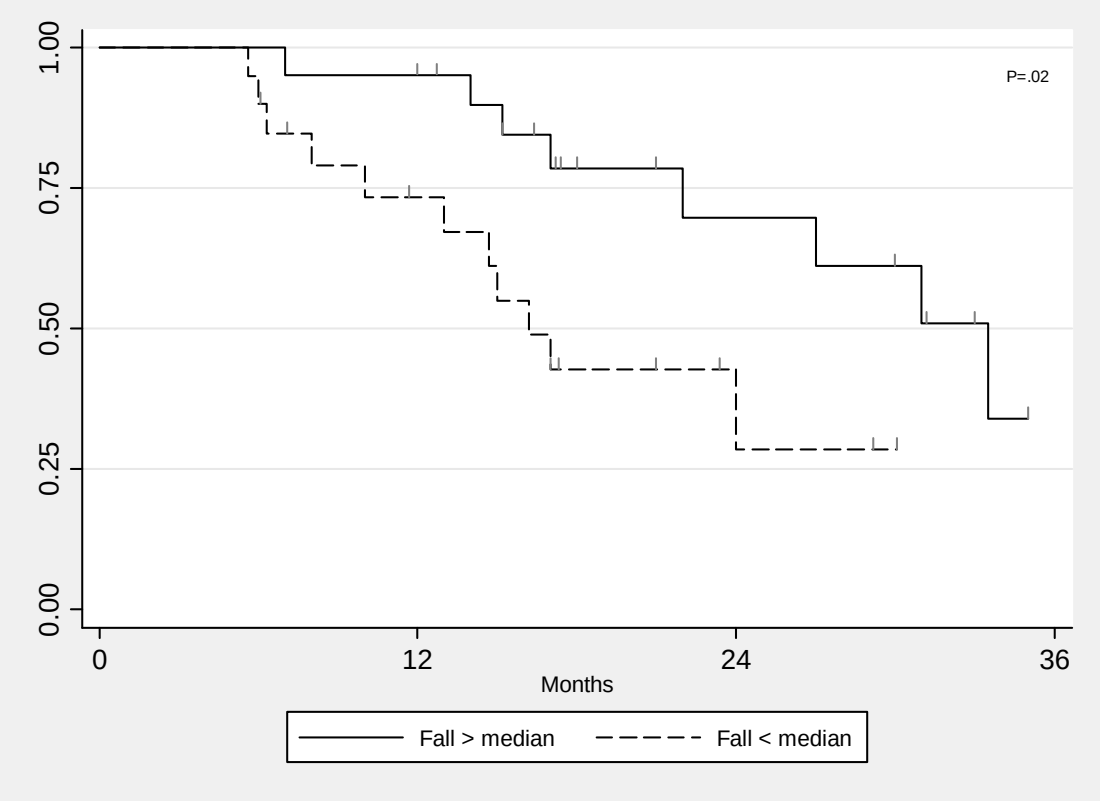

Figure 3.2: The relationship between vessel density reduction and overall survival. This Kaplan Meier curve indicates that patients experiencing a great than the median fall in CD31 expression have a better prognosis. Survival was measured from the time of surgery (n=48). This Kaplan Meier curve was created in collaboration with a Barts Experimental Cancer Medicine Centre statistician. A statistical comparison was performed using the log-rank test.

3.3.3 The effect of VEGFR-TKI treatment on FGF-2 expression in matched patient samples

The molecular mechanism underlying resistance to VEGFR-TKI therapy is not fully understood, but the resistance process is likely to be multi-factorial [75]. It has been proposed that tumours can compensate by switching to non-VEGF pro-angiogenic factors. The pro-angiogenic factor FGF-2 is anticipated to be a key player in this process. Several preclinical studies have highlighted the potential of FGF-2 to stimulate angiogenesis in this setting [67, 68] including a paper by Welti et al, in collaboration with our group, which demonstrated that the addition of FGF-2 can undermine sunitinib efficacy in an *in vitro* model of angiogenesis [69].

To investigate the impact of FGF-2 on TKI-induced MVD reduction and patient outcome, TMAs were stained and scored for FGF-2 expression. FGF-2 was expressed in the nucleus and cytoplasm of tumour cells and, in some cases, vessels also stained positive for FGF-2 (examples are shown in Figure 3.3). Consequently, cores were scored separately for these three compartments. 31 matched pairs of tissue were present and deemed scorable after the staining process. This tissue was scored by both a trained pathologist [Rukma Doshi] and the author. For each core, scores for the nucleus and cytoplasm were generated by estimating the percent of tissue stained, which was multiplied by an estimate of the strength of staining (0 = negative, 1 = weak, 2 medium, 3 strong). For vessels, cores were scored as positive if FGF-2 expression could be seen in one or more vessels. In cases where more than one core was present an average score was taken.

In matched samples, there was no significant difference between the pre- and post-treatment levels of FGF-2 expression in either the vessels or the nuclear compartment of tumour cells. In the cytoplasmic compartment, expression of FGF-2 was significantly higher post-treatment [median rise 124%, $p<0.01$, see Figure 3.3 (d)]. Baseline levels FGF-2 expression did not correlate with patient outcome in any of the 3 tumour compartments. Furthermore, the degree of cytoplasmic FGF-2 increase was not associated with an increased risk of death (1.03; 95% CI 0.33-3.22, $p=0.96$).

(a) Example of tissue classified as negative for cytoplasmic FGF2, with strong and moderate and nuclear staining

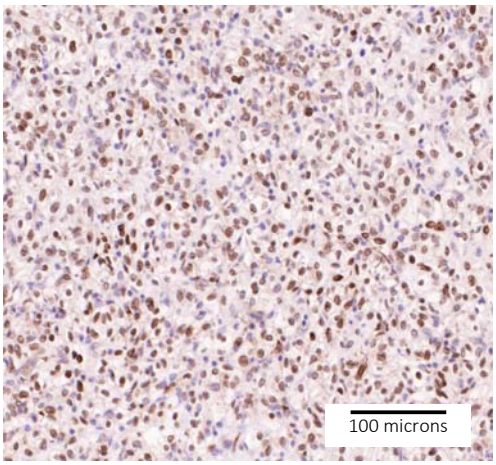

(b) Example of tissue classified as negative for nuclear FGF2, with strong cytoplasmic staining and FGF2 positive vessels

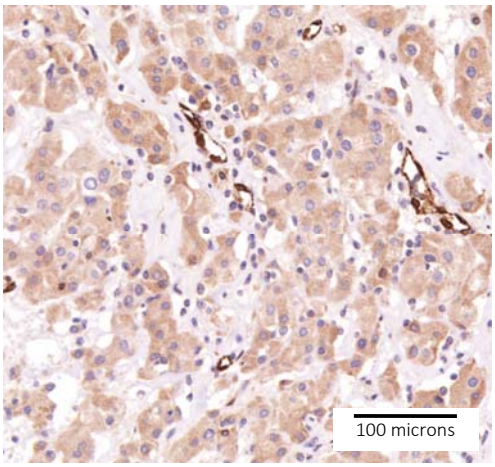

(c) Change in FGF2 nuclear staining

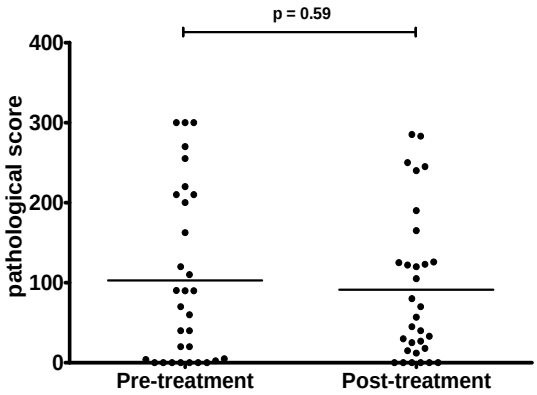

(d) Change in cytoplasmic staining

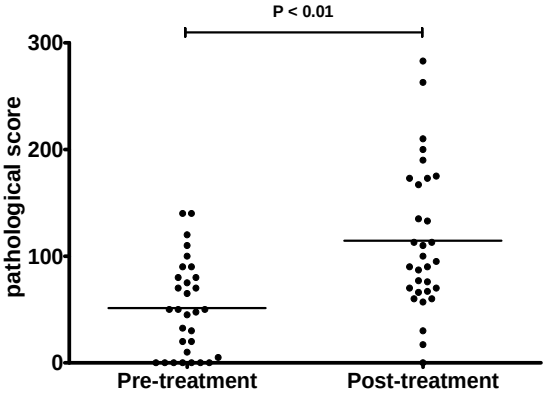

Figure 3.3: Change in FGF-2 expression pre- and post- VEGFR-TKI therapy. Panels (a) and (b) shows examples of FGF2 staining in nephrectomy tissue with strong expression in the nuclear and cytoplasmic compartments respectively. Panel (c) and (d) shows the impact on FGF-2 expression pre- and post-treatment in patient-matched tissue (n=31).

3.3.4 The effect of VEGFR-TKI treatment on MET receptor in matched patient samples

Further to FGF-2, the HGF/MET receptor pathway has been implicated as an alternative angiogenic pathway capable of promoting resistance to VEGFR-TKIs[69, 71]. MET receptors expressed on endothelial cells are thought to be activated by ligand, Hepatocyte Growth Factor (HGF), which can be expressed by endothelial cells themselves, tumour cells or stromal cells such as fibroblasts.

Further to angiogenesis, several preclinical studies show that VEGFR-TKIs can induce up-regulation of MET receptor in the tumour compartment, which may promote invasion and metastasis [70, 76].

To investigate the impact of this signaling pathway on TKI-induced microvessel reduction and patient outcome, TMAs were stained and scored for MET receptor, scoring the tumour cells and vessels separately. 41 matched pairs of tissue were present and met quality control standards. These were scored by a trained pathologist [Colan Ho-Yen] and the author. For each core, scores for the tumour compartment were generated in a similar manner to FGF-2 (% of tumour positive multiplied by an estimate of the strength of staining; 0 = negative, 1 = weak, 2 medium, 3 strong). For vessels, the percent of MET receptor positive vessels was calculated with reference to another CD31-stained section, located in a tissue section adjacent to MET receptor-stained tissue.

In the tumour compartment, there was no significant difference between the pre-treatment and post-treatment levels of MET receptor. However, treatment did induce a statistically significant increase in MET receptor in vessels. This increase in MET receptor did not predict patient outcome as measured by either overall survival or disease progression.

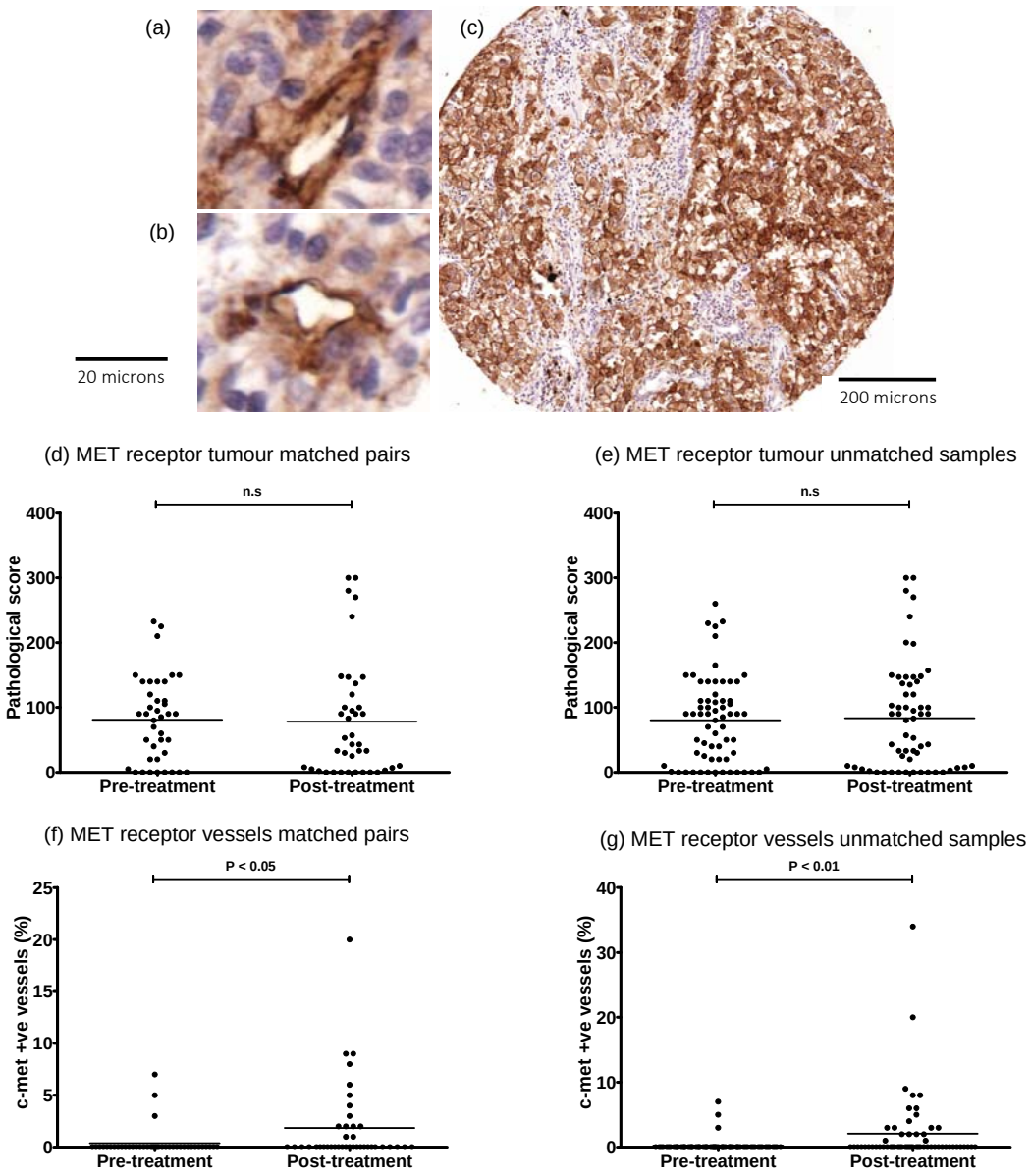

Figure 3.4: Change in MET receptor expression pre- and post- VEGFR-TKI therapy. Examples of MET positive vessels can be seen in panels (a) and (b) and panel (c) shows a tumour core with a tumour compartment classified as strongly positive. Panels (d) and (e) refers to the tumour compartment, whereas panels (f) and (g) shows the impact on MET receptor in tumour-associated vessels (n=41).

3.3.5 The effect of VEGFR-TKI treatment on Ki67 in matched and unmatched patient samples

Ki67 is a nuclear protein expressed in cells in all active phases of the cell cycle, but absent in resting cells (G_0). IHC of Ki67 is commonly used to establish the growth fraction of a tumour sample. A high Ki67 index has been associated with poor prognosis in multiple tumour types including renal cell carcinoma [77] [78] [79]. Compared to FGF-2 and HGF/MET receptor there is comparatively little previous work looking at a link between Ki67 and VEGFR-TKI resistance, but there is some evidence that baseline levels of Ki67 index may be prognostic in patients treated with VEGFR-TKIs, albeit in a different tumour type [80]. Consequently, TMAs were stained and scored for Ki67 expression. Scoring involved estimating the proportion of tumour cells that were Ki67-positive and this was performed by a trained pathologist [Dan Berney]. When there were multiple cores available to score for the same patient, the mean score was used.

The Ki67 index increased post-treatment in both analyses [Fig 3.4]. However, restricting the analysis to matched patient samples, the increase did not reach statistical significance (median rise 26%, p=0.14). Furthermore, the level of increase during treatment was not associated with a significant increase in the risk of death [2.08 (95% CI; 0.68-1.46, p=0.13)]. Unlike previously published data in pancreatic neuroendocrine cancer, baseline levels of Ki67 were not predictive of patient outcome to VEGFR-TKI in this setting [80]. It should be noted that Ki67 is an essential part of tool for the prognostic classification of pancreatic neuroendocrine cancer. Although some research has suggested that renal tumors with high Ki67 may predict for poor prognosis [77], this correlation does not appear to be as strong as in pancreatic neuroendocrine cancer.

(a) Ki67 – matched pairs of tissue

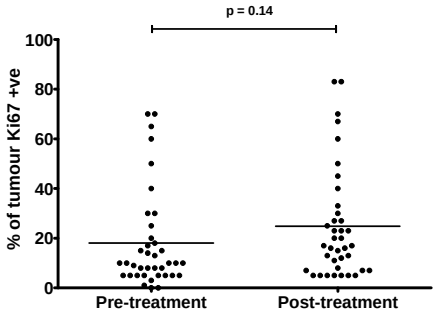

(b) Ki67 – all tissue samples

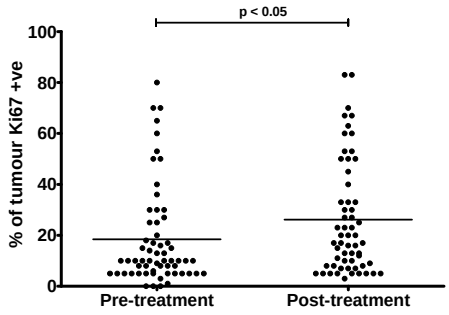

Figure 3.5: Change in Ki67 index pre- and post- VEGFR-TKI therapy. Panel (a) uses the mean score per patient when multiple cores are available and restricts analysis to patients for which matches tissue was scorable (n=38). Panel (b) also uses the mean score per patient but incorporates unmatched biopsies and nephrectomies (biopsies n=61, nephrectomies n=59).

3.3.6 Heterogeneity

Phenotypic and functional heterogeneity arise among cancer cells. This heterogeneity can influence therapy outcome, particularly when the target of molecular therapy is inconsistently expressed on tumour cells. Furthermore, heterogeneity can adversely affect biomarker analysis if sample bias confuses biomarker identification.

Multiple samples were taken from within the same treated tumors to investigate heterogeneity of tumour biomarker expression (n= 5). Significant intra-tumour heterogeneity was observed for all biomarkers investigated (Figure 3.6). Further analysis using array CGH and DNA methylation analysis (MethylCap-seq) showed the observed variability seen at the protein level was largely driven by genetic rather than epigenetic instability. This work was carried out in conjunction with external collaborators and does not form part of this thesis (data not shown).

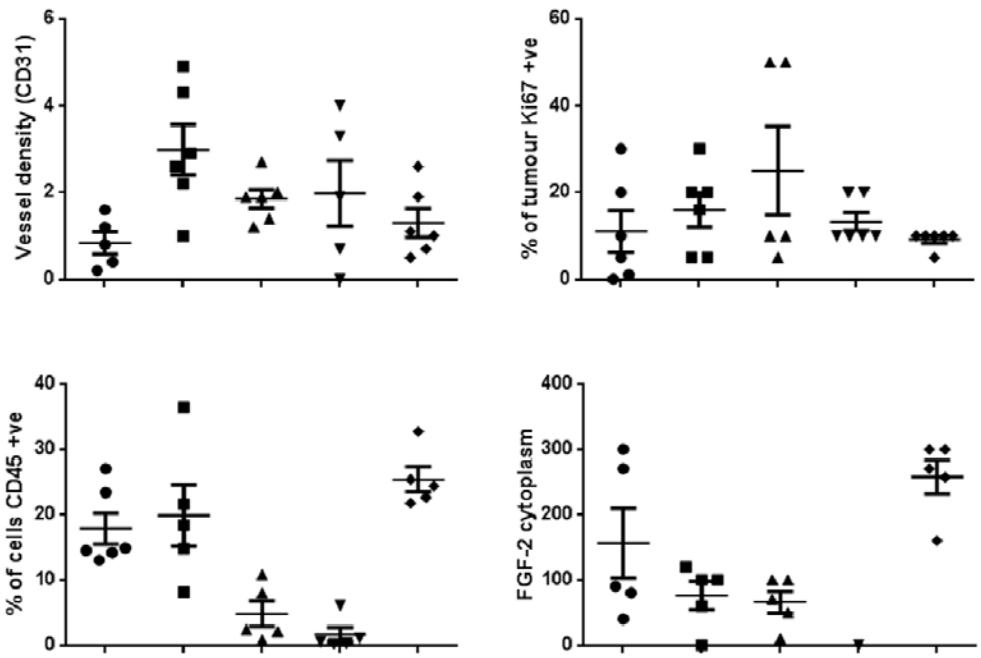

Figure 3.6: Examples of intra-tumour heterogeneity in treated samples. IHC scores for CD31, Ki67, CD45 and FGF-2 are shown from patients with at least five cores available from different tumor regions taken after treatment.

3.3.7 Developing a preclinical model of 'sunitinib resistance'

Clinical experience suggests that while most RCC patients benefit from VEGFR-TKI treatment, tumours inevitably acquire a resistant phenotype. In a recent paper, Huang et al [39] showed that xenografts were capable of replicating the clinical experience. That is to say, tumours in xenografts that were continuously treated with sunitinib were initially well controlled by treatment but then appeared to develop a resistant phenotype as tumour growth returned.

We attempted to replicate the published models in order to further investigate which factors help promote the resistance process. The development of a sunitinib-resistant preclinical model was partly motivated by the desire to challenge resistant tumours with a SRC inhibitor, which we hypothesised may be effective in this setting.

Following the protocol outlined with by Huang et al [39] 786-O xenografts were established in 6-8 week old female SCID mice by s.c. injection of 5×10^6 cells into the animal's flank. 30 days post inoculation, when tumours were measurable and growing consistently (tumour volumes 0.3-0.8 cm^3) mice were treated with 40mg/kg sunitinib once daily by oral gavage. As seen in the previously published work [39], tumours initially regressed before rebounding [Figure 3.7 (d)]. Minimum measurements were recorded between Day 17 and Day 28. The degree of treatment-induced tumour regression correlated with the size of the tumour prior to treatment onset [Figure 3.7 (e)].

In contrast A498 xenografts, also continuously treated with sunitinib (40mg/kg O.D), benefitted from strong tumour regression upon treatment onset, but showed no signs of rebound after sustained treatment for over 40 days.

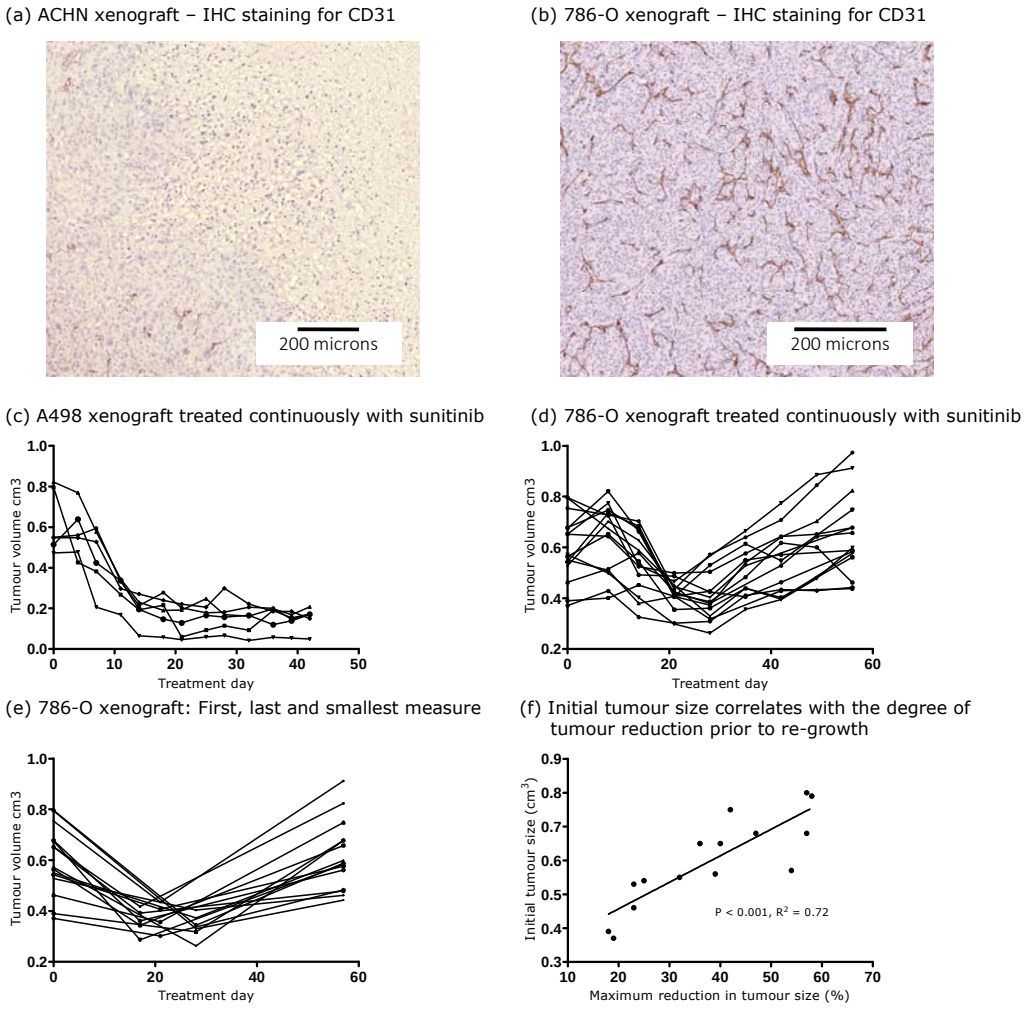

Figure 3.7: Investigating 3 different RCC xenografts as potential models for VEGFR-TKI resistance. Panel (a) is an example of a vehicle treated ACHN tumour 45 days post inoculation. Sections were IHC stained for CD31. Panel (b) shows an example of a CD31-stained vehicle treated 786-O xenograft. Panel (c) shows the effect of sunitinib (40mg/kg O.D) treatment on tumour volume in 6 mice harbouring A498 xenografts. Panel (d) shows the effect of the same treatment regimen on 15 mice harbouring 786-O tumours. Panel (e) represents the same mice, but only the first and last measures smallest are shown. Panel (f) shows the positive correlation between the size of tumour prior to treatment onset and the subsequent drug-induced tumour shrinkage (calculated as the difference between the first measure and the smallest measure).

3.4 Discussion

Preclinical models have shown that VEGFR-targeted therapy can affect vessel function, permeability and induce normalisation [81]. Furthermore, preclinical studies invariably show that TKIs are capable of reducing MVD in these models. Typically, these preclinical models involve fast-growing tumours set within the highly vascular subcutaneous microenvironment and so its not clear how representative these models are of the clinical setting [81]. Furthermore, the value of MVD as a pharmacodynamic marker of anti-angiogenic drug efficacy has been questioned since, over a period of time, vessel reduction may be expected to result in a similar reduction in viable tumour mass leaving the intercapillary distance largely unchanged [82].

Very few clinical studies have been designed in a way that allows the direct measurement of treatment-induced MVD reduction. When this has been possible, a significant decrease in MVD has not always been observed [83]. Moreover, when a decrease is observed, the studies have been underpowered to investigate the impact on patient outcome [84].

The design of 3 recently completed clinical trials gave us access to biopsy tissue taken before any treatment and patient tissue taken from the same patients 3 months after VEGFR-TKI treatment onset. This allowed us to examine the degree of MVD reduction in RCC patients for the first time. Since matched tissue was available in the majority of these patients we had the opportunity to assess the correlation between MVD reduction and patient outcome. A greater than average reduction in vessel density was associated with increased overall survival. To our knowledge, this is the first study to demonstrate a direct correlation between reduced vessel density and patient outcome in the clinical setting.

In addition to examining the degree of vessel density reduction, we also investigated whether the absolute levels (both pre-treatment and post-treatment) correlated with patient outcome. In both cases, absolute vessel density did not correlate with overall survival.

The pro-angiogenic potential of FGF-2 is long established [85]. In more recent times, FGF-2 has been proposed as a key mediator of drug-resistance in mRCC [69] [37]. Increased circulating concentrations of FGF-2 have been reported in patients progressing on VEGF-targeted therapy [86]. Because FGF-2 exerts a paracrine effect to promote angiogenesis [87], the level of FGF-2 at the tumour site, rather than the level of FGF-2 in the circulating pool, would seem to be the more relevant measurement.

FGF-2 expression can occur in both the cytoplasmic and nuclear compartments. Furthermore, the subcellular location is thought to play a role on the function of FGF-2 [88]. Consequently, tissue was scored for nuclear and cytoplasmic FGF-2 separately. Nuclear FGF-2 was unaffected, but VEGFR-TKI therapy increased expression of cytoplasmic FGF-2 expression at the tumour site. However, we found no significant correlation between the degree of FGF-2 up-regulation and patient survival. Furthermore, FGF-2 expression levels (both pre- and post-treatment) did not correlate with patient outcome.

Other clinical studies have collected on-treatment patient blood samples to investigate circulating factors that may contribute to resistance [89]. Our approach to look at pre- and post-treatment tissue samples has both benefits and limitations. One clear advantage is the ability to look at tumour expression in situ. This is potentially important in view of recent evidence that TKI treatment can induce a systemic up-regulation of pro-angiogenic factors, which occurs in a tumour-independent manner [35]. Blood sample measurements incorporate both tumour-derived and systemic expression of these factors, confusing any analysis. Our approach confirms that there was a significant increase in the pro-angiogenic ligand FGF-2 and this occurred in the tumour compartment in direct proximity to the target vessels.

However, the non-invasive nature of blood sample collection allows multiple samples to be taken which can be compared to tumour response on a dynamic basis. For example, FGF-2 was shown to increase in the blood of TKI-treated glioblastoma patients at the time of progression [90]. In this study, we analysed

FGF-2 expression at one post-treatment timepoint - three months into therapy. At this stage, as a requirement to perform the nephrectomy, none of the patients contributing to the matched tissue pairs had progressed. Consequently, what our analysis does show is that mRCC tumours can up-regulate FGF-2 in response to VEGF-targeted therapy. This occurred in patient still responding to treatment. The extent to which FGF-2 expression contributes resistance is not clear from our study.

Preclinical studies suggest VEGFR-TKI therapy can up-regulate expression of MET receptor in tumor cells, potentially promoting tumor invasion and metastasis [70, 76]. In this study we found no evidence for up-regulation of MET receptor at the tumour site. However, we did see up-regulation of MET receptor in tumour-associated vessels. Up-regulation of MET receptor in the vascular compartment could provide an alternative pro-angiogenic signal for endothelial cells in the presence of its ligand, hepatocyte growth factor (HGF). Previous work suggests that HGF may also be up-regulated in response to VEGFR-TKI which could work synergistically with MET receptor up-regulation [71]. In the absence of a suitable antibody, it was not possible to investigate whether HGF expression was effected by treatment in the TMA. Moreover, despite efforts to obtain an antibody that measured levels of phosphorylated MET receptor we could not find an antibody that passed our quality control in terms of demonstrating specific binding to the target. As a result we were not able to measure MET receptor activation in addition to total MET receptor levels.

Ki-67 is a measure of tumour proliferation and provides an independent marker of tumour aggressiveness in several cancer types, including renal carcinoma [77] [78] [79]. This marker was chosen to test the hypothesis that these drugs have an effect on tumour cellular proliferation, potentially leading to a more aggressive tumour phenotype. VEGF TKI treatment may result in dynamic changes at the molecular level that lead to a more resistant, aggressive tumour phenotype. While a significant increase in Ki67 was seen when taking into account all samples (including unpaired samples [Figure 3.5 (b)]) the primary focus of our analysis is the matched tissue samples. In this tissue a statistically significant change in Ki67 was not observed [Figure 3.5 (a)].

Molecular heterogeneity is challenging because sampling bias may prevent detection of biologically significant changes in biomarker expression. Intra-tumor heterogeneity can occur at the genetic level, but can also be impacted by epigenetics and regional differences in the tumor microenvironment. Investigating biomarkers at the protein level, rather than at the DNA level, can be particulary problematic because protein expression can be affected by all three of the above variables i.e. protein expression can be altered by the underlying genotype, epigenetics and the local microenvironment.

Heterogeneous protein expression can be particularly unhelpful when dealing with small biopsies that may not necessarily reflect the pattern of biomarker expression in the tumors that they represent. One potential strategy to mitigate the effect of tumor heterogeneity is to use multiple tissue samples from the same patient. Where possible we employed this strategy in our biomarker analysis.

Analysis of multiple samples taken from different regions within the same tumour indicated significant intra-tumour heterogeneity in our RCC tumour sample set, supporting previous results in this tumour type [91]. Despite this heterogeneity, we still observed significant changes in several key biomarkers, including CD31, MET receptor and FGF2. Arguably, the ability to detect significant changes in these biomarkers across a sample that is intrinsically heterogeneous, acts to further reinforce the significance of these changes.

There are several shortcomings to this work. The tissue originated from three different studies, although these studies were very similar in design. A decision was made to concentrate on matched tumour samples. While this allowed a direct comparison of pre- and post-treatment tissue, it potentially biased the sample set. Not all patients were able to have sequential tissue taken due to lack of excess tissue for sampling and patients coming off study. The tissue samples allowed us to investigate biomarker changes that occurred in conjunction with treatment in the presence of vessel density reduction. However, without time-matched controls it is possible that the observed increases in FGF-2, MET receptor and Ki67 are simply indicative of normal disease progression.

Efforts to understand resistance have been hampered by the lack of representative preclinical models. Moreover, the lack of suitable preclinical models has hampered drug development efforts to counteract the onset of acquired resistance. To investigate the potential efficacy of SRC inhibitors in anti-VEGF resistance a preclinical model of sunitinib resistance was developed. Initial attempts to develop a model based on the ACHN cell line were unsuccessful. Vehicle treated tumours were observed to have large necrotic centres surrounded by a limited amount of viable tumour. ACHN cells are VHL wild-type and so may not express as much VEGF ligand as xenografts based on VHL mutated cell lines such as A498 or 786-O. In line with this hypothesis, IHC staining for the vessel marker CD31 shows that ACHN had relatively low vessel density [Figure 3.7 (a) and (b)].

A498 tumours grew more successfully and responded well to sunitinib treatment. Unfortunately we could not generate a 'resistant model' because we failed to observe tumour re-growth [Figure 3.7 (c)].

In line with previously published work by Huang et al [39], all 15 786-O xenograft tumours initially responded to treatment leading to tumour regression. Furthermore, in 15 out of 15 tumours, re-growth in excess of 20% was observed in response to sustained sunitinib treatment. In the clinical setting a growth in excess of 20% would meet the threshold required to be classified as 'progressive disease' under RECIST criteria [33]. In contrast, Huang et al found that 3 out of 18 tumours failed to re-grow. These tumours were not considered to be resistant to sunitinib. In fact, the molecular profile of these 3 'sensitive' tumours were compared to the 'resistant' tumours to look for drivers of resistance. In their publication, Huang et al do not show growth trajectories prior to sunitinib treatment. Nor do they confirm that tumours were measured over time prior to treatment to increase confidence that any tumour regression observed could be attributed to treatment. In our protocol, to be included in the study, tumours needed to demonstrate consistent growth at 3 consecutive time-points prior to treatment onset. In this way, we hoped to avoid including tumours that simply did not 'take' properly. Tumours that don't 'take' properly may have a growth profile that could be confused with a sustained response to sunitinib i.e. tumours that fail to develop resistance.

This 786-O xenograft model forms the primary focus of the *in vivo* work contained in the next two chapters of this thesis. In Chapter 4 we use this model to investigate the use of SRC inhibitors to overcome resistance. In Chapter 5 we investigate what was driving resistance in the 786-O model and revert back to the RCC patient tissue samples to verify whether a similar process could be observed in the clinic.

Chapter 4:

Investigating the potential of SRC-TKIs in Renal Cell Carcinoma therapy

4.1 Introduction

Anti-angiogenic therapy has revolutionised the treatment of metastatic renal cell carcinoma (RCC). But while VEGFR-TKIs provide a significant clinical benefit, responsive patients inevitably relapse. A number of 'acquired resistance' mechanisms have been proposed, most prominently; (1) a renewed capability to induce angiogenesis and (2) the promotion of metastasis. SRC in best known for its role in the focal adhesion complex, a pathway is thought to play a central role in cell motility, adhesion and the metastatic process. In addition, published data, albeit in non-RCC tumour models, suggests that SRC kinase can regulate pathways involved in angiogenesis. Consequently the addition of a SRC kinase inhibitor to VEGFR-TKI therapy may provide a rational combination.

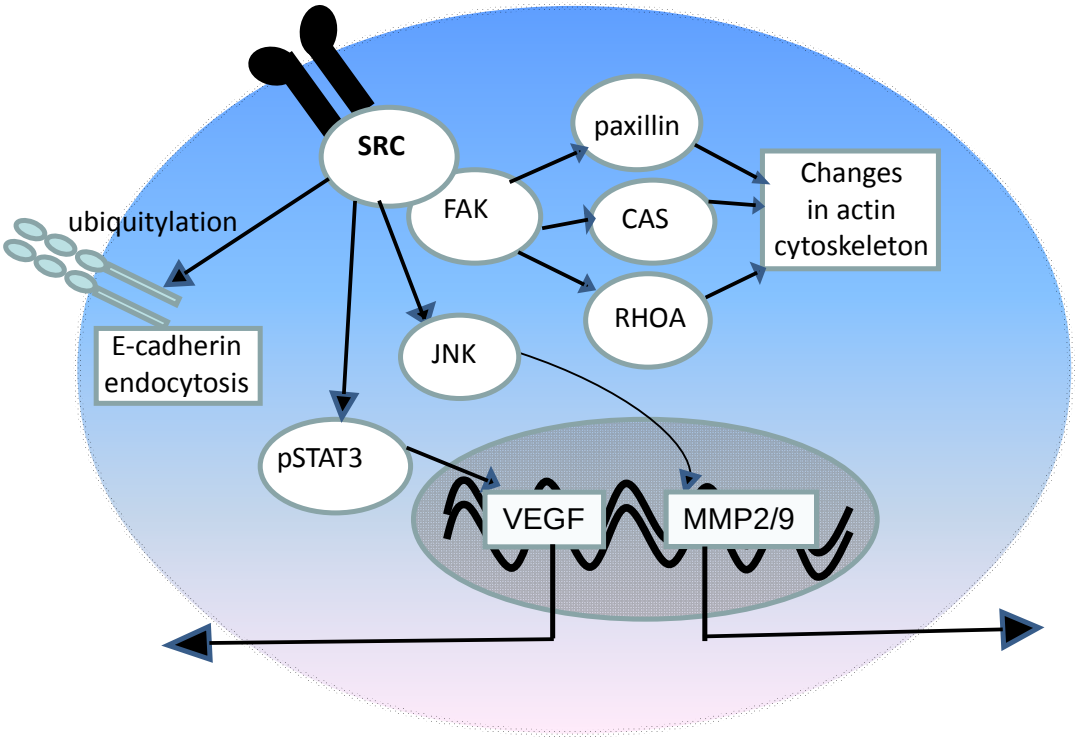

Figure 4.1: SRC is thought to be central to a number of pathways involved in metastasis and angiogenesis.

4.2 Aims of chapter

The work presented in this chapter investigates the effect of the SRC kinase inhibitors saracatinib and dasatinib in various preclinical models. The ultimate goal was to establish whether the addition of SRC kinase inhibitors to VEGFR-TKI therapy could provide a rational combination, but SRC kinase inhibition as monotherapy was also investigated. Treatment effect on cell viability and migration was investigated *in vitro*, before moving into the 786-O xenograft model. Using this xenograft model the effect of SRC inhibition on apoptosis, proliferation and angiogenesis were investigated. Furthermore, the effect on gene expression was analysed in an effort to better understand the mechanism of action on the observed anti-tumour effect.

4.3 Results

4.3.1 Cell line selection for functional assays

Prior to undertaking functional studies, a panel of 12 cell lines was characterized for SRC expression and activity levels. Auto-phosphorylation of residue Y419, located in the kinase domain, is required for full activity and has been proposed as a biomarker for SRC-TKI efficacy [92]. Conversely, SRC can be negatively regulated by phosphorylation at residue Y530, which causes the protein to lock into a closed structure with the kinase domain inaccessible [93].

Cell lysates from the cell line panel were probed for total SRC protein, SRC phosphorylated at residue Y419 and SRC phosphorylated at Y530. All cell lines expressed SRC protein, but there was a significant difference in the phosphorylation status of the different cell lines. Four well-characterised cell lines were chosen for future functional studies, A498, ACHN, 786-O and Caki-1. As figure 4.1 (a) shows these cell lines had quite different phosphorylation profiles with the ACHN cell line having very little SRC protein phosphorylated at the Y530 site, which renders the protein inaccessible and inactive. Whereas the A498 cell line showed a comparatively high proportion of protein phosphorylated at Y530 and less auto-phosphorylation of the Y419 residue.

4.3.2 The effect of dasatinib on SRC kinase activity

Initial in vitro functional studies were conducted using the commercially available SRC TKI, dasatinib (cell viability assays were repeated using the SRC inhibitor saracatinib, which was donated by AstraZeneca, prior to conducting any xenograft studies). Dasatinib is an orally active small molecule shown to be a dual SRC / Abl TKI[62]. The drug was developed, primarily, as a second line treatment for the treatment of chronic myelogenous leukemia (CML) [59]. CML is associated with the t(9;22) chromosomal translocation, which generates the oncogenic BCR-ABL fusion gene. More recently, the potential of dasatinib to

inhibit metastasis has been investigated through its inhibition of SRC kinase [94]. We confirmed dasatinib's ability to inhibit SRC kinase activity in our panel of 4 RCC cell lines before proceeding with functional assays. Figure 4.1 (b) indicates that dasatinib reduced phosphorylation of the Y419 residue, in a dose-dependent manner. Compared to the other cell lines, dasatinib seemed more capable of reducing SRC activity of the ACHN cell line at the lowest dose level investigated (10 nm).

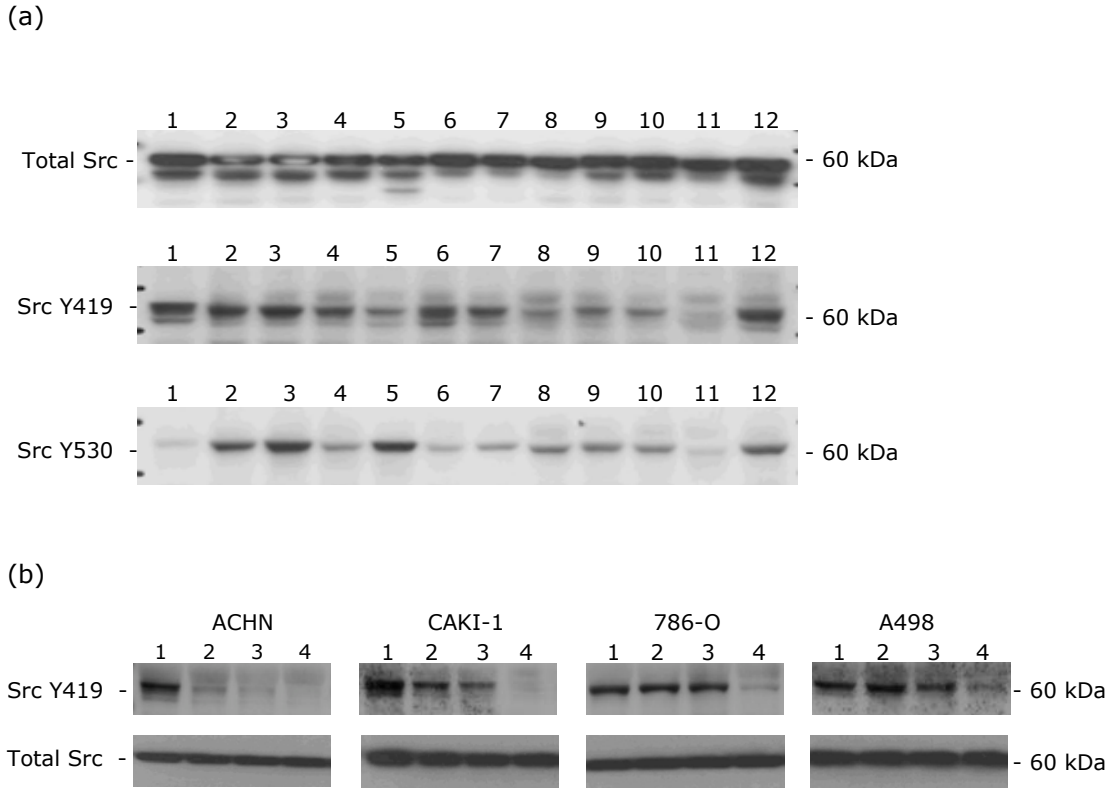

Figure 4.2: **Characterisation of SRC protein levels and phosphorylation status in a panel of 12 RCC cell lines and the effect of dasatinib on SRC activity on 4 cell lines chosen for functional assays.** Panel (a) shows the result of 12 cell lines probed for total SRC and phosphorylated SRC-Y419 by western blot. The cells probed were (1) ACHN (2) CAKI-1 (3) CAKI-2 (4) CAL54 (5) A498 (6) 786-O, 769-P, RCC6, RCC7, RCC12, RCC38 and RCC42. Panel (b) demonstrates the effect of dasatinib on the SRC kinase activity on 4 cell lines chosen for functional assays. Lysates were harvested 6 hours after adding (1) 0nM (2) 10nM (3) 50nM or (4) 250nM of dasatinib.

4.3.3 The effect of dasatinib on cell viability

To determine the effect of dasatinib on cell viability an MTS assay was performed treating cells for both 24 and 72 hours. Figure 4.3 (a) shows the impact of dasatinib on cell viability after 72 hours of dasatinib treatment. A498 appeared the most resistant to treatment with ACHN the most sensitive cell line [Figure 4.3 (a)]. A similar pattern was seen at 24 hours (data not shown).

Cell viability assays were also carried out using an alternative SRC inhibitor, saracatinib. Again, a similar pattern was seen with A498 was the most resistant to treatment, followed by 786-O with the drug having the most impact on ACHN cell viability (data not shown).

It was noted that the two VHL -/- cell lines A498 and 786-O were the most resistant cell lines. Given the high prevalence of VHL mutation in RCC, further experiments were conducted to determine whether the loss of functional VHL could promote resistance to SRC inhibitors.

We hypothesised that if VHL mutation was conferring resistance, it may be through reduced degradation the HIF (hypoxia-inducible factor) transcription factors. Therefore, by stablising HIF transcription factors in VHL wild-type cells we hypothesized resistance would occur. Efforts were made to stablilise HIF both with the use of a hypoxia incubator (oxygen was set to 1%) and with a pharmacological agent (dimethyloxalylglycine). Western blots showed successful stabilisation by these methods, but the lack of oxygen and treatment effects resulted in a significant loss in cell viability making it impossible to test whether HIF stabilisation promoted resistance (data not shown).

Consequently we used the RCC4 VHL +/- isogenic cell line to test our hypothesis. We compared the effect of dasatinib treatment on stably transfected RCC4 cell lines expressing vector alone (RCC4) or wild-type VHL (RCC4 + VHL-WT). As shown in Figure 4.3 (b), VHL loss did promote resistance to dasatinib confirming out hypothesis.

(a)

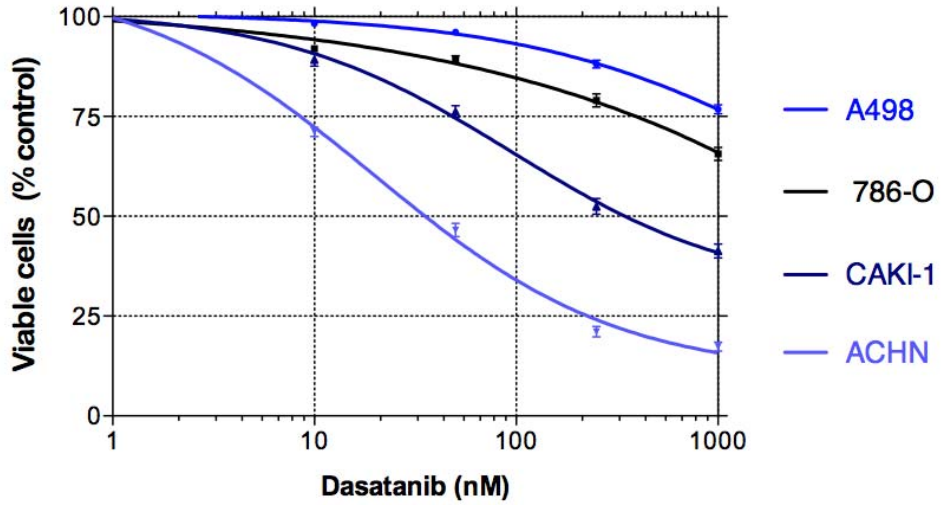

(b)

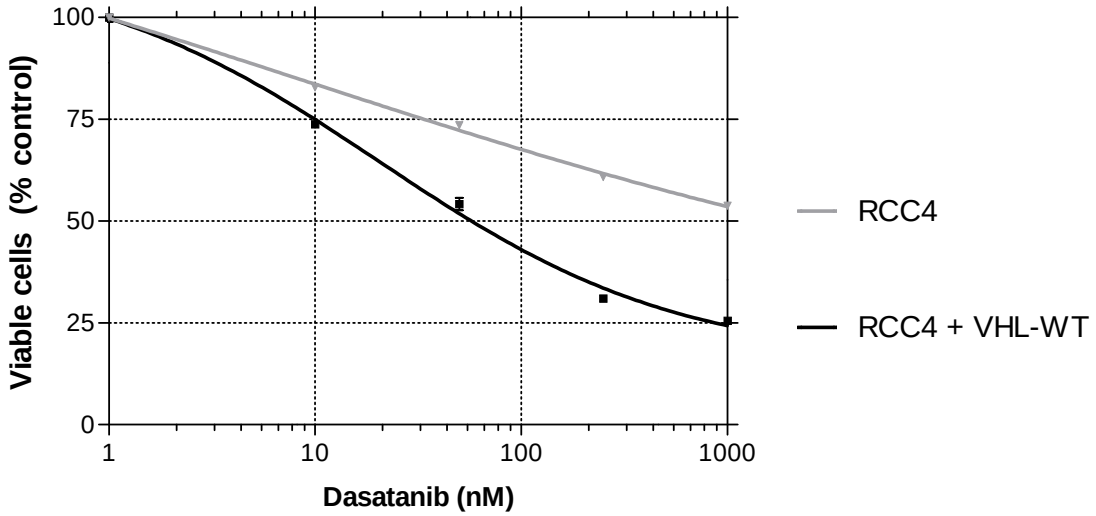

Figure 4.3: The effect of dasatinib on cell viability. Panel (a) compares the treatment effect on four cell lines. Panel (b) demonstrates that VHL loss promotes resistance in the isogenic VHL+/- RCC4 cell line. In both experiments, cells were seeded at 3-6 x 10^3 cells per well on 96-well plates and cultured in 100ul of RPMI-media overnight. The following day, 100ul of dasatinib was added to achieve a range of final concentration between 0uM and 1uM. Cell viability was determined at 72 hours following the manufacturer's protocol (MTS assay, Promega).

4.3.4 The effect of dasatinib of cell motility and migration

SRC inhibitors have demonstrated the ability to reduce cell motility using cell lines originating from several different tumour types. To confirm that SRC inhibitors could reduce motility of RCC cells in vitro, all four cell lines were plated into 6 well plates and incubated until cells were more than 90% confluent (24-48 hours). A scratch was made in each well and an image taken. Media was replaced with media containing 10nM, 50nM, 250nM of dasatinib. A well with no dasatinib added was used as a control. Assays were performed in triplicate. After 18 hours incubation a further image was taken and the distance between the cells where the original scratch took place was observed. In all 4 cell lines a visible difference in the migration rate could be seen at the 10nM dose level when compared to control wells. A representative image showing the effect on 50nM can be seen below. Similar experiments were performed with the SRC inhibitor saracatinib generating similar results (data no shown).

To better quantify the effect of SRC inhibition on migration, transwell migration assays were performed. Media containing 5% serum was used as the chemo-attractant agent. As figure 4.4(b) shows, dasatinib reduced cell migration in a dose-dependent manner in all RCC cell lines tested. The reduction in migrated cells reached statistical significance ($p<0.01$) at 50nM and above in all cell lines, but only ACHN reached statistical significance at the 10nM dose level.

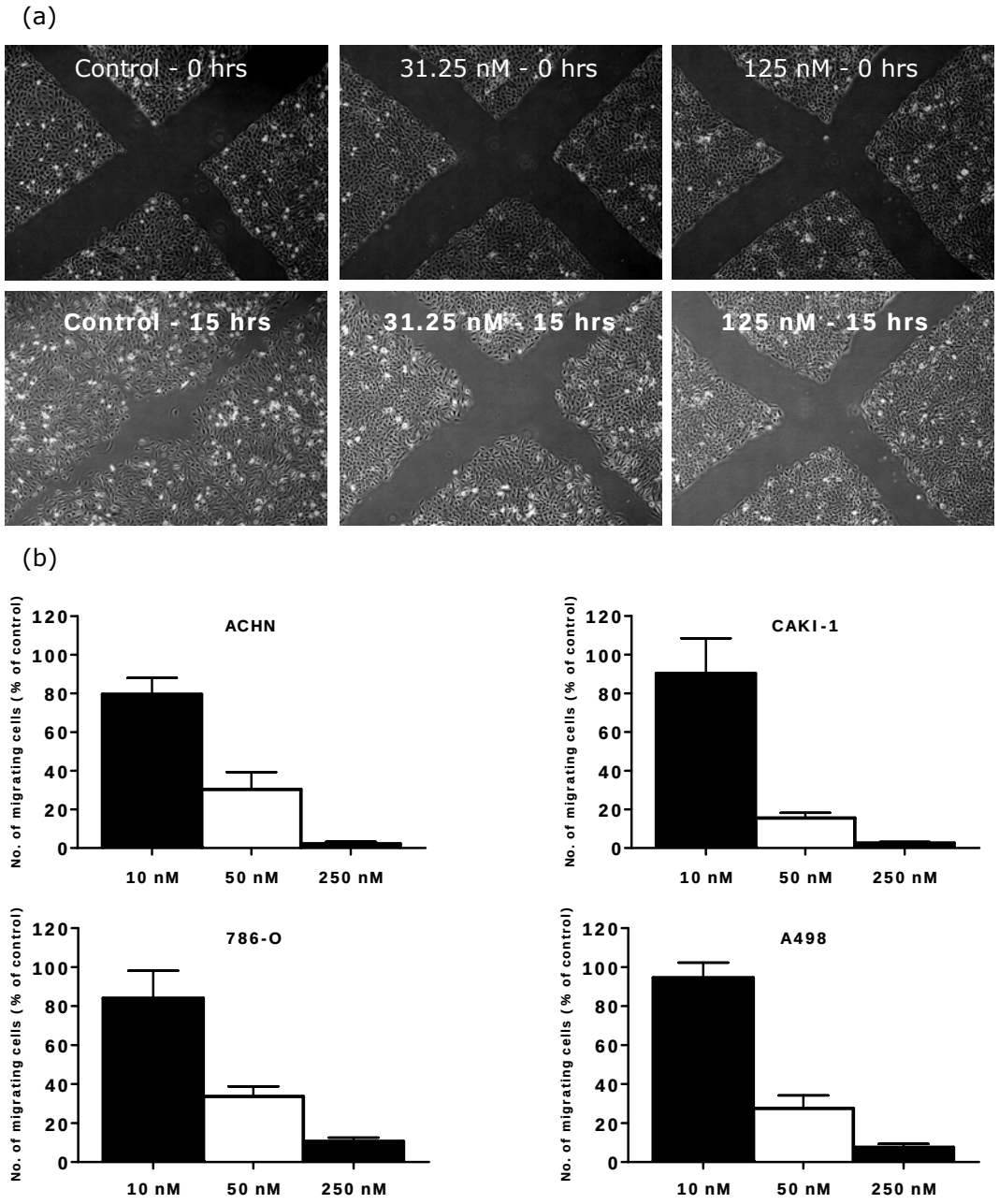

Figure 4.4: The effect of dasatinib cell migration. Panel (a) shows a representative image of a scratch assay. 7.5 x 10^4 cells per well were plated and incubated for 24-48 hours until cells were confluent. A cross was scratched into the monolayer using a 1ml pipette tip, cell washed in PBS and media replaced with containing 50nM dasatinib or 0nM dasatinib (control). A further image was taken 18 hours later to measure dynamic changes in cell migration. Panel (b) shows the results of transwell assays (n=3) performed on the four cell lines. Briefly, 2.5 x 10^5 cells per added to each transwell and incubated for 3 hours to allow cells to adhere to the transwell membrane. Media was removed before 200ul of serum-free media containing 0-250ul of dasatinib was added to the upper chamber of the transwell. The lower chamber contained, 500ul of media, containing the same concentration of dasatinib as the upper chamber, with the addition of 5% fetal calf serum. Cells were allowed to migrate towards serum for 18 hours before being, fixed, stained with haematoxylin and counted.

4.3.5 Saracatinib effects biomarkers of the focal adhesion complex and phospho-STAT3 in the 786-O xenograft model

The 786-O model was used to investigate the effect of SRC inhibitors on pharmacodynamic biomarkers *in vivo*. For this purpose, a short-term chronic dose study (once-daily dosing for 4 days) was conducted. SRC inhibitor monotherapy (saracatinib) and its combination with the VEGFR-TKI cediranib was investigated.

786-O xenografts were established in the flank of SCID mice into one of 4 groups; vehicle, saracatinib monotherapy, cediranib monotherapy or the combination of saracatinib and cediranib (n = 7 for the vehicle group and n= 5 for all other treatment groups). Tissue was harvested 3 hours after the final dose.

At 25mg/kg, saracatinib visibly reduced the phosphorylation of FAK and paxillin, both key players in the focal adhesion complex and known downstream targets of SRC [Figure 4.1 (a)-(b)].

Phospho-STAT3 is also thought to be regulated by SRC and through this interaction regulate the expression of VEGF [95]. Saracatinib significantly down-regulated phospho-STAT3 ($p<0.01$ [Figure 4.5 (c)] Although sunitinib has been suggested to reduce STAT3 phosphorylation [96] [65], we could find no evidence of this [Figure 4.5 (c)].

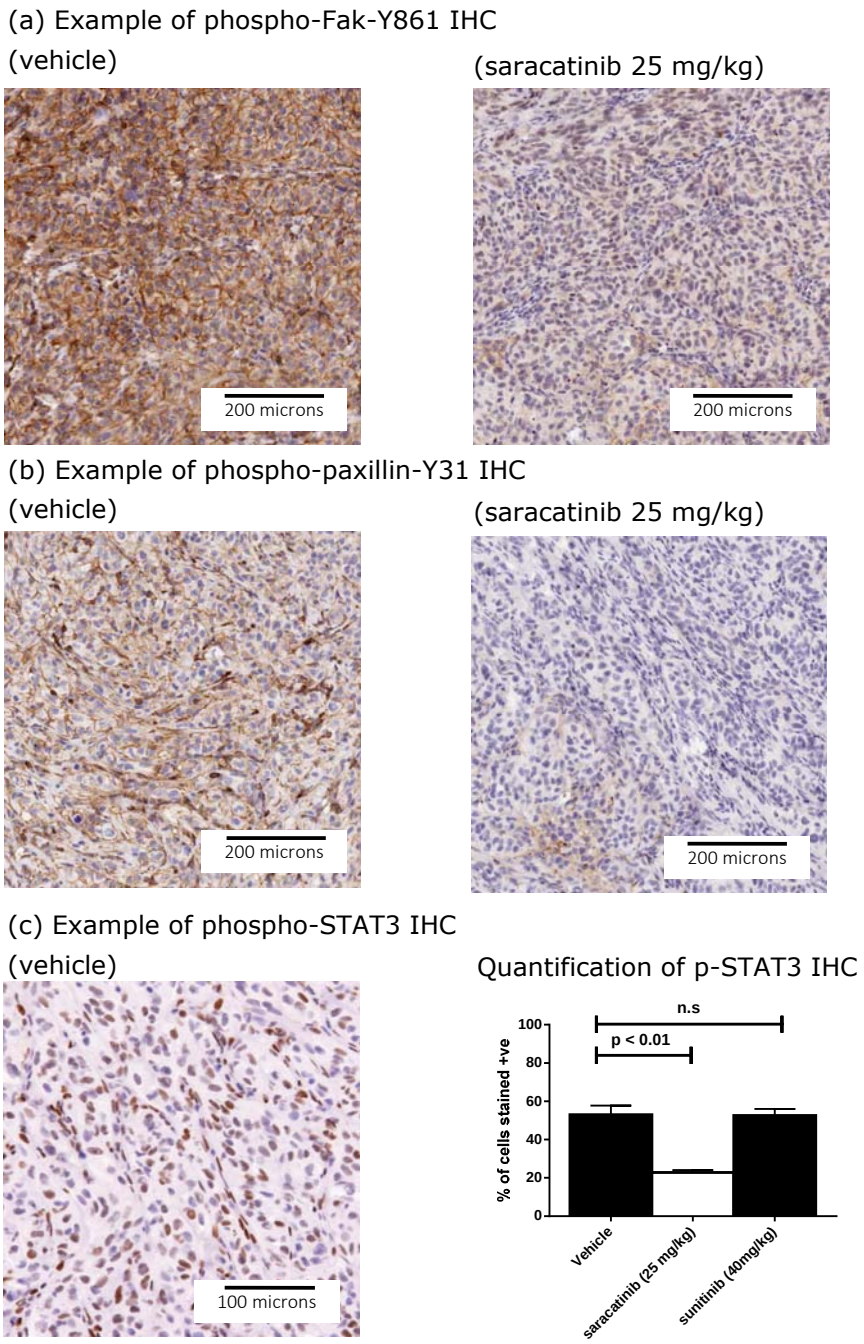

Figure 4.5: The effect of saractinib on pharmacodynamic biomarkers. Panel (a) and (b) are representative examples of the effect of SRC inhibition on the activity of the focal adhesion complex proteins FAK and paxillin respectively. Panel (c) shows an example of phospho-STAT3 IHC staining and the resulting quantification using image analysis software. Saracatinib significantly down-regulated phospho-STAT3 ($p<0.01$).

4.3.6 Saracatinib decreases VEGF gene expression but this does not affect vessel density

SRC is thought to regulate VEGF ligand expression through its interaction with STAT3 [95]. We hypothesized that by reducing STAT3 activity [Figure 4.5 (c)] SRC inhibitors could decrease VEGF expression and so reduce vessel density.

In line with our hypothesis, Figure 4.6 (a) shows that VEGF-A gene expression was significantly reduced, both in the tumour and host compartments. However, this did not translate into a significant change in vessel density [Figure 4.6 (c)].

In addition to saracatinib monotherapy, the effect of saracatinib / cediranib (VEGFR-TKI) combination therapy was investigated. Cediranib monotherapy significantly increased the expression of VEGF and MMP2 in the host [Figure 4.6 (b)]. As suggested by previous studies, saracatinib monotherapy significantly reduced the expression of both genes, further supporting our hypothesis that the addition of a SRC inhibitor to anti-angiogenic therapy may provide a rational combination. However, when combined with cediranib, rather than reducing gene expression (compared to cediranib monotherapy) saracatinib exacerbated the up-regulation ($p<0.01$).

Staining for CD31 revealed that there was a trend in favour of reduced vessel density in the combination arm but this did not reach statistical significance [Figure 4.6 (c)].

(a) Effect of saracatinib treatment on VEGF expression

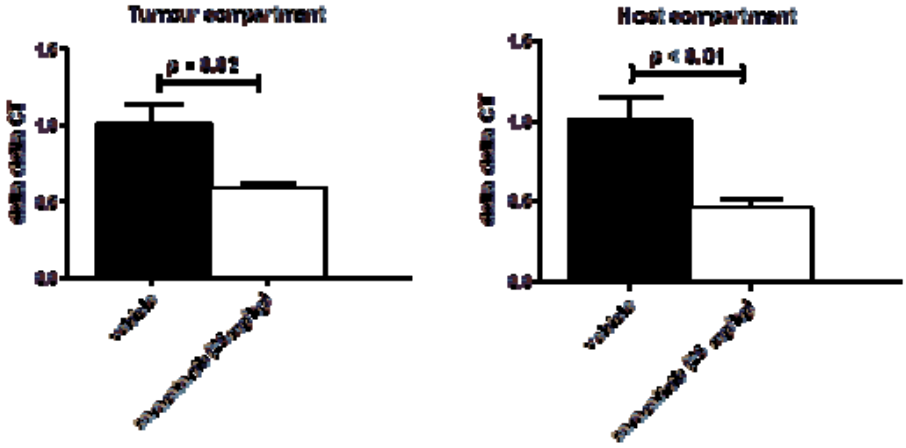

(b) Effect of saracatinib monotherapy and combination therapy on gene expression

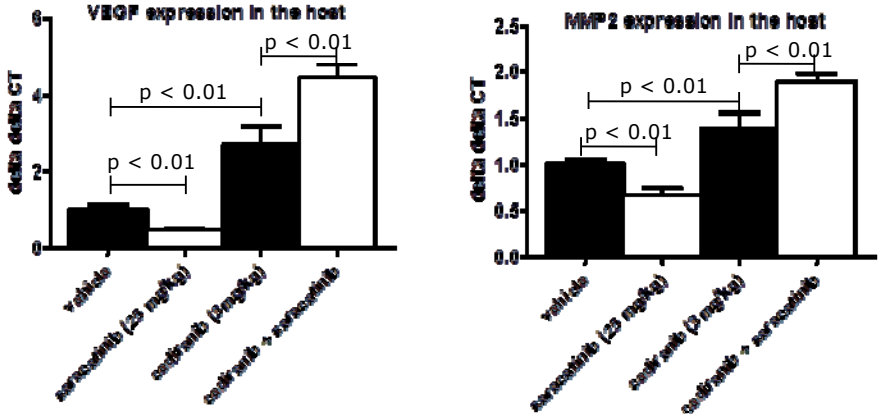

(c) Effect of saracatinib monotherapy and combination therapy on vessel density

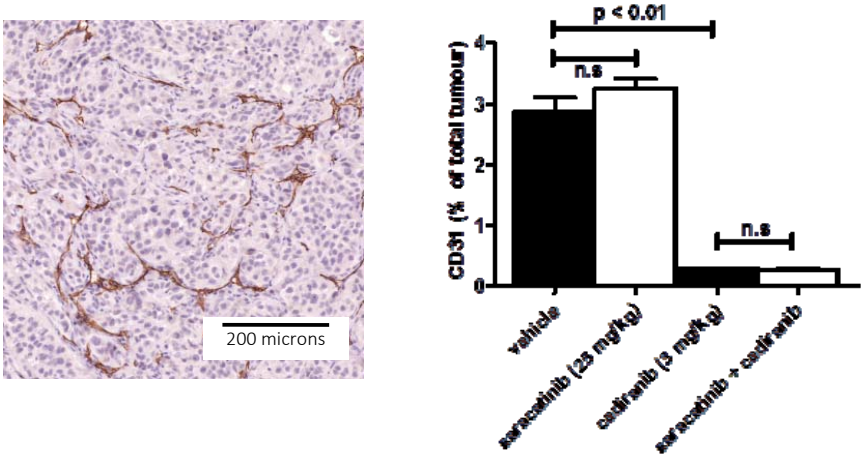

Figure 4.6: The effect of saracatinib on VEGF expression and vessel density: Panel (a) shows the effect of saracatinib on VEGF expression. Panel (b) shows the effect of saracatinib monotherapy and combination therapy on gene expression and panel (c) shows treatment effect on vessel density (measured at Day 4).

4.3.7 The effect of saracatinib treatment on cell viability and proliferation in vivo

To test whether saracatinib monotherapy, or its combination with cediranib effected cell viability or proliferation, treated tissue (4 days) was stained for cleaved caspase 3 and Ki67 and compared with controls.

Neither saracatinib, cediranib nor the combination had any effect on Ki67 levels, indicating no treatment effect on proliferation [Figure 4.7 (a)].

Saracatinib monotherapy did not have a significant effect on cleaved caspase 3 expression indicating treatment had no effect on the proportion of apoptotic cells [Figure 4.7 (b)]. Staining indicated that cediranib did significantly increase the proportion of apoptotic cells ($p<0.01$). The addition of saracatinib to cediranib further increased the proportion of apoptotic cells, but the increase did not reach statistical significance.

Although the effect didn't reach statistical significance, the trend in favour of increased apoptosis in the combination, together with previous data showing that saracatinib could decrease STAT3 activity [Figure 4.5 (c)] led us to further investigate a potential synergistic mechanism of action for the combination therapy. STAT3 is thought to regulate the expression of the several anti-apoptotic genes including BCL-X_L and BCL-2. We hypothesised that if saracatinib was down-regulating these anti-apoptotic genes, it could increase the ability of cediranib to induce the apoptosis seen in the monotherapy. PCR was conducted to look for evidence of this potential mechanism of action. We found no significant change in the level of BCL-X_L or BCL-2 expression level in treated tumours (data not shown).

(a) Effect of saracatinib treatment on proliferation

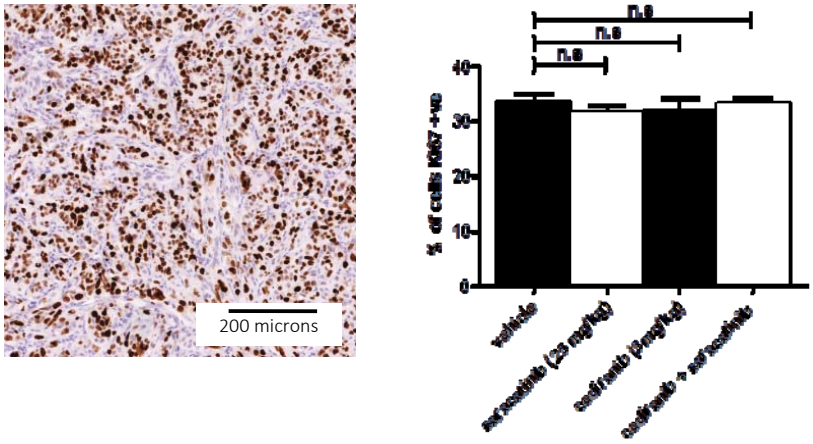

(b) Effect of saracatinib treatment on apoptosis

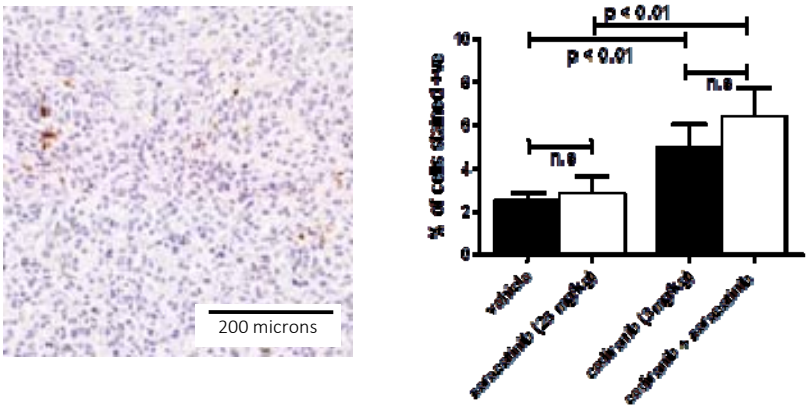

Figure 4.7: The effect of saracatinib on cell viability and proliferation in 786-O xenografts: Tissue taken after 4 days of treatment was stained for Ki67 (panel a) and cleaved caspase 3 (panel b) to investigate the effect on proliferation and apoptosis respectively.

4.3.8 Saracatinib reduces tumour growth both as monotherapy and in combination with the VEGFR-TKI cediranib

To investigate the effect of the respective monotherapies and combination treatment on tumour growth, mice were inoculated with 786-O cells and tumours measured twice weekly with calipers until they reached palpable size. To qualify for the study, tumours needed to have recorded volume growth on both of the two prior measurement days before randomisation.

Animals were randomised into one of 4 treatment groups (n = 12); the SRC inhibitor saracatinib at 25 mg/kg, the novel anti-VEGF cediranib at 3mg/kg, a combination of the two drugs (25mg/kg + 3mg/kg) or vehicle. Randomisation date occurred on day 30 – at that stage tumour volumes ranged from 0.2-0.8 cm^3. All drugs and vehicle were administered once daily by oral gavage. The effect on tumour growth can be seen in Figure 4.8 (a).

All therapeutic arms significantly slowed tumour growth versus vehicle (saracatinib $p < 0.05$, cediranib and the combination $p < 0.01$). Furthermore combination therapy achieved tumour regression, as opposed to just slowing tumour growth. Combination therapy was significantly more effective than either monotherapy ($p < 0.01$).

We were most interested in investigating the potential benefits of SRC inhibitors in tumours that had acquired a 'resistant' phenotype. As shown previously [Figure 3.7], in our hands 100% of sunitinib-treated 786-O xenografts demonstrated a growth rebound after initial regression. 30 mice were treated with 40 mg/kg sunitinib for 22 days. Mice were randomised into one of two arms at Day 22; (1) cediranib at 3mg/kg or (2) cediranib plus saracatinib at (3mg/kg + 25mg/kg). Again combination treatment was more effective than cediranib monotherapy ($p < 0.01$). In contrast to treatment naïve xenografts, combination therapy was not able to induce tumour regression in tumours pre-treated with sunitinib.

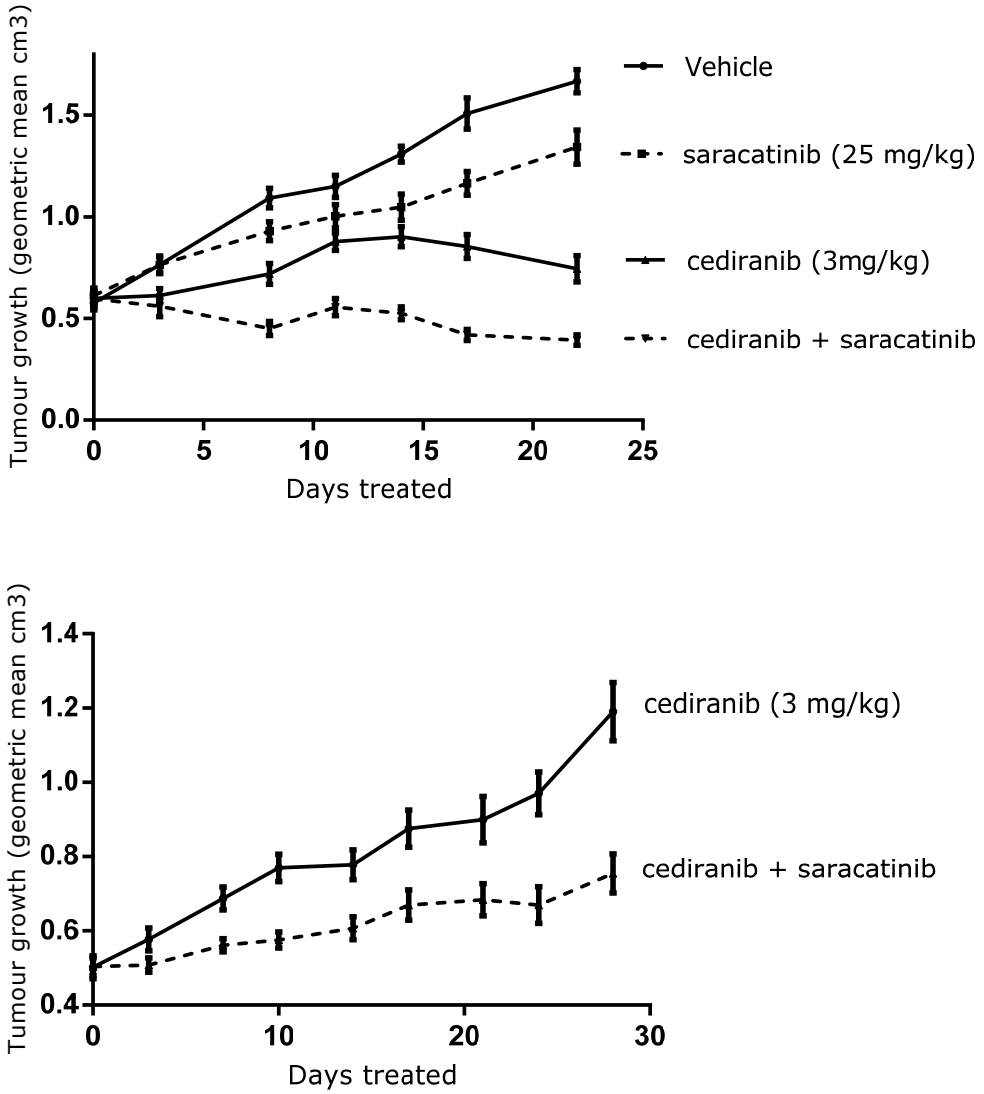

Figure 4.8: The anti-tumour effect of saracatinib monotherapy and in combination with the anti-VEGF drug cediranib: Panel (a) shows the effect of therapy in treatment naïve xenografts. Animals received saracatinib 25 mg/kg, cediranib 3mg/kg a combination of the two drugs (25mg/kg + 3mg/kg) or vehicle once daily by oral gavage (n=12). Tumour volumes represent the geometric mean of the treatment group (n=12). Error bars represent SEM. Panel (b) shows the effect of different therapy in xenografts pre-treated with 40 mg/kg sunitinib for 22 days. Animals were then treated with cediranib 3mg/kg a combination of saracatinib and cediranib (25mg/kg + 3mg/kg) by oral gavage (n=15).

4.4 Discussion

SRC has been shown to regulate a number of pathways involved in tumourgenesis [54]. SRC protein expression and activity has been shown to correlate with progression and site-specific metastasis in several different tumour types [97] [98] [55] [99]. SRC inhibition has been shown to reduce cell motility and growth in multiple disease-specific preclinical models [100] [101] [102]. Furthermore, SRC inhibitors have been shown to act synergistically with other treatment modalities [103] [104]. A 'test panel' of 4 cells lines was selected to investigate the effect of SRC inhibitors in preclinical models of RCC both as a monotherapy and as combination therapy in conjunction with anti-VEGF treatment.

MTS assays demonstrated that the SRC inhibitors dasatinib [Figure 4.3 (a)] and saracatinib (data not shown) affected RCC cell viability. The size of this effect varied greatly between the different cell lines. Previous work highlights the potential of VHL mutation to promote drug resistance through either the NF-Kβ or HIF-alpha pathway [105] [106]. Based on the observation that treatment effect correlated with VHL status in the four cell lines tested, we hypothesized that VHL loss was promoting resistance to SRC TKI treatment.

Initial studies to investigate this hypothesis used either a hypoxic incubator or small molecule HIF-stabilising agents to stabilize HIF in VHL wild-type cells (data not shown). Interpreting the results of these studies was confounded by the effect of hypoxic conditions (or stabilizing agents) on cell growth. However, the use of the RCC4 VHL+ / VHL- isogenic cell lines demonstrated that VHL was promoting resistance to dasatinib [Figure 4.3 (b)] and saracatinib (data not shown). This result has subsequently been corroborated by another group using two different VHL+/ VHL- isogenic cell lines of RCC origin, ACHN and SN12C [107].

Transwell migration assays and scratch assays confirmed the ability of SRC inhibitors to reduce the motility and migration of all RCC cell lines tested [Figure 4.4]. This effect was observed in all cell lines at a dose level (10nm) that precluded any treatment effect on cell viability being the primary driver for the observed decrease in cell migration. Metastasis has been proposed as a key

mechanism of resistance to anti-VEGF treatment [40] [41]. The confirmation that SRC inhibitors decrease migration of RCC cell lines highlights the potential for a potential synergistic combination with anti-VEGF treatment.

A major limitation of our work is that we did not test the potential benefit of SRC inhibition in a preclinical model of anti-VEGF-induced metastasis. Instead, we focused our animal studies a resistance model characterized by growth rebound of the primary tumour.

By replicating previous work by Huang et al [39] we developed a preclinical model of sunitinib resistance [Figure 3.7]. In their paper Huang et al described a model of renewed angiogenesis driven by up-regulation of IL-8. SRC has been implicated as a key mediator of IL-8 expression in a number of cell lines suggesting SRC inhibition may impact this resistance mechanism in the 786-O model [108] [60] [109]. In addition, SRC has been implicated in the regulation of VEGF expression [110] [111] [95]. Finally, recent work has suggested that SRC inhibitors can directly affect migration and survival of endothelial cells thereby reducing angiogenesis [58]. Taken together, these results suggest the addition of a SRC inhibitor to anti-VEGF therapy may delay or prevent renewed angiogenesis in the 786-O preclinical model.

Saracatinib was able to significantly reduce phospho-STAT3 levels in the 786-O xenograft [Figure 4.5 (c)]. Moreover, saracatinib treatment reduced VEGF gene expression in both the tumour and host compartments [Figure 4.6 (a)]. However, the observed VEGF reduction did not translate into a significant reduction in vessel density when compared to time-matched controls [Figure 4.6 (c)]. Another key limitation to our work is the reliance on one timepoint (tissue was taken 3 hours after the Day 4 dose) to analyze vessel density, gene expression and other biomarkers by IHC. VEGF gene expression investigated 3 hours after dosing may not be reflective of the treatment effect over the course of treatment.

The anti-VEGF drug cediranib was used to investigate the potential synergy of adding a SRC inhibitor to anti-angiogenic therapy. The addition of saracatinib to the anti-VEGF drug cediranib failed to significantly reduce vessel density beyond that observed with cediranib monotherapy [Figure 4.6 (c)]. It should be noted

that cediranib monotherapy reduced vessel density by approximately 90% which arguably left little scope for a further improvement in vessel density reduction after just 4 days of treatment. Interestingly, while saracatinib monotherapy showed a treatment-induced reduction in VEGF and MMP2 gene expression, when comparing gene expression in combination treated tumours to cedarinib monotherapy-treated tumours, expression of these two pro-angiogenic genes was significantly increased in the combination arm [Figure 4.6 (b)].

As Figure 4.8 shows, extended treatment with saracatinib lead to a significant reduction in 786-O xenograft growth when compared to control treated tumours. IHC analysis did not reveal the mechanism of action. We could find no evidence for increased apoptosis or reduced proliferation in the saracatinib arm [Figure 4.7].

The primary focus of this work was to investigate the potential of SRC inhibition in combination with anti-VEGF treatment. As Figure 4.7 shows, when combined with cediranib, saracatinib did provide an additive benefit. Again, IHC analysis did not provide a definitive mechanism of action for this effect. Ki67 was not significantly different between combination treatment and the cedarinib monotherapy arms. Cedarinib significantly increased apoptosis compared to vehicle treated tumours and combination therapy further increased the number apoptotic cells, but the effect did not reach statistical significance. Conceivably, the ability of cediranib to induce apoptosis may be enhanced by saracatinib's ability to reduce STAT3 activity. In addition to regulating VEGF expression, up-regulation of the STAT3 pathway has been shown to promote anti-apoptotic gene expression [112] [113]. Similarly inhibition of STAT3 has been shown to sensitize cells to pro-apoptotic signals, reducing drug resistance [114] [115]. Further investigation of this potential synergistic mechanism of action is warranted.

In the final study 786-O xenografts were pre-treated with sunitinib until all tumours displayed a 'resistant' phenotype i.e. tumours were growing in response to continuous sunitinib treatment having initially regressed in response to treatment. Tumours were randomized to either cediranib monotherapy or combination therapy. Tumours receiving combination therapy grew less rapidly than cediranib monotherapy tumours. However, even tumours receiving combination therapy could not be prevented from growing suggesting the

molecular mechanisms driving tumour resistance to anti-VEGF therapy could not be completely overcome by the addition of the SRC inhibitor [Figure 4.8]. Chapter 5 investigates the potential mechanisms of acquired resistance in the 786-O xenograft. Several pro-angiogenic genes were upregulated in response to sunitinib treatment including FGF-2, MET receptor and PGF. A retrospective analysis found that the addition of saracatinib to cediranib did not affect gene expression of any of these alternative pro-angiogenic factors.

There are a number of shortcomings with the work contained in this chapter. Firstly, xenograft work was based on one tumour model with tissue taken at one timepoint. Although the addition of the SRC inhibitor seemed to improve efficacy compared to anti-VEGF monotherapy, biomarker analysis provided little insight into the mechanism of action. Nevertheless, we did show that VHL mutation can promote resistance to the direct effect of SRC inhibitors on RCC cell viability. Furthermore, we showed saracatinib was capable of inhibiting STAT3 activation in an animal model, highlighting one potential mechanism by which SRC inhibitors may synergize with anti-angiogenic therapy. Further work is warranted to explore these preliminary observations. In particular, biomarker analysis using patient tissue from an ongoing study investigating cediranib plus saracatinib in sunitinib-resistant patients may provide insight into whether VHL status or baseline levels of STAT3 activation have any impact on treatment response.

Chapter 5:

Using the 786-O xenograft model to investigate VEGF-TKI resistance in Renal Cell Carcinoma

5.1 Introduction and aims of chapter

Xenografts have frequently been used to investigate mechanisms of angiogenesis and the interaction of tumour cells with their microenvironment. Unfortunately the majority of these xenograft models don't accurately reflect the clinical reality of renal cancer. The majority of RCC patients initially benefit from anti-angiogenic therapy, but inevitably these tumours develop a resistant phenotype over the course of treatment. A model that more accurately reflects this pattern of acquired resistance could provide a useful research tool.

Huang et al used 3 different RCC xenograft models that displayed some capability of tumour regrowth, after initially responding to sunitinib treatment [39]. In A498 and SN12C xenograft models a minority of tumours developed a resistant phenotype. In contrast, the majority of 786-O tumours (15 out of 18) were capable model capable developing a resistant phenotype when exposed to continuous sunitinib treatment. By examining plasma taken at study end, the authors went on to show that IL-8 was higher in 786-O xenografts demonstrating a resistant phenotype (n=15) than xenografts that continued to show sensitivity (n=3). Further experiments showed that blocking IL-8 had some therapeutic benefit to these 15 resistant tumours.

In line with Huang et al we demonstrated that 786-O xenografts are capable of developing a resistant phenotype under continuous therapy, whereas no A498 xenografts showed any evidence of tumour regrowth when the study was terminated (Figure 3.7). The majority of work contained in this chapter aims to better characterise the drivers of resistance in the 786-O xenograft model.

Tissue was taken at three timepoints; Day 4, Day 22 and Day 57. At Day 4 tumours had not yet developed resistance to sunitinib treatment. Tissue taken at this timepoint was used to perform pharmacodynamic studies to better understand sunitinib's mechanisms of action. Experimental techniques included IHC staining of tumour tissue, flow cytometry to investigate the effect on the myeloid cells and PCR to investigate gene expression on the tumour and host compartments.

By Day 57 tumour growth had rebounded in all cases. By comparing biomarkers at Day 4 with tissue taken at later timepoints, we show that dynamic changes occurred in gene expression in both the tumour compartment and the host. Vessel density showed a modest rebound in resistant tumours and collagen deposition increased in treated tumours by the later timepoints.

Finally, tumour tissue taken from RCC patients was used to examine whether the xenograft observations are representative of processes occurring in the clinical setting.

5.2 Results

5.2.1 Pharmacodynamic study investigating sunitinib in the 786-O xenograft model

Prior to any work investigating resistance mechanisms, a pharmaco-dynamic study was performed using tissue taken after 4 days treatment with sunitinib or vehicle. Tissue taken at 4 days was not necrotic allowing entire sections to be examined by IHC.

IHC was performed to examine CD31 a tumour vessel marker. CD31 protein was specific for tumour vessels [Figure 5.1 (b)] enabling computer-aided quantification of vessel density, using visually-trained parameters. Vessel density was defined as the percent of total tissue stained positive for CD31 protein. By Day 4 vessel density was 90% lower in sunitinib treated tumours when compared to time-matched vehicle treated controls [Figure 5.1 (b)]. Mean vessel density was 2.85% in vehicle-treated tumours vs 0.28% in the sunitinib arm ($p<0.01$).

Sunitinib increased cleaved caspase 3 significantly [Figure 5.1 (c)] indicating an increase in the number of cells undergoing apoptosis. The proliferation index, defined as the proportion of cells staining positive for Ki67, also increased significantly in sunitinib-treated tumours.

While vessel reduction and the increase in apoptotic cells could help explain the observed effect of sunitinib on tumour size, an increase in the proliferation index was not expected. Furthermore, this result was observed in tissue taken after 4 days of treatment, prior to development of a resistance phenotype. This result was further investigated and details can be found in section 5.2.3.

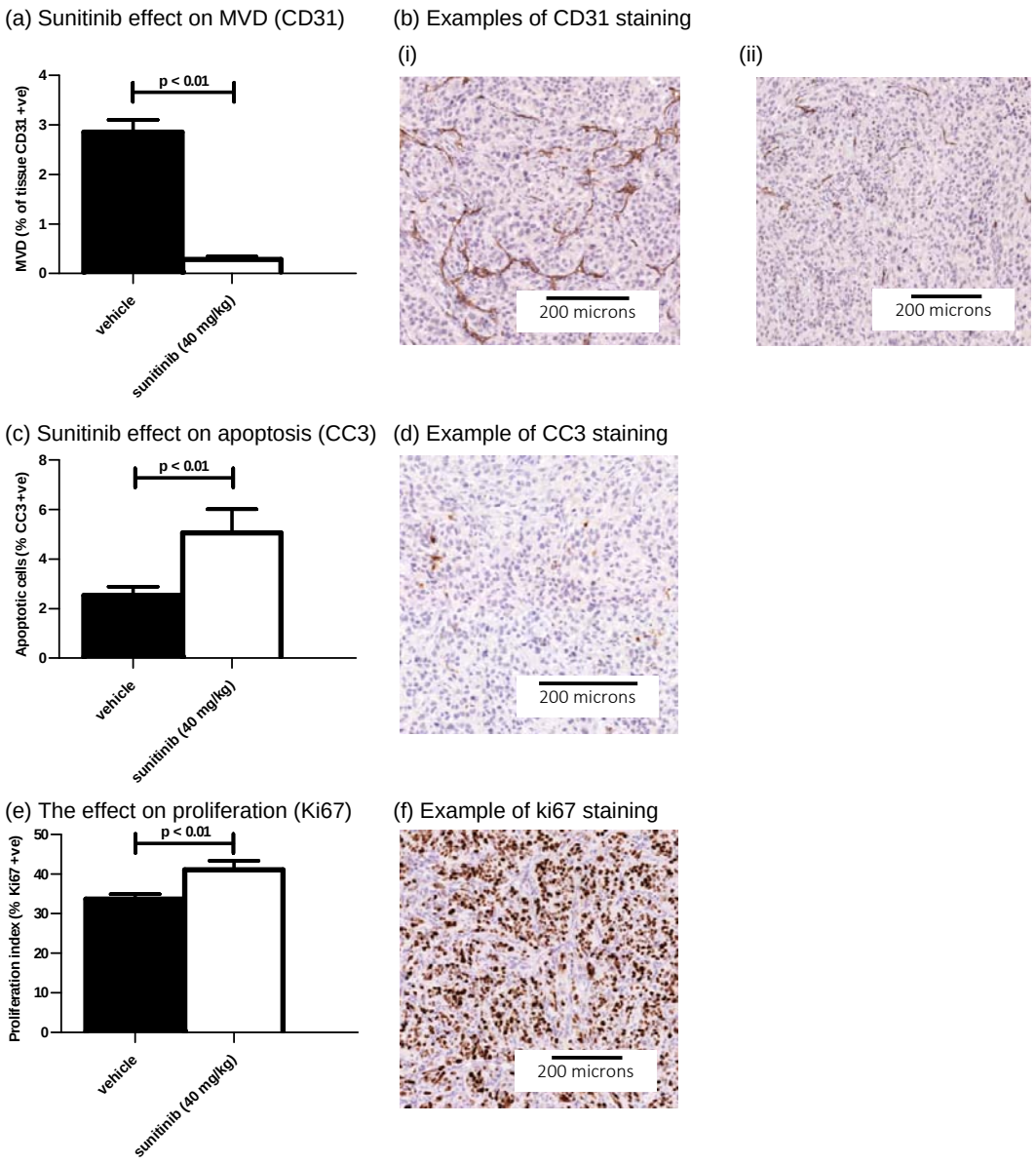

Figure 5.1: Pharmacodynamic study in tissue taken after 4 days treatment with sunitinib or vehicle. Panels (a) and (b) show an example of CD31 and its quantification (all quantification was done using the ARIOL system with visually trained parameters). The example indicates the level of vessel density in a (i) vehicle-treated tumour and (ii) sunitinib treated tumour. Panel (d) shows and example of cleaved caspase 3 (CC3) IHC in a sunitinib treated tumour. CC3 is a marker of apoptosis. Panels (e) and (f) show the effect on proliferation as determined by Ki67 staining.

5.2.2 The effect of the VEGF-TKIs sunitinib and cediranib on the myeloid compartment

As part of previous work conducted by our group it was observed that spleen weights were affected by sunitinib treatment. In this previous study, spleens were collected at the end of extended anti-tumour studies [48]. The pharmaco-dynamic study allowed us to investigate whether spleen weights were affected over a shorter period. It also allowed us to investigate the effect on different myeloid cell types.

Figure 5.2 (c) shows that spleen weights were significantly reduced after 4 days of sunitinib treatment. To investigate the effect on the myeloid compartment, bone marrows were flushed at necropsy and harvested cells were assessed by flow cytometry. By gating cells based on forward and side-scatter, the proportion of monocytes, granulocytes and lymphocytes were quantified.

Panels (a) and (b) shows raw flow cytometer data and the gates used to distinguish cell types. Gates R1, R2, R3 and R4 were taken to represent red blood cells, lymphocytes, monocytes and granulocytes respectively.

Figure 5.2 (d)-(f) shows sunitinib significantly reduced the proportion of monocytes and lymphocytes in the bone marrow (both $p<0.01$), but did not have a statistically significant effect on the granulocyte population. The experiment was repeated at a further timepoint (Day 22) and with a different anti-VEGFr TKI (cediranib) with similar results (data not shown).

.

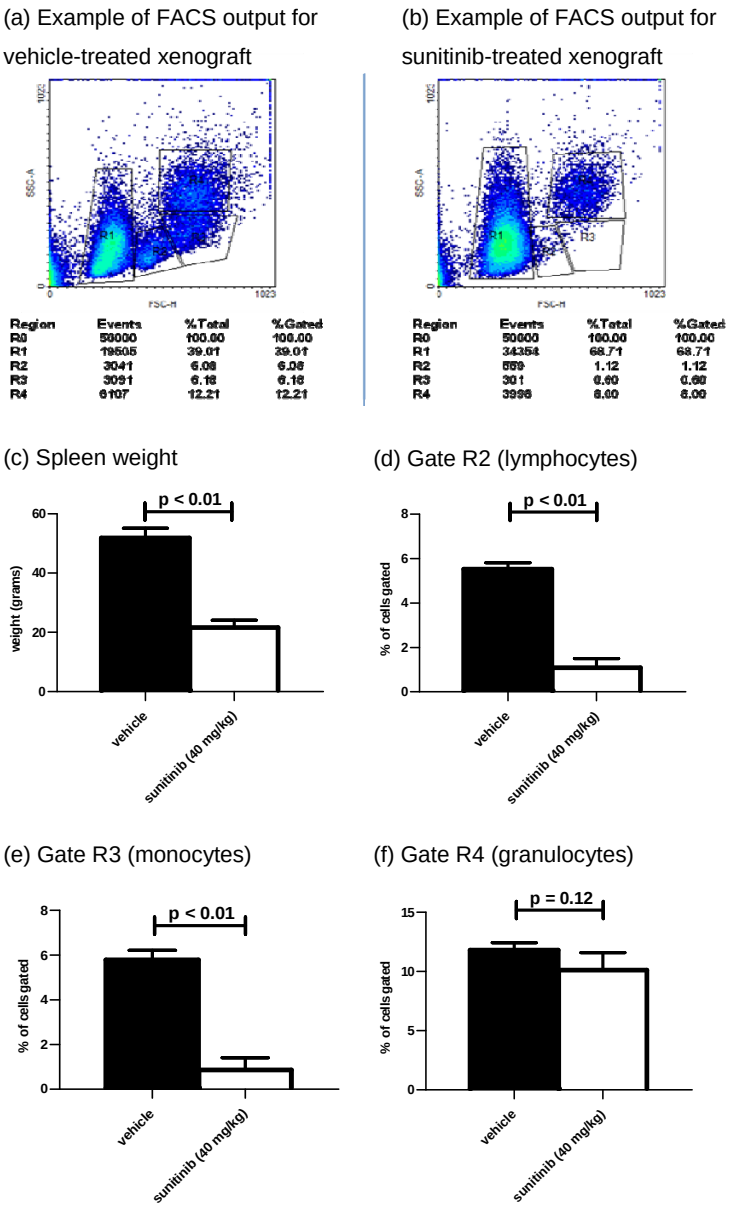

Figure 5.2: Pharmacodynamic study using bone marrow harvested after 4 days therapy. Panels (a) and (b) show raw flow cytometer data - gates R1, R2, R3 and R4 were taken to represent red blood cells, lymphocytes, monocytes and granulocytes respectively. Panels (d) - (f) shows the results of the analysis on the different cell types. Panel (c) shows the difference in spleen weights harvested from mice after 4 days therapy.

5.2.3 The impact of sunitinib on tumour-associated myeloid cells

Flow cytometry established an effect on myeloid cells in the bone marrow and spleen weights suggested an effect on circulating myeloid cells. Furthermore, data using human and mouse-specific PCR indicated a significant reduction in host cells within the tumour [Figure 5.3 (a)]. IHC was used to investigate whether this translated to a reduction in myeloid-derived cells within the tumour microenvironment. IHC staining for F4/80 positive cells was used to quantify macrophage content. Panels (b) and (d) indicate that macrophages were abundant in 786-O tumours and represented a significant proportion of non-tumour cells at the tumour site (unlike epithelial derived tumour cells epithelial derived murine cells do not stain positive for cytokeratin). Quantification of the F4/80 staining of vehicle of sunitinib-treated tumours indicated sunitinib significantly reduced macrophage content by 4 days.

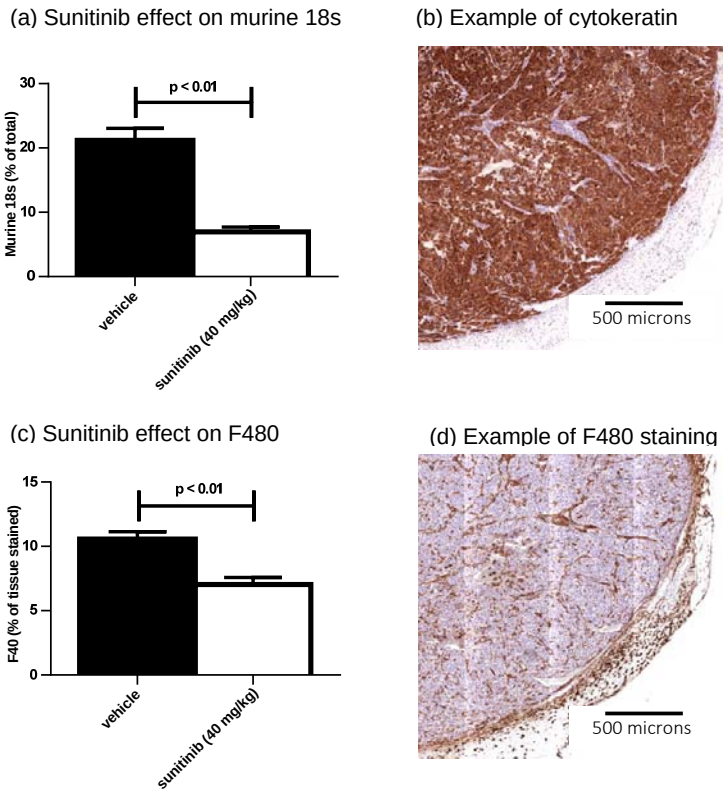

Figure 5.3: The effect of sunitinib on stromal cells *in situ*. Panel (a) shows the result of a PCR experiment to quantify the relative amount of tumour and host cells at the tumour site. Human and mouse-specific probes for 18s demonstrated fewer mouse cells were present in tissue taken from sunitinib-treated tumours. Panel (b) is an example of pan-cytokeratin staining which indicates which cells are of human origin and so tumour cells. Panel (d) shows and example of F4/80 staining for macrophages and panel (c) shows the effect of sunitinib on the macrophage content of 786-O xenografts.

Xenograft sections were stained for Ki67 to investigate treatment effect on cell proliferation. Ki67 staining was not homogenous. In fact the pattern of positive cells was similar to that seen in cytokeratin staining [Figure 5.4 (a) and (c)]. Since sunitinib had reduced both macrophages and vessels at the tumour site, we hypothesised that a sunitinib-induced reduction in non-malignant cells could explain the earlier observation that sunitinib increased the proportion of Ki67+ve cells [Figure 5.1 (e)].

In order to test this hypothesis, sections were dual-stained for Ki67 and cytokeratin by IFC and the results visualised by confocal microscope [Figure 5.4 (d)]. Counting cells positive for both cytokeratin and Ki67 allowed us to quantify the proportion of proliferating cells in the tumour compartment. Sunitinib treatment had no effect on the proportion on tumour cells that were Ki67+ve (data not shown) supporting our hypothesis.

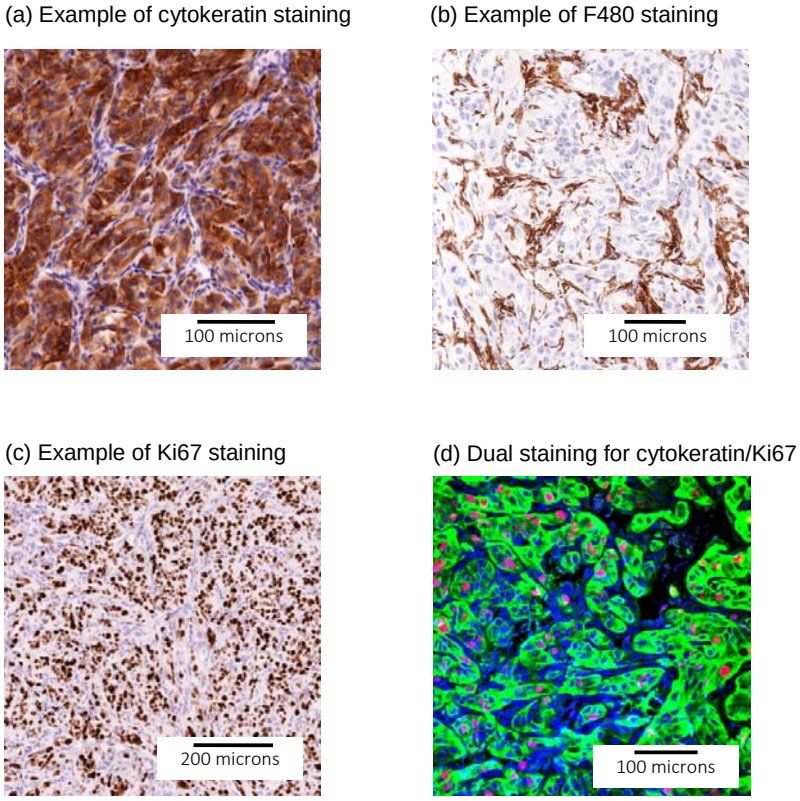

Figure 5.4: The effect of sunitinib on Ki67 staining in the tumour compartment of 786-O xenografts. Panels (a) – (c) shows examples of IHC stains; (a) pan-cytokeratin distinguishes tumour cells, (b) F480 stains for macrophages (c) shows the pattern of Ki67 staining. Panel (d) shows the result of tumour dual stained for cytokeratin (green) and Ki67 (red). DAPI (blue) shows cell nuclei.

5.2.4 The effect of sunitinib treatment on gene expression in tumour cells and the host compartment

In the clinical setting, sunitinib can generate tumour responses and improvements in Progression Free Survival (PFS), but acquired resistance translates to a limited long term survival benefit. Pre-clinical studies aimed at explaining drivers of acquired resistance have focused on several mechanisms including:

- Angiogenic factors such as basic fibroblast growth factor (FGF-2), the hepatocyte growth factor (HGF) / MET receptor pathway and placental growth factor (PGF) that can complement VEGF-A, providing alternative mechanisms to recruit endothelial cells and promote their growth in situ.

- Inflammatory cytokines and host immune / myeloid cells, which can also drive angiogenesis and support tumour progression.

- An increase in metastatic potential, driven by the tumour cell ability to invade local tissue before travelling to distant sites. Genes involved in matrix remodeling, such as the matrix metalloproteases and genes involved in a tumour cell's motility and adhesion such as snail, slug and the cadherins may help drive this process.

To investigate what was driving resistance in the 786-O model a panel of genes thought to be involved in angiogenesis, metastasis and tumour-stromal interaction were selected. PCR probes for these genes were tested for specificity for human or mouse (this work was carried out at AstraZeneca independently of this project). In this way, gene expression in the tumour and host compartments of 786-O xenografts could be investigated separately.

Tissue was taken at 3 timepoints (unlike the Huang et al which only reported on tissue taken at study completion). This allowed investigation of dynamic changes to relevant biomarkers over the course of treatment and disease progression; tissue from sensitive tumours was taken after 4 days of therapy, tissue was taken again after sustained treatment (22 days) and finally at 57 days when all tumours were displaying a resistant phenotype (Figure 5.5).

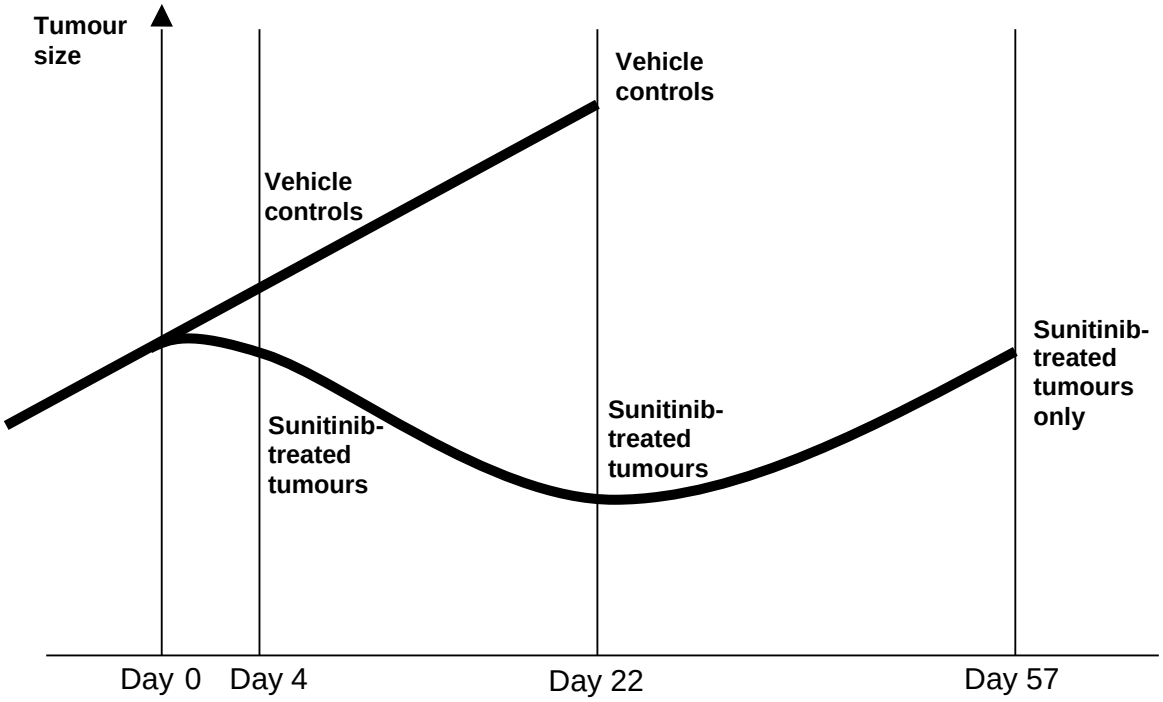

Figure 5.5: Experiment design allowed tissue to be taken at three timepoints. At Day 4 tissue from vehicle and sunitinib-treated was taken. Sunitinib-treated tumours were sensitive to sunitinib at this time-point (n=7 in the vehicle arm and n=5 in the treatment arm). Tissue was taken from both arms at Day 22 (n=7 in the vehicle arm and n=5 in the treatment arm). This was the latest time-point available to take tissue from vehicle-treated tumours because tumour size was approaching the limit allowable under the project license. Finally tissue was taken at Day 57 (n=15). By this timepoint all tumours were growing (>20% growth from the lowest measurement taken in all cases) and so were classified as displaying a resistant phenotype.

High throughput PCR (Fluidigm) was performed on tissue taken at the 3 different time-points using species-specific assays (n=7 for vehicle, n=5 for sunitinib-treated tumours). The proportion of human and mouse tissue in each sample was controlled for with primers targeting human and mouse specific 18s rRNA primers.

After removing results from genes that did not produce Ct values within 40 cycles, we generated data for 112 human-specific and 156 mouse-specific primers. Figures 5.6 and 5.7 show gene expression data generated from human and mouse-specific probes respectively. Delta-delta-CT values were calculated with reference to the mean CT value of vehicle treated in tissue taken at 4 days.

Figure 5.6: Gene expression data relating to the tumour compartment of 786-O xenografts. At Day 4 sunitinib-treated tumours were classed as sensitive to treatment, whereas all tumours displayed a resistant phenotype by day 57. Species-specific probes were used, with the data above relating to probes validated as specific to cells of human origin, but not murine cells (the host compartment).

Figure 5.7: Gene expression data relating to the host compartment of 786-O xenografts. At Day 4 sunitinib-treated tumours were classed as sensitive to treatment, whereas all tumours displayed a resistant phenotype by day 57. Species-specific probes were used, with the data above relating to probes validated as specific to cells of murine origin, but not human cells (the tumour compartment).

Two genes with significantly different expression profiles between sunitinib-treated and vehicle-tumours were chosen to validate the gene expression data at the protein level. In terms of the tumour compartment (Figure 5.6), the three genes with the largest fold-increase in gene expression at Day 57 versus Day 4 (vehicle) were PGF (placental growth factor, 12.2-fold increase, $p<0.01$) ENG (endoglin, 8.9-fold increase, $p<0.01$) and S100A4 (6.4-fold increase, $p<0.01$). These genes were selected to validate the gene expression data.

To investigate the increase in PGF, an ELISA was performed on serum harvested from both vehicle and sunitinib-treated mice at the 3 time-points. As Figure 5.8 (d) - (e) shows, PGF concentration was significantly increased at Day 57. When data was normalised to allow for differences in tumour size, PGF concentration was 11.6-fold higher in sunitinib-treated mice (Day 57) than (Day 4) vehicle-treated mice ($p<0.01$). This was consistent with the earlier gene expression analysis.

To quantify S100A4 and endoglin protein expression levels, IHC was performed on whole xenograft sections. Although endoglin could be visualised in the vessels of human tumours (used as a positive control) the protein could not be visualised in any xenograft sections including sunitinib-treated tumours harvested at Day 57 (concentrations up to 1:3 were tried). S100A4 protein could be visualized by IHC. Examples of staining can be seen in Figure 5.8 (a) – (b). Quantification using image analysis software with visually trained parameters confirmed S100A4 protein was significantly increased in 'resistant' Day 57 tumours as compared to tissue taken at Day 4 ($p<0.01$). This was consistent with the earlier gene expression analysis.

(a) Example of S100A4 staining in tissue taken at 4 days

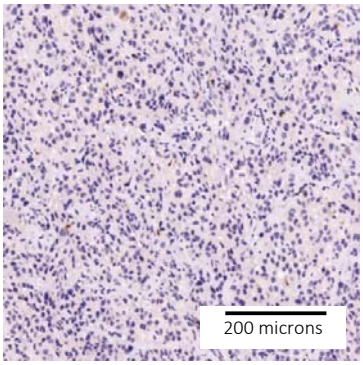

(b) Example of S100A4 staining in resistant model

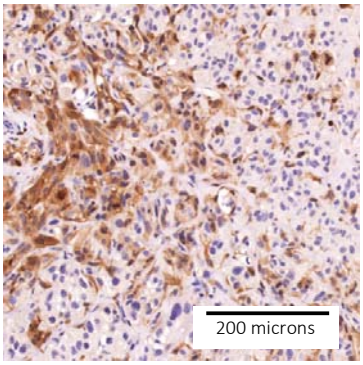

(c) Quantification of S100A4 IHC staining

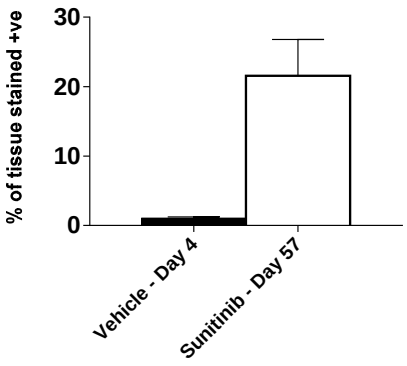

(d) PGF quantification by ELISA (raw data)

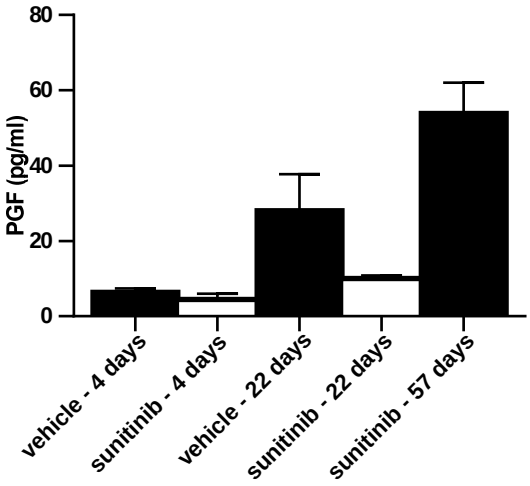

(e) PGF quantification by ELISA (normalised to take into account tumour size)

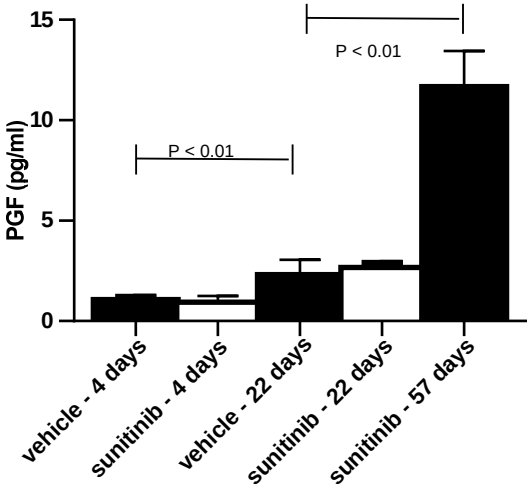

Figure 5.8: Validation of gene expression data at the protein level. Panel (a) and (b) show examples of S100A4 staining from tissue taken at Day 4 and Day 57 respectively. Panel (c) shows the quantification of staining results using image analysis software with visually trained parameters. Panels (d) and (e) show the results of an ELISA performed to quantify PGF levels in the serum of mice harvested at days 4, 22 and 57. Panel (e) normalised the data to take into account the difference in tumour size between the various study groups.

Results of the gene expression analysis showed that multiple pro-angiogenic ligands were up-regulated in sunitinib-treated tumours in both the host and tumour compartments. In the host compartment VEGF-A, PGF, FGF-2, HGF and its target MET receptor were all significantly up-regulated by Day 22 [Figure 5.9 (d)]. Furthermore, the anti-angiogenic ligand DLL4 was significantly down-regulated.

In the tumour compartment, VEGF-A and PGF were up-regulated by Day 22 [Figure 5.9 (c)], but FGF-2, HGF and DLL4 were not significantly different (data not shown). Both VEGF-A and PGF are known to be regulated by the HIF-1 and HIF-2 transcription factors. A separate PCR confirmed up-regulation of the HIF-2 transcription factors (the 786-O cell line is HIF-1 null).

CD31 staining showed that vessel density continued to reduce after Day 4 reaching a minimum vessel density at Day 22. After this, a modest but significant rebound occurred by Day 57 (the 'resistant' tumours). In these tumours, vessels were not homogenously distributed but were present in patches, which were also populated by a high proportion of non-endothelial host cells. An example of this can be seen in Figure 5.9 (b).

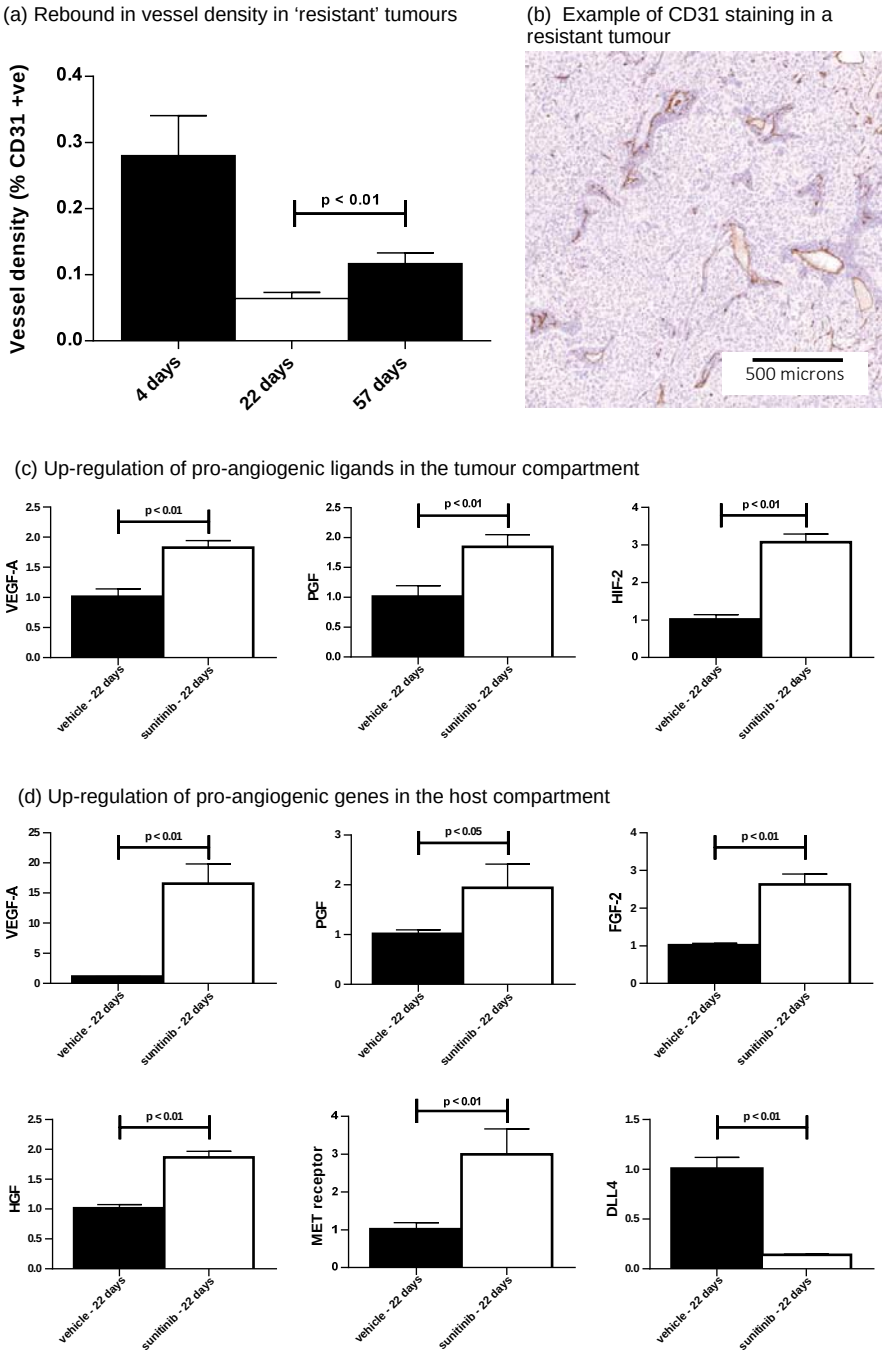

Figure 5.9: Up-regulation of multiple pro-angiogenic factors and rebound in vessel density. Panel (a) shows that vessel density rebounds with time as tumours become resistant to sunitinib. An example of CD31 staining in 'resistant' tumours is shown in panel (b). Panel (c) shows the tumour compartment up-regulates VEGF-A and PGF ligands. While panel (d) shows non-malignant host cells upregulate VEGF-A to a much more significant degree as well as a number of other alternative angiogenic factors including FGF-2 and the HGF-Met receptor pathway.

In addition to genes associated with angiogenesis, Figure 5.6 shows that treatment affected a number of other genes implicated in tumour progression. When comparing sunitinib-treated tumours to their corresponding vehicle-treated controls, a number of genes were significantly up-regulated in treated tumours including several inflammatory factors (including IL-6, CCL5, CXCL10), proteases involved in tissue remodeling (MMP2, cathepsin b) and genes central to the clotting system (tissue plasminogen activator, SERPINE1 and SERPINE2). In the majority of cases, these genes are most affected at Day 22 when treatment had its maximum effect on vessel density reduction [the four most up-regulated genes at Day 22 can be seen in Figure 5.10 (a)].

A comparison was made between vehicle groups at Day 4 and Day 22 to investigate whether genes were changing with time independently of treatment. In the tumour compartment 10 genes (cathepsin b, CCL2, cytokine-like protein1, FGF18, IL1 receptor1, IL6 receptor, neuroplin1 , neuropilin 2, placental growth factor, S100A4) were significantly up-regulated in vehicle treated tumours at Day 22 versus Day 4 (all $p<0.05$). A further two genes (MMP9 and MMP13) were significantly down-regulated at Day 22 versus Day 4 ($p<0.05$).

Of the 10 genes up-regulated at the later timepoint, three genes (placental growth factor, FGF18 and S100A4) were up-regulated in sunitinib-treated tumours at Day 57 compared to both the vehicle and sunitinib arms at Days 4 and 22 [see Figure 5.10 (b)]. Consistent with this data at the gene expression level, placental growth factor concentration levels were significantly up-regulated in the serum of mice at Day 22 versus Day 4 in vehicle-treated tumours. Concentration levels continued to increase and by Day 57 PGF was significantly higher than either sunitinib or vehicle-treated tumours at Day 22 [see Figure 5.8 (e)].

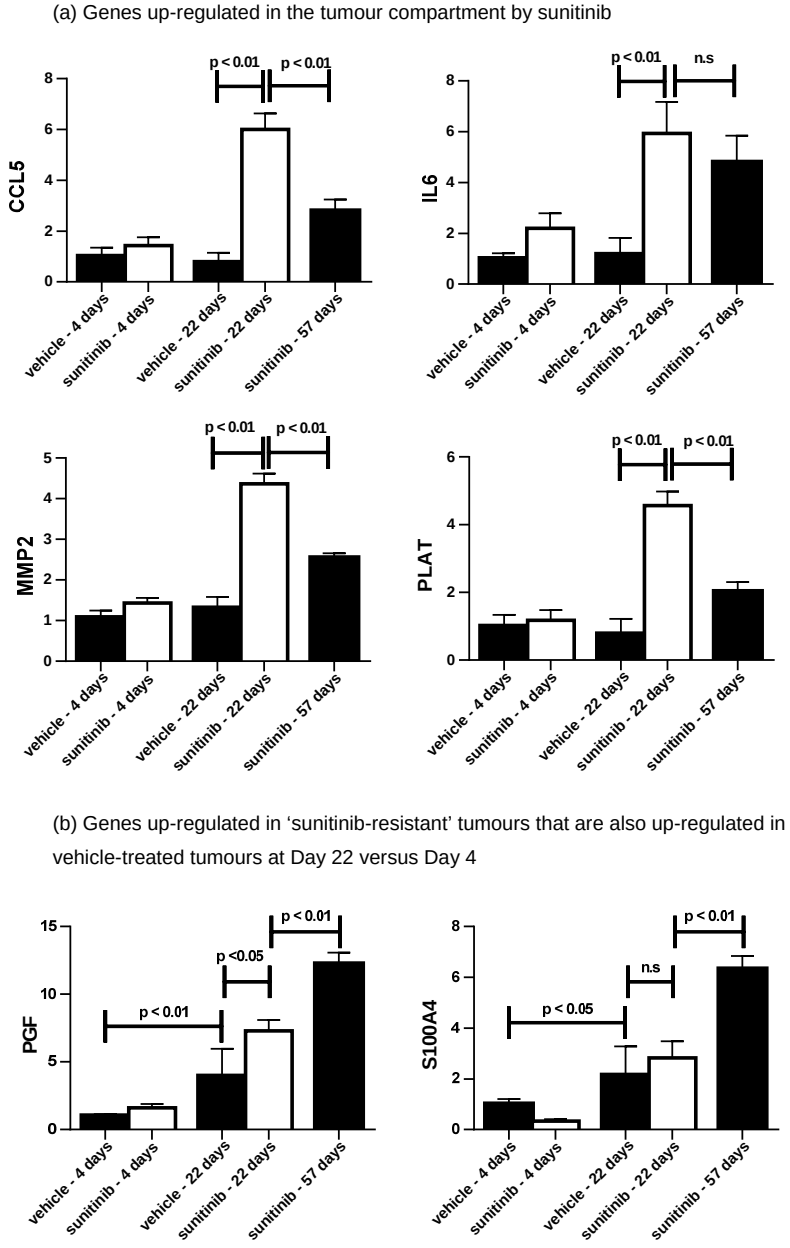

Figure 5.10: Gene up-regulation in the tumour compartment. Panel (a) show examples of inflammatory, protease and clotting genes significantly up-regulated in sunitinib-treated tumours at Day 22. Panel (b) shows and example of two genes up-regulated in vehicle-treated tumours at Day 22 versus Day 4, which are also significantly up-regulated in sunitinib-treated tumours at Day 57 compared to Day 22.

One of the proposed mechanisms of resistance is a treatment, or hypoxia, induced increase in the tumours metastatic potential. Genes thought to be involved in this process include proteases involved in invasion and tissue remodeling (which could derive from both the tumour and host compartments) in addition to genes involved in tumour cell's epithelial to mesenchymal transition.

A number of proteases were up-regulated in both the tumour and host by Day 22 compared to the corresponding vehicle-treated tumours. These included MMP2 [3.4-fold increase in the tumour ($p<0.01$) and 3.6-fold increase in the host ($p<0.01$)] and MMP9 [no significant up-regulation in the tumour, but a 2.3-fold increase in the host ($p<0.01$)].

In terms of genes indicating an epithelial-to-mesenchymal transition in the tumour compartment, the transcription factor SNAIL was significantly up-regulated at Day 22 [2.2-fold increase ($p=0.04$)]. However, although there was a decrease in E-cadherin (CDH1) and an increase in CDH11, a cadherin whose expression is associated with a mesenchymal phenotype, neither of these changes quite reached statistical significance [CDH1 2.8-fold decrease ($p=0.06$) and CDH11 1.9-fold increase ($p=0.06$)].

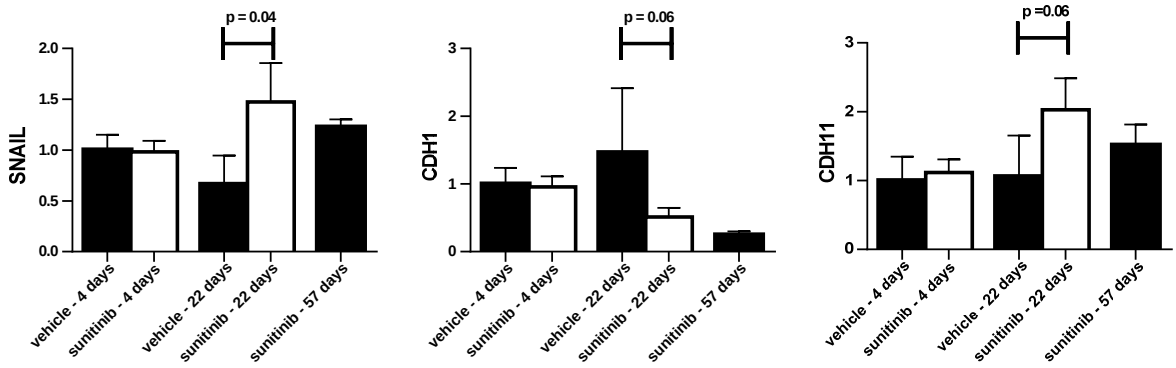

Figure 5.11: Gene expression of genes in the tumour compartment thought to regulate epithelial-to-mesenchymal transition.

5.2.5 The potential role of methylation in the 'sunitinib-resistant' phenotype

S100A4 was significantly up-regulated in 'resistant' tumour tissue taken at Day 57 when compared to treated tissue at Day 4, However, at Day 22 protein levels were not significantly different between sunitinib-treated and vehicle-treated tumours. S100A4 has been shown to be associated with metastasis. An inverse relationship between e-cadherin has been noted and recently one group has shown that overexpression of S100A4 can drive metastasis in a RCC xenograft model [116]. This same group noted that S100A4 was regulated by methylation.

Using O-miner, an online tool developed at Barts Cancer Institute that allows re-analysis of gene expression data taken from publicly deposited raw microarray data files, a panel of RCC cell lines was re-analysed to investigate which genes were most up-regulated when treated with the de-methylation agent 5-azacytidine. In line with previous findings S100A4 was among the most affected genes. Interestingly, placental growth factor, which was also highly up-regulated at Day 57, also appeared among the list of most up-regulated genes.

786-O cells were de-methylated with 5-azacytidine *in vitro* and PCR was conducted to investigate S100A4 and PGF expression. De-methylation was found to significantly up-regulate both S100A4 [log-fold change 4.3 ($p<0.01$)] and PGF [log-fold change 5.0 ($p<0.01$)] confirming previous microarray data.

To date, 'resistant' xenograft tumours have not been investigated for changes in methylation status.

Gene symbol	Gene name	Log-fold change	Gene location
DAZL	deleted in azoospermia-like	6.041207250	3p24.3
CCL20	chemokine (C-C motif) ligand 20	5.491894177	2q33-q37
GTSF1	gametocyte specific factor 1	5.257688717	12q13.13
MAEL	maelstrom homolog (Drosophila)	5.118489475	1q24.1
MMP1	matrix metallopeptidase 1	4.607410577	11q22.3
NFE4	transcription factor NF-E4	4.595544903	7q22.1
COL1A1	collagen, type I, alpha 1	4.175204324	17q21.33
WDR66	WD repeat domain 66	4.159705878	12q24.31
COL1A1	collagen, type I, alpha 1	4.109540555	17q21.33
GREM1	gremlin 1	4.057677289	15q13.3
COL6A3	collagen, type VI, alpha 3	4.020847357	2q37
GREM1	gremlin 1	3.973137918	15q13.3
HORMAD1	HORMA domain containing 1	3.573127135	1q21.3
LAPTM5	lysosomal protein transmembrane 5	3.471547104	1p34
CST6	cystatin E/M	3.463559096	11q13
LOC654433	hypothetical LOC654433	3.404553620	2q13
LY6K	lymphocyte antigen 6 complex, locus K	3.336944199	8q24.3
H19	H19	3.329118595	11p15.5
S100A4	**S100 calcium binding protein A4**	**3.199693292**	**1q21**
SFN	Stratifin	3.080317536	1p36.11
HCLS1	hematopoietic cell-specific Lyn substrate 1	3.001811876	3q13
SYCP3	synaptonemal complex protein 3	2.947403641	12q
DENND2A	DENN/MADD domain containing 2A	2.883159126	7q34
PSG9	pregnancy specific beta-1-glycoprotein 9	2.705099983	19q13.2
FERMT3	fermitin family member 3	2.660193311	11q13.1
ISG20	interferon stimulated exonuclease gene 20	2.652711541	15q26
KRT34	keratin 34	2.583364730	17q21.2
PGF	**placental growth factor**	**2.568622368**	**14q24.3**
LOC728449	hypothetical protein LOC728449	2.557249674	10q11.22
CCL5	chemokine (C-C motif) ligand 5	2.495092384	17q11.2-q12

Table 5.1: Genes most significantly up-regulated when a panel of RCC cell lines were treated with the de-methylation agent 5-azacytidine.

5.2.6 Sunitinib up-regulates genes associated with fibrosis and is associated with increased collagen deposition

Using the gene expression data, Ingenuity Pathway Analysis (IPA) was conducted to better understand processes and pathways involved with 786-O resistance. This was conducted separately in the tumour compartment and the host compartment respectively.

Table 5.1 shows the results of the IPA analysis suggesting genes up-regulated in the 786-O. Interestingly, genes associated with fibrosis were consistently up-regulated in both tumour and host gene expression pathway analysis. Fibrosis is characterised by excessive deposition of connective tissue components, particularly collagen. In order to investigate whether up-regulation of fibrosis-related genes was accompanied by increased collagen deposition, tumours were stained with sirius red. Collagen content was quantified using image analysis software. As Figure 5.12 shows, collagen density at the tumour site was significantly increased by sunitinib treatment.

	Tumour compartment	
	Day 22 - sunitinib v's vehicle	**sunitinib resistant (Day 57) v's sunitinib sensitive (Day 4)**
1	Coagulation	**Hepatic Fibrosis**
2	**Hepatic Fibrosis**	Coagulation
3	Glioma invasiveness	Macrophages, Fibroblasts & Endothelial in RA
4	Macrophages, Fibroblasts & Endothelial in RA	Glioma invasiveness
5	Osteoclasts and osteoblasts in RA	Ephrin receptor signalling

	Host compartment	
	Day 22 - sunitinib v's vehicle	**sunitinib resistant (Day 57) v's sunitinib sensitive (Day 4)**
1	**Hepatic Fibrosis**	**Hepatic Fibrosis**
2	Bladder Cancer	IL-8 signaling
3	IL-8 signaling	Glioma invasiveness
4	Clathrin-mediated endocytosis	Stem cell pluripotency
5	FGF signaling	Axonal guidance signalling

Table 5.2: Results of Ingenuity pathway analysis: All genes whose expression was significantly affected ($p<0.05$) by sunitinib-treatment (column 1) or the resistance process (column 2) were included in the IPA analysis.

(a) Example of collagen staining in a sunitinib-treated xenograft

(b) Quantification of collagen density

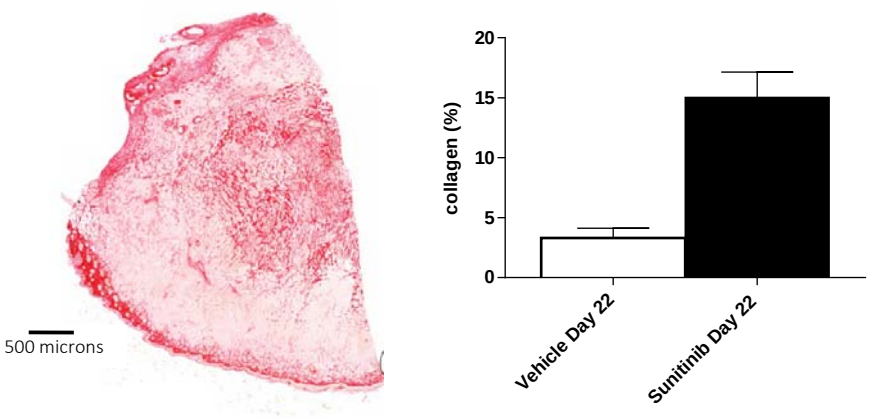

Figure 5.12: Results of staining for collagen density in vehicle and sunitinib treated tumours. Panel (a) shows an example of a sunitinib-treated tumour stained for collagen. Panel (b) indicates that collagen was significantly denser in sunitinib-treated tumours than the corresponding vehicle-treated tumours.

5.2.7 Investigating whether key xenograft findings occur in the clinical setting

VEGFr-TKI treated RCC patient tissue was used to investigate whether unexpected findings from the xenograft model were occurring in the clinical setting.

Cells of myeloid origin were significantly decreased in sunitinib-treated tumours both in the bone marrow and at the tumour site. Tumours were stained for total myeloid cell content by targeting CD45. As 5.13 (a) shows there was no significant difference in total myeloid content between the two groups.

In flow cytometry analysis of xenograft's bone marrow, the proportion of lymphocytes was significantly reduced. RCC samples were stained for CD3 +ve cells, a marker of T lymphocytes. No difference was seen between the pre- and post-treatment samples [Figure 5.13 (b)]. However, the proportion of FOXP3 +ve cells was significantly reduced [Figure 5.13 (c)]. FOXP3 is thought to be a marker of T-reg cells a subset of T-lymphocytes.

The RCC patient tissue was a combination of sunitinib (n=58) and pazopanib-treated (27) samples. For all biomarkers stained, including all markers in Chapter 3 (CD31, FGF-2, Met receptor, Ki67) and markers in data not presented in this thesis (phosphorylated s6K and PDL-1) a comparison was made between the effects of the two drugs. In the majority of cases, there was no difference in the effects of the 2 drugs. However, sunitinib but not pazopanib, resulted in a significant reduction in the expression of CD45 and CD3 [median change -84% vs. +13% ($p<0{\cdot}05$); median change -38% vs. +117% ($p<0{\cdot}05$) respectively].

TMAs were constructed avoiding necrotic regions and areas with a high proportion of connective tissue. Consequently we used whole sections to the effects of sunitinib treatment on collagen deposition.

As seen in the xenograft tumours, sunitinib treatment (12-16 weeks of therapy) was associated with a significant increase in collagen density at the tumour site (Figure 5.14).

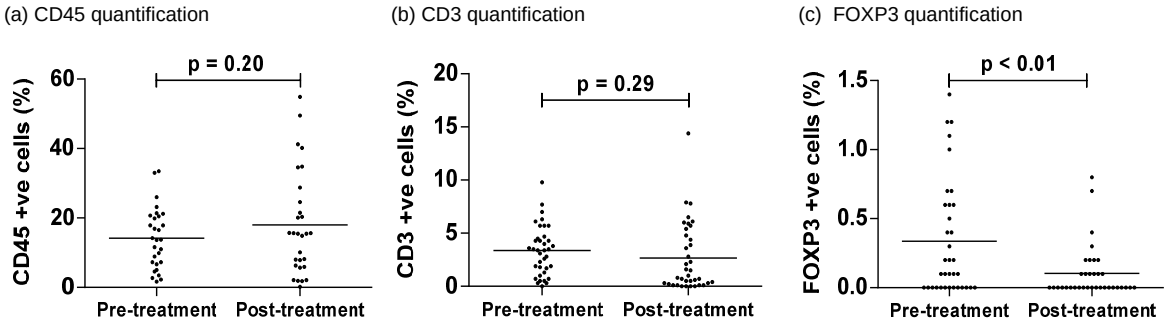

Figure 5.13: VEGFr-TKI treated RCC patient tissue stained for the immune markers CD45 (all myeloid cells) CD3 (T cells) and FOXP3 (T-reg cells).

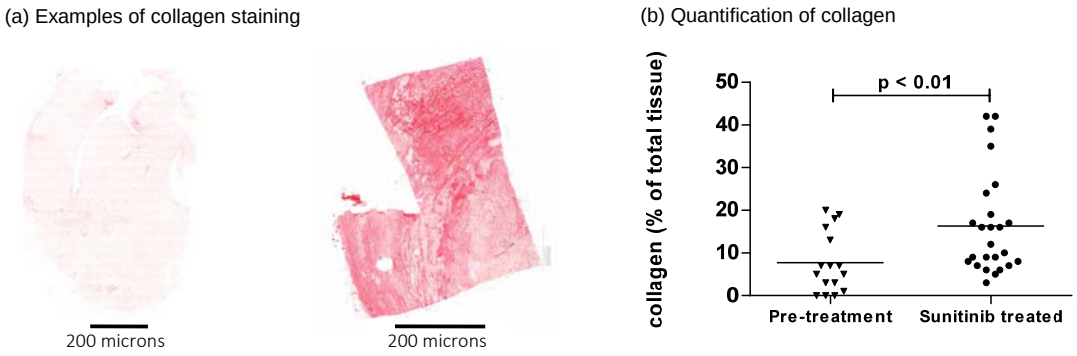

Figure 5.14: Comparison of collagen density staining of VEGFr-TKI treated and untreated RCC patient samples. Panel (a) shows an example of a low collagen density untreated tissue sample and a treated tissue sample with high collagen density as seen by the increased amount of Sirius Red. Panel (b) indicates that collagen was significantly denser in sunitinib-treated tumours.

5.3 Discussion

Before looking for resistance mechanisms, xenograft tissue taken after 4 days of treatment was used to examine the pharmacodynamics effect of sunitinib treatment on 786-O tumours. The 4-day time point was chosen because it was thought to provide enough time for pharmacodynamics effects to take place, but not too long for treated tumour sizes to be significantly different from vehicle treated controls. Nevertheless, the fact that we only have tissue from this one timepoint is a limitation of this study. Furthermore, the choice to take tissue 2 hours after the last sunitinib (or vehicle) dose provides another important limitation, particularly in the context of trying to measure biomarkers that are thought to change significantly over treatment cycles, such as the anti-apoptotic marker, cleaved caspase 3. Notwithstanding these limitations, IHC analysis conducted on this tissue did provide some interesting insights.

Sunitinib is thought to work primarily by reducing tumour vessel density thereby decreasing oxygen and nutrient supply to malignant cells. 4 days after treatment onset tumour vessel density was already 90% lower in sunitinib-treated xenografts than in vehicle controls [Figure 5.1 (a)]. Given that these tumours had grown for 28 days prior to treatment onset, this degree of reduction suggests sunitinib pruned existing vessels in this xenograft, rather than simply reducing new vessel formation.

A 90% decrease in tumour vessel density after just 4 days suggests the sunitinib dose used in the 786-O model had a much more significant effect than we may expect to take place in the clinical setting. A pre- and post-treatment analysis in the clinical setting saw a 49% median decrease in tumour vessel density [Section 3.1]. This highlights a further limitation of our xenograft work. Many of the dynamic changes seen in biomarkers, such as changes in gene expression, may be indirect results of the hypoxic environment caused by sunitinib in this model. If this model is not representative of the clinical setting, it reduces our ability to translate these findings into a meaningful context.

FACS analysis on the bone marrow at Day 4 revealed a significant immune-suppressive effect. Furthermore, PCR results using human and mouse-specific

18s probes indicated a significant reduction in non-malignant cells at the tumour site. Due to size of this effect, and previous IHC staining that revealed that vessels comprised approximately 3% of the total tissue, we hypothesized that sunitinib was impacting other non-malignant cells, in addition to endothelial cells. IHC staining showed that sunitinib reduced macrophage content at the tumour site.

To investigate whether a similar effect was occurring in the clinical setting, RCC tumour samples pre- and post- anti-VEGFr treatment were stained for CD45, a common marker for cells of haematopoietic origin. No difference in the percent of CD45+ve cells was seen between pre- and post-treatment tissue. A subgroup analysis looking at patients treated with sunitinib (excluding patients treated with pazopanib) a significant reduction in CD45 cells was seen post-treatment. Previous work taking peripheral blood from patients before and after sunitinib treatment suggests sunitinib is having a myelosuppressive effect, at least in peripheral blood [45]. To our knowledge no previous work has shown a reduction in myeloid cells at the tumour site of RCC patients following anti-VEGFr treatment. In addition to their role in immune evasion [44], myeloid cells are thought to supply pro-angiogenic ligands and so promote resistance to anti-VEGFr therapy resistance [45 117]. Conceivably a reduction of certain myeloid cells at the tumour site could contribute to sunitinib's observed efficacy. However, our subgroup analysis looking at sunitinib-treated patients only, reduces an already modest sample size and limits our ability to draw conclusions with any confidence.

A similar subgroup analysis, looking at patients who received sunitinib specifically, showed that treatment significantly reduced CD3 cells at the tumour site. Preclinical models have previously suggested that directly targeting VEGFR-2 does not impede T-cell infiltration at the tumour site, but may in fact promote infiltration through vascular normalization [118]. However, sunitinib is multi-targeted TKI, which affects several other kinases at clinically relevant doses. Other groups have shown that sunitinib can reduce T-cell proliferation [119]. Sunitinib and pazopinib impact other kinases to different degrees. It is possible that sunitinib has a direct off-target effect on immune cells which does not happen with pazopinib therapy and the pre and post-treatment tissue IHC corroborates our xenograft work suggesting that sunitinib significantly decreases

immune infiltrate at the tumour site. Different agents have previously been reported to have effects on different subsets of immune cells [120]. Again, our subgroup analysis is based on a small sample size reducing our ability to draw conclusions with confidence.

FOXP3, a marker for regulatory T cells, is the one immune biomarker that did reduce significantly when analyzing the pre- and post-treatment samples as a whole i.e. not relying on a subgroup analysis focusing specifically on sunitinib-treated patients [Figure 5.6 (c)]. Sunitinib's ability to reduce FOXP3 T cells has previously been reported [45, 64]. Again this previous work focuses on peripheral blood rather than tumour tissue. It has been suggested that the effect on FOXP3 cells is mediated directly through the VEGF-A/VEGFR2 rather than any off-target kinase inhibition [121]. If the VEGF pathway is the main pathway involved it may help explain why this effect was seen in both sunitinib and pazopinib patient tissue. Regardless of the pathways involved, the ability to reduce FOXP3 cells at the tumour site may contribute to improved outcomes associated with anti-VEGFr therapy.

Turning to the tumour compartment, our pharmacodynamics analysis on the 786-O xenograft model showed an increase in the apoptotic marker cleaved caspase 3 in sunitinib-treated tumours. Sunitinib has been suggested to act directly on cells to induce apoptosis in part through reduction in STAT3 activity [65, 96]. We found no evidence that sunitinib had any effect on STAT3 activity in this model [Figure 4.5 (c)]. Furthermore, there was no evidence for a change in gene expression of pro- and anti-apoptotic genes thought to be regulated by STAT3 such as BCL-XL and BCL-2 (data not shown). We cannot rule out a direct effect on tumour cells leading to apoptosis, mediated by a different pathway, but the increase in apoptosis may be explained by the observed reduction in vessel density, reducing oxygen supply and nutrients to tumour cells. We could not validate this finding in our RCC patient tissue (data not shown). This could have been partly due to the time delay between the last treatment dose and the nephrectomies being performed, but we also experienced technical difficulties with cleaved caspase staining that may have masked any effect. Tumour tissue appeared susceptible to non-specific staining that made quantification of cleaved caspase positive tumour cells a difficult task.

An increase in the percentage of Ki67 was also observed at Day 4. Because of the pattern of staining, and evidence that the proportion the host had decreased in sunitinib-treated tumours [Figure 5.3], we hypothesized that this effect was driven by a reduction in the proportion on less proliferative non-malignant cells in the tissue analyzed, rather than an effect on the tumour cells themselves. Subsequent dual-staining for Ki67 and cytokeratin confirmed this [Figure 5.4 (d)]. Furthermore, we saw no increase in the percentage of Ki67 in the tumour compartment at later time periods. As such, we could find no evidence in the 786-O xenograft to support our observation in clinical tissue that anti-VEGFr treatment promotes a more proliferative, aggressive phenotype which may contribute to resistance [Figure 3.5].

The primary reason for conducting the xenograft studies was to look for mechanisms of resistance. By replicating the 786-O xenograft model employed by Huang et al [39] we were able to obtain xenograft tissue while tumours were sensitive to treatment (Day 4) and at a later date when tumours were classified as "resistant" since tumour growth had rebounded in all 15 tumours having initially shrunk in response to treatment (Day 57). We also obtained tissue at Day 22. This timepoint is more difficult to characterize since it could be seen as the point of maximum response but could equally be seen as a timepoint when many of the resistance mechanisms driving regrowth of tumours were already in place [Figure 5.5].

In all 15 tumours that were treated for 57 Days, the initial response to treatment lead to a tumour volume decrease that was in excess of 30%, the required threshold to be classified as a Partial Response under RECIST criteria [122]. Furthermore, in 15/15 tumours regrowth was in excess of 20%, the threshold that must be exceeded to be classified as Progressive Disease under RECIST guidelines.

PCR analysis was conducted on the tissue taken at each timepoint to look dynamic changes in gene expression that may highlight resistance mechanisms in the 786-O model. Rather than looking for specific genes, an effort was made look for pathways and processes that were potentially contributing to resistance. Moreover, although the use of mouse and human specific probes allowed us to investigate the host and tumour compartments separately, an effort was made

to look for potential co-operation between the two compartments. Unsurprisingly a number of pro-angiogenic genes were upregulated in both the host and tumour compartment [Figures 5.6, 5.7 and 5.9]. Up-regulation of these genes was most significant at Day 22 which was also the timepoint when vessel density was at its lowest [Figure 5.9 (a)]. Presumably host and tumour cells up-regulated genes in compensation to the hypoxic microenvironment and hypoxia was greatest at Day22.

Pro-angiogenic genes were up-regulated to a greater degree in host cells compared to the tumour compartment. This is perhaps unsurprising since many of these genes such as VEGF-A or MET receptor are known to be mediated by the VHL-HIF pathway. Under hypoxic conditions the transcription factor HIF-alpha is allowed to stabilize resulting in up-regulation of pro-angiogenic genes [8]. While this process is likely to have driven the observed increase in VEGF-A and other pro-angiogenic genes in host cells, the tumour compartment, consisting of VHL-null cells would not have experienced the same process. Since 786-O cells are VHL-null, the HIF-alpha transcription factors are not labeled for proteasomal degradation even under normoxic conditions i.e. HIF-alpha was allowed to stabilize even in vehicle treated tumours and so the difference between pro-angiogenic gene expression in vehicle and sunitinib-treated tumours was not so great. The increase in VEGF-A in the tumour compartment could be explained by increased HIF-2 gene expression [Figure 5.9 (c), note 786-O cells are HIF-1 null].

HIF transcription factors are also thought to regulate certain genes associated with metastasis and the promotion of mesenchymal phenotype such as SNAIL [20]. Interestingly, SNAIL was up-regulated in the tumour compartment versus time-matched vehicle controls [$p<0.05$, Figure 5.5]. E-cadherin, which is thought to be negatively regulated by SNAIL was decreased at the same time point, but this decrease fell short of statistical significance ($p=0.06$). These results highlight one potential resistance mechanism that may be invoked in response to anti-angiogenic therapy.

Many other genes were up-regulated at Day 22. Of note several inflammatory genes were effected in both the tumour and host compartments including IL-6 which was significantly up-regulated in both compartments. As noted previously

with the up-regulation of several pro-angiogenic genes, the increase in inflammatory gene expression was greatest at Day 22. Although Huang et al reported that sunitinib decreased IL-8 expression and "reactivation of tumor angiogenesis was accompanied by a significant increase of IL-8 release" [39], we found neither a decrease in IL-8 in sensitive tumours at Day 4 nor an increase in IL-8 in resistant tumours at Day 57. Since we were investigating gene expression and Huang et al used ELISA assays, it may be that the decrease and subsequent increase occurred at the protein level. However, Huang et al based their conclusion taken at one time point (study end) after comparing IL-8 levels in tumours that had a resistant phenotype with tumours that failed to rebound to draw conclusions. In the Huang et al study, tumours that showed a resistant phenotype had similar levels of IL-8 to non-treated controls. It seems conceivable that the conclusion of Huang et al was incorrect. Rather than decreasing before rebounding to the original levels as they suggest, IL-8 may remain at a constant level throughout the treatment course.

The significant modulation of inflammatory markers is interesting in the context of the earlier discussion of FOXP3 T cells. The up-regulation of several pro-inflammatory cytokines provides another potential mechanism by which sunitinib may improve type 1 T cell function.

Our PCR analysis revealed several genes that were significantly up-regulated at Day 57 despite sunitinib seemingly having little effect on gene expression when treated tumours were compared with time-matched controls at Day 22. PGF and S1004a both fall into this category. Interestingly, both genes were up-regulated in vehicle-treated tumours at Day 22 compared to vehicle-treated tumours at Day 4. This raises the possibility that time rather than treatment is the key driver of the observed up-regulation of these 2 genes. That is to say that PGF and S100A4 were up-regulated as a result of the natural progression of disease. Interestingly, although sunitinib may not be directly causing the up-regulation of PGF or S100A4, both genes could contribute to sunitinib resistance, PGF by promoting new vessel formation and S100A4 through promotion of a mesenchymal, metastatic phenotype.

Both PGF and S100A4 are known to regulated in part by methylation. We showed that 786-O cells significantly up-regulate both genes in response to a

de-methylation agent. Further work could demonstrate whether this was the mechanism involved in the 786-O xenograft model.

Ingenuity Pathway analysis was conducted in an effort to better explain what pathways were involved in the resistance process. The suggestion that several genes involved in fibrosis were up-regulated, lead us to look for collagen deposition. Sunitinib was demonstrated to significantly increase collagen content in the 786-O xenograft model and we then validated that this process was occurring in the clinic using RCC patient tissue. Collagen is thought to promote blood vessel development and contribute to pathological angiogenesis [123] [124] [125]. Collagen is also thought to promote tumour cell metastasis [126]. Consequently, increased collagen deposition could promote the resistance process through both tumour revascularization and increasing the tumour's metastatic potential.

One limitation of our work is that although we demonstrate sunitinib increases collagen deposition in both xenograft and RCC sample tumours, we did not characterise the collagen type. Although 90% of collagen in the human body is Type 1 [127], which is thought to be pro-angiogenic and metastasis promoting, we cannot discount increased deposition of other collagens such as type XVIII collagen, which are thought to have anti-angiogenic properties.

There are several other limitations to the work carried out in this chapter. The xenograft work is based on one model at one dose level, which may not be reflective of the clinical setting. Certainly the work focused on the immune system is undermined by the use of SCID mice, which are severely immune-compromised. Moreover, by the time tumours demonstrated a resistance phenotype, all vehicle-treated tumours had been sacrificed leaving us without any time-matched controls. Gene expression analysis in the host compartment was complicated by the fact that sunitinib significantly decreased the number of host cells at the tumour site. Although we could allow for the general decrease in host cells using a mouse specific 18s probe we could not account for sunitinib changing the composition of the remaining host cells. It is possible that some of the gene expression changes we saw in the host compartment merely reflect a change in the composition of remaining host cells.

In summary, the gene expression analysis showed that several different pro-angiogenic and pro-metastatic pathways were activated by the time tumours were rebounding. Some of these genes seemed to be up-regulated to compensate for the hypoxic microenvironment caused by sunitinib therapy. Other genes such as S100A4 and PGF, although up-regulated at the time of resistance, and potentially contributing to that process, appeared to be up-regulated due to the natural course of disease, rather than as a response to therapy. Due to the prior selection of genes thought to potentially play a role in tumourgenesis, most of the genes and pathways implicated in this study have been previously implicated in the resistance process. Despite this, gene pathway analysis suggested a wound healing or 'fibrosis-like' process was taking place and this lead to the novel finding that VEGFr TKIs increase collagen deposition in both xenograft and RCC patient tissue. To our knowledge, collagen deposition has not previously been described as a potential resistance mechanism to anti-VEGFr therapy. Due the potential for collagen to affect both angiogen

esis and metastasis further investigation of this novel finding is warranted.

Chapter 6:

Summary and Future Work

VEGFr-TKIs are established as first line therapy for metastatic RCC [128, 129]. A minority of tumours are inherently resistant to therapy while a larger proportion are initially sensitive and subsequently acquire a resistant phenotype [75]. There are currently no clinically validated biomarkers that predict VEGFr TKI treatment response or the onset of acquired resistance [130]. Moreover, when resistance occurs, current second line treatment offers only a modest improvement in patient survival [131].

For patients presenting with metastatic disease current standard of care is for nephrectomy which takes place prior to treatment onset. Prior nephrectomy together with the difficulty in accessing metastatic tissue has meant that most biomarker studies to data have focused on tumour samples taken prior to therapy despite preclinical data that suggests treatment induces dynamic changes in tumour biology [37, 132]. We hypothesise that it is important to understand these dynamic changes in order to understand the mechanisms that mediate acquired resistance, and make informed choices about how to treat patients that become resistant to these agents.

This majority of work contained in this thesis is aimed at improving our understanding of the molecular drivers of acquired resistance. To this end a preclinical model of resistance was used together with tissue taken from RCC patients prior to planned nephrectomy and after 12-16 weeks of TKI therapy. In both preclinical and clinical tissue, a wide range of molecular changes were observed:

Treatment resulted in the up-regulation of multiple pro-angiogenic factors. FGF-2 and HGF-MET receptor have long been thought to provide alternative pathways by which tumours can escape VEGF-targeted therapy. Both pathways were seen to be up-regulated in clinical samples; cytoplasmic FGF-2 and MET

receptor on tumour vessels were significantly increased. In our preclinical model, FGF-2 ligand and MET receptor were both increased in non-malignant cells residing in the tumour microenvironment. No increase was in tumour cells. In addition, VEGF and PGF were seen to be up-regulated in our preclinical model in both the tumour and hose compartments (technical problems with the IHC prevented their measurement in clinical samples). Our preclinical model suggested that the highest up-regulation of VEGF ligand and MET receptor coincided with the maximum reduction in vessels density, potentially indicating a compensatory mechanism. Interestingly, PGF increased with time even in vehicle treated tumours. Moreover, PGF was up-regulated to the greatest degree at the last time-point, not at the point of maximum vessel reduction (a similar expression profile was observed for s100a4, a gene implicated in promoting renal cancer metastasis).

This raises an interesting hypothesis, the dynamic molecular changes that lead to acquired resistance observed in the clinic may occur through two distinct processes:

- the tumour may up-regulate pathways to compensate for hypoxia caused by VEGFr-TKI treatment
- the natural course of disease is associated with changes in gene expression over time and some of these genes up-regulated later timepoints may contribute to a resistant phenotype

A major limitation of our analysis of clinical tissue is that time-matched controls were not possible. As a result, we cannot discount the possibility that the natural course of disease is contributing to the observed molecular changes in sequential patient tissue.

In addition to the multiple pro-angiogenic factors up-regulated by treatment, several genes associated with metastasis were affected in the preclinical model. Metastasis is thought to be play an important role in VEGFr-TKI resistance. A major limitation of our preclinical work was our sole focus on the primary tumour site. 786-O xenografts do not easily metastasise beyond the primary tumour when cells are inoculated sub-cutaneously. Moreover, tumours were measured with callipers rather than using imaging equipment so any metastasis

would not have been observed. Consequently, although it can be verified that VEGFr-TKI treatment affected genes associated with metastasis, there is no evidence that this translated into the generation of metastatic tumours.

Ki67 analysis of clinical tissue showed an increase in the proliferation index of treated tumours, however this did not reach statistical significance in matched samples and tumour Ki67 was not significantly affected in our preclinical model. Nevertheless the observed increase in Ki67 in clinical samples suggests further investigation of this potential resistance mechanism is warranted.

In summary, several different pathways were affected by VEGFr-TKI therapy and many of these genes have been previously implicated as drivers of resistance. Because of the unique nature of the clinical tissue samples, this is (to our knowledge) the first time that these resistance mechanisms have been validated in clinical tissue. Two important conclusions could be drawn from this headline result. Firstly, the results question the use of tissue taken prior to treatment onset to select patients likely to benefit from VEGFr-TKI treatment disease. Secondly, the addition of therapy targeting any one of the many resistance pathways implicated, for example the FGF-2 or MET receptor inhibitors, may have an incremental on treatment efficacy. However, the number of different pro-angiogenic and pro-metastatic pathways affected by VEGFR-TKI treatment, and potentially contributing to acquired resistance, suggests that targeting any one of these individual pathways in isolation may not to lead to a long-lasting improvement in treatment response. In line with hypothesis dovitinib, a dual VEGFr-FGFr TKI, failed to show a significant improvement over sorafenib in patients that had previously progressed on VEGFr-TKI therapy [133].

A key motivation of developing a preclinical model of resistance was the ability to test treatment combinations that may delay or prevent resistance occurring. Before conducting the in depth resistance analysis described above, we hypothesised that SRC inhibitors may provide a rationale combination with VEGFr-TKIs to delay or prevent acquired resistance. This hypothesis was based on work by other groups that the SRC pathway can affect the two key mechanisms of resistance, namely metastasis and (renewed) angiogenesis. The data shows that combining the SRC inhibitor with VEGFr-TKI therapy had an

additive anti-tumour effect in our preclinical model of resistance, when compared to VEGFr-TKI monotherapy. However, gene analysis suggested that the addition of the SRC inhibitor had no significant effect on any of the molecular pathways associated with VEGFr-TKI resistance described above. A major limitation of the work investigating the potentially utility of SRC inhibition was the failure to identify a molecular mechanism by which the SRC inhibitor was providing this additive anti-tumour effect. Future work in clinical samples taken from patients treated with the VEGFr-TKI SRC inhibitor combination may provide insight here. In particular, we hypothesise from the preclinical data that VHL status and phospho-STAT3 activity may influence efficacy. Future translational efforts in clinical samples will prioritize these two biomarkers.

Additional work is ongoing using the sequential tissue taken from VEGFr-TKI treated patients. Some of this work may overcome some of the limitations with the work contained in the thesis. Perhaps the most important future work will expand the investigation into the effect of VEGFr-TKI on the immune system of patients. The ultimate goal of any translational research should be aimed at improving patient outcome through increased and sustained response to treatment. Of all the current drug candidates currently in clinical trials for RCC patients, immunotherapeutic approaches arguably hold the most promise. Unlike VEGFr-TKI treatment, where acquired resistance inevitably leads to tumour progression, immunotherapy has been associated with sustained treatment responses, and in some cases, remission. Consequently, the addition of an effective immunotherapy agent to VEGFr-TKI therapy holds promise. However, the effects of VEGFr-TKI therapy on immune compartment may complicate matters. Moreover, the preliminary work contained in this thesis suggests that different TKIs may have substantially different effects on CD3+ T cells the key effector cell of some of the most promising immunotherapies in clinic trials. Further work is needed to understand the effects on T cells and other key effector cells. IHC reagents are available to identify subpopulations of T cells. In addition to investigating the effects on CD4+ and CD8+ cells, it would be insightful to understand the effects on markers of immune-suppression. An increasing body of evidence suggests that PD-1 and CTLA4 expression play an important role in tumourgenesis. In addition it would be interesting to investigate expression of LAG-3 and TIM-3, which are known to be transiently expressed on CD8+ and CD4+ T cells respectively [134].

In addition, it would be insightful to understand the effect on other cell types important to mounting an immune reaction. In particular, NK cells should also be prioritized in part due to their ability to induce antibody-dependent cell-mediated cytotoxicity (ADCC). ADCC has been shown to be an important mechanism of action for antibody therapy. Any effect the different VEGFr-TKIs have on NK cell number and activation could be an important factor for immunotherapies currently in clinic, particularly immunotherapies that are thought to benefit from ADCC.

There are several limitations to the work described in this thesis. For the most part, the preclinical work was limited to one xenograft model (786-O cell line) in a SCID mouse. Extending the work to further xenograft models and taking tissue at further timepoints may help elucidate which genes are the key drivers of the resistance process. Unfortunately there are no clear cell renal carcinoma models that grow in immuno-competent mice, which limits the value of any further preclinical investigation of the effect of VEGFr-TKIs on immune response. Consequently, patient tissue is likely to be more insightful when examining the effect of VEGFr-TKI on the immune compartment.

Antibody-drug conjugates (ADCs) are empowered antibodies that harness the specificity of antibody therapies with the cell killing effects of chemotherapy. This class of drug have demonstrated efficacy in other tumour types, particularly breast cancer, and may prove to be effective in the RCC setting, despite the previous failures of traditional chemotherapies. An important hypothesis to emerge from this work is that derives from the Ki67 IHC work in sequential tissue. Our data, although not conclusive, suggests that VEGFr-TKI may lead to a more aggressive, proliferative phenotype. A proliferative phenotype may help sensitize cells to ADCs, particularly those drugs using cell-cycle dependent tubulin polymerisation inhibitors. Further investigation of the effect of VEGFr-TKIs of tumour cell proliferation may provide important insight into the use of ADCs in combination with, or subsequent to, VEGFr-TKI therapy.

Gene expression analysis of the xenograft tumours lead us to hypothesise that VEGFr-TKI treatment was leading to a process resembling fibrosis or wound healing. Since fibrosis is characterised by increased collagen deposition, collagen volume in the xenograft tumours was investigated. VEGFr TKIs resulted in a

significant increase in collagen deposition and this result was validated in clinical samples. To our knowledge, this has not been noted in either preclinical models or clinical tissue. Since collagen is thought to promote pathological angiogenesis [123] [124] [125] and metastasis [126] it is conceivable that increased collagen deposition represents a novel mechanism of resistance that contributes to tumour progression. However, a number limitations to our work prevents us from drawing such a conclusion at this stage.

As yet, the type of collagen deposited in the preclinical or clinical tissue has not been characterized. Different collagens are thought to have different effects on angiogenesis and cell signaling within the tumour compartment. Collagen has been shown to have pro- and anti-tumour effects within the same tumour type [135, 136], while it's impact in our work has not been established. It may be possible to address this in our preclinical model with the use of an anti-fibrotic agent, reducing collagen deposition. Any such efforts may be complicated by the fact that many drugs used to reduce fibrosis also have direct effects on vessels and blood flow [137, 138]. Intriguingly, retrospective analysis suggests that patients presenting on anti-fibrotic agents had significantly higher progression free survival [139]. Further work is warranted to better understand whether increased collagen deposition contributes to VEGFr TKI resistance and whether the use of anti-fibrotic agents can help slow tumour progression.

References

1. Vogelstein, B. & Kinzler, K.W. The multistep nature of cancer. *Trends Genet* **9**, 138-41 (1993).

2. Hanahan, D. & Weinberg, R.A. The hallmarks of cancer. *Cell* **100**, 57-70 (2000).

3. Hanahan, D. & Weinberg, R.A. Hallmarks of cancer: the next generation. *Cell* **144**, 646-74 (2011).

4. Qian, B.Z. & Pollard, J.W. Macrophage diversity enhances tumor progression and metastasis. *Cell* **141**, 39-51 (2010).

5. Murdoch, C., Muthana, M., Coffelt, S.B. & Lewis, C.E. The role of myeloid cells in the promotion of tumour angiogenesis. *Nat Rev Cancer* **8**, 618-31 (2008).

6. Drake, C.G., Jaffee, E. & Pardoll, D.M. Mechanisms of immune evasion by tumors. *Adv Immunol* **90**, 51-81 (2006).

7. Kerbel, R.S. Tumor angiogenesis: past, present and the near future. *Carcinogenesis* **21**, 505-15 (2000).

8. Baldewijns, M.M. et al. VHL and HIF signalling in renal cell carcinogenesis. *J Pathol* **221**, 125-38 (2010).

9. Kerbel, R.S. Tumor angiogenesis. *N Engl J Med* **358**, 2039-49 (2008).

10. Rafii, D.C., Psaila, B., Butler, J., Jin, D.K. & Lyden, D. Regulation of vasculogenesis by platelet-mediated recruitment of bone marrow-derived cells. *Arterioscler Thromb Vasc Biol* **28**, 217-22 (2008).

11. Rusnati, M. et al. A distinct basic fibroblast growth factor (FGF-2)/FGF receptor interaction distinguishes urokinase-type plasminogen activator

induction from mitogenicity in endothelial cells. *Mol Biol Cell* **7**, 369-81 (1996).

12. Bussolino, F. et al. Hepatocyte growth factor is a potent angiogenic factor which stimulates endothelial cell motility and growth. *J Cell Biol* **119**, 629-41 (1992).

13. Waugh, D.J. & Wilson, C. The interleukin-8 pathway in cancer. *Clin Cancer Res* **14**, 6735-41 (2008).

14. Schoenfeld, J. et al. Active immunotherapy induces antibody responses that target tumor angiogenesis. *Cancer Res* **70**, 10150-60 (2010).

15. Rundhaug, J.E. Matrix metalloproteinases and angiogenesis. *J Cell Mol Med* **9**, 267-85 (2005).

16. Willis, B.C. & Borok, Z. TGF-beta-induced EMT: mechanisms and implications for fibrotic lung disease. *Am J Physiol Lung Cell Mol Physiol* **293**, L525-34 (2007).

17. Zhang, Q. et al. Wnt/beta-catenin signaling enhances hypoxia-induced epithelial-mesenchymal transition in hepatocellular carcinoma via crosstalk with hif-1alpha signaling. *Carcinogenesis* **34**, 962-73 (2013).

18. Ding, H. et al. Sonic hedgehog signaling mediates epithelial-mesenchymal communication and promotes renal fibrosis. *J Am Soc Nephrol* **23**, 801-13 (2012).

19. Talbot, L.J., Bhattacharya, S.D. & Kuo, P.C. Epithelial-mesenchymal transition, the tumor microenvironment, and metastatic behavior of epithelial malignancies. *Int J Biochem Mol Biol* **3**, 117-36 (2012).

20. Luo, D., Wang, J., Li, J. & Post, M. Mouse snail is a target gene for HIF. *Mol Cancer Res* **9**, 234-45 (2011).

21. Yang, M.H. et al. Direct regulation of TWIST by HIF-1alpha promotes metastasis. *Nat Cell Biol* **10**, 295-305 (2008).

22. Lam, J.S., Shvarts, O., Leppert, J.T., Figlin, R.A. & Belldegrun, A.S. Renal cell carcinoma 2005: new frontiers in staging, prognostication and targeted molecular therapy. *J Urol* **173**, 1853-62 (2005).

23. Siegel, R., Naishadham, D. & Jemal, A. Cancer statistics, 2012. *CA Cancer J Clin* **62**, 10-29 (2012).

24. Gu, F.L., Cai, S.L., Cai, B.J. & Wu, C.P. Cellular origin of renal cell carcinoma--an immunohistological study on monoclonal antibodies. *Scand J Urol Nephrol Suppl* **138**, 203-6 (1991).

25. Schmidt-Ott, K.M., Lan, D., Hirsh, B.J. & Barasch, J. Dissecting stages of mesenchymal-to-epithelial conversion during kidney development. *Nephron Physiol* **104**, p56-60 (2006).

26. Gnarra, J.R. et al. Mutations of the VHL tumour suppressor gene in renal carcinoma. *Nat Genet* **7**, 85-90 (1994).

27. Herman, J.G. et al. Silencing of the VHL tumor-suppressor gene by DNA methylation in renal carcinoma. *Proc Natl Acad Sci U S A* **91**, 9700-4 (1994).

28. Motzer, R.J., Bander, N.H. & Nanus, D.M. Renal-cell carcinoma. *N Engl J Med* **335**, 865-75 (1996).

29. Glaspy, J. Therapeutic options in the management of renal cell carcinoma. 2002;: . *Sem Oncol* **29**, 41-6 (2002).

30. Kim, P.G.a.S. Renal cell carcinoma. *Curr Opin Oncol* **14**, 280-5 (2002).

31. Nathan, P.D. & Eisen, T.G. The biological treatment of renal-cell carcinoma and melanoma. *The Lancet Oncology* **3**, 89-96 (2002).

32. Motzer, R.J. et al. Sunitinib versus interferon alfa in metastatic renal-cell carcinoma. *N Engl J Med* **356**, 115-24 (2007).

33. Roskoski, R., Jr. Sunitinib: a VEGF and PDGF receptor protein kinase and angiogenesis inhibitor. *Biochem Biophys Res Commun* **356**, 323-8 (2007).

34. Francia, G., Emmenegger, U. & Kerbel, R.S. Tumor-associated fibroblasts as "Trojan Horse" mediators of resistance to anti-VEGF therapy. *Cancer Cell* **15**, 3-5 (2009).

35. Ebos, J.M., Lee, C.R., Christensen, J.G., Mutsaers, A.J. & Kerbel, R.S. Multiple circulating proangiogenic factors induced by sunitinib malate are tumor-independent and correlate with antitumor efficacy. *Proc Natl Acad Sci U S A* **104**, 17069-74 (2007).

36. Carmeliet, P. et al. Synergism between vascular endothelial growth factor and placental growth factor contributes to angiogenesis and plasma extravasation in pathological conditions. *Nat Med* **7**, 575-83 (2001).

37. Casanovas, O., Hicklin, D.J., Bergers, G. & Hanahan, D. Drug resistance by evasion of antiangiogenic targeting of VEGF signaling in late-stage pancreatic islet tumors. *Cancer Cell* **8**, 299-309 (2005).

38. Welti, J.C. et al. Fibroblast growth factor 2 regulates endothelial cell sensitivity to sunitinib. *Oncogene* **30**, 1183-93 (2011).

39. Huang, D. et al. Interleukin-8 mediates resistance to antiangiogenic agent sunitinib in renal cell carcinoma. *Cancer Res* **70**, 1063-71 (2010).

40. Ebos, J.M. et al. Accelerated metastasis after short-term treatment with a potent inhibitor of tumor angiogenesis. *Cancer Cell* **15**, 232-9 (2009).

41. Paez-Ribes, M. et al. Antiangiogenic therapy elicits malignant progression of tumors to increased local invasion and distant metastasis. *Cancer Cell* **15**, 220-31 (2009).

42. Gupta, G.P. & Massague, J. Cancer metastasis: building a framework. *Cell* **127**, 679-95 (2006).

43. Brahimi-Horn, M.C., Chiche, J. & Pouyssegur, J. Hypoxia and cancer. *J Mol Med (Berl)* **85**, 1301-7 (2007).

44. Kusmartsev, S. & Gabrilovich, D.I. Role of immature myeloid cells in mechanisms of immune evasion in cancer. *Cancer Immunol Immunother* **55**, 237-45 (2006).

45. Ko, J.S. et al. Direct and differential suppression of myeloid-derived suppressor cell subsets by sunitinib is compartmentally constrained. *Cancer Res* **70**, 3526-36 (2010).

46. Ko, J.S. et al. Sunitinib mediates reversal of myeloid-derived suppressor cell accumulation in renal cell carcinoma patients. *Clin Cancer Res* **15**, 2148-57 (2009).

47. Bolontrade, M.F., Zhou, R.R. & Kleinerman, E.S. Vasculogenesis Plays a Role in the Growth of Ewing's Sarcoma in Vivo. *Clin Cancer Res* **8**, 3622-7 (2002).

48. Welti, J.C. et al. Contrasting effects of sunitinib within in vivo models of metastasis. *Angiogenesis* **15**, 623-41 (2012).

49. Rous, P. Landmark article (JAMA 1911;56:198). Transmission of a malignant new growth by means of a cell-free filtrate. By Peyton Rous. *JAMA* **250**, 1445-9 (1983).

50. Rubin, H. Quantitative relations between causative virus and cell in the Rous no. 1 chicken sarcoma. *Virology* **1**, 445-73 (1955).

51. Martin, G.S. The hunting of the Src. *Nat Rev Mol Cell Biol* **2**, 467-75 (2001).

52. Yeatman, T.J. A renaissance for SRC. *Nat Rev Cancer* **4**, 470-80 (2004).

53. Geahlen, R.L., Handley, M.D. & Harrison, M.L. Molecular interdiction of Src-family kinase signaling in hematopoietic cells. *Oncogene* **23**, 8024-32 (2004).

54. Irby, R.B. & Yeatman, T.J. Role of Src expression and activation in human cancer. *Oncogene* **19**, 5636-42 (2000).

55. Talamonti, M.S., Roh, M.S., Curley, S.A. & Gallick, G.E. Increase in activity and level of pp60c-src in progressive stages of human colorectal cancer. *J Clin Invest* **91**, 53-60 (1993).

56. Webb, D.J. et al. FAK-Src signalling through paxillin, ERK and MLCK regulates adhesion disassembly. *Nat Cell Biol* **6**, 154-61 (2004).

57. Zamir, E. & Geiger, B. Molecular complexity and dynamics of cell-matrix adhesions. *J Cell Sci* **114**, 3583-90 (2001).

58. Liang, W. et al. Antitumor activity of targeting SRC kinases in endothelial and myeloid cell compartments of the tumor microenvironment. *Clin Cancer Res* **16**, 924-35 (2010).

59. Steinberg, M. Dasatinib: a tyrosine kinase inhibitor for the treatment of chronic myelogenous leukemia and philadelphia chromosome-positive acute lymphoblastic leukemia. *Clin Ther* **29**, 2289-308 (2007).

60. Trevino, J.G. et al. Expression and activity of SRC regulate interleukin-8 expression in pancreatic adenocarcinoma cells: implications for angiogenesis. *Cancer Res* **65**, 7214-22 (2005).

61. Green, T.P. et al. Preclinical anticancer activity of the potent, oral Src inhibitor AZD0530. *Mol Oncol* **3**, 248-61 (2009).

62. Lombardo, L.J. et al. Discovery of N-(2-chloro-6-methyl- phenyl)-2-(6-(4-(2-hydroxyethyl)- piperazin-1-yl)-2-methylpyrimidin-4- ylamino)thiazole-5-carboxamide (BMS-354825), a dual Src/Abl kinase inhibitor with potent antitumor activity in preclinical assays. *J Med Chem* **47**, 6658-61 (2004).

63. Wedge, S.R. et al. AZD2171: a highly potent, orally bioavailable, vascular endothelial growth factor receptor-2 tyrosine kinase inhibitor for the treatment of cancer. *Cancer Res* **65**, 4389-400 (2005).

64. Finke, J.H. et al. Sunitinib reverses type-1 immune suppression and decreases T-regulatory cells in renal cell carcinoma patients. *Clin Cancer Res* **14**, 6674-82 (2008).

65. Xin, H. et al. Sunitinib inhibition of Stat3 induces renal cell carcinoma tumor cell apoptosis and reduces immunosuppressive cells. *Cancer Res* **69**, 2506-13 (2009).

66. Kerbel, R. & Folkman, J. Clinical translation of angiogenesis inhibitors. *Nat Rev Cancer* **2**, 727-39 (2002).

67. Rini, B.I. & Atkins, M.B. Resistance to targeted therapy in renal-cell carcinoma. *Lancet Oncol* **10**, 992-1000 (2009).

68. Lieu, C., Heymach, J., Overman, M., Tran, H. & Kopetz, S. Beyond VEGF: inhibition of the fibroblast growth factor pathway and antiangiogenesis. *Clin Cancer Res* **17**, 6130-9 (2011).

69. Welti, J.C. et al. Fibroblast growth factor 2 regulates endothelial cell sensitivity to sunitinib. *Oncogene* **30**, 1183-93 (2010).

70. Cooke, V.G. et al. Pericyte depletion results in hypoxia-associated epithelial-to-mesenchymal transition and metastasis mediated by met signaling pathway. *Cancer Cell* **21**, 66-81 (2012).

71. Shojaei, F. et al. HGF/c-Met acts as an alternative angiogenic pathway in sunitinib-resistant tumors. *Cancer Res* **70**, 10090-100 (2010).

72. Powles, T. et al. The outcome of patients treated with sunitinib prior to planned nephrectomy in metastatic clear cell renal cancer. *Eur Urol* **60**, 448-54 (2011).

73. Bex, A. et al. A phase II study of presurgical sunitinib in patients with metastatic clear-cell renal carcinoma and the primary tumor in situ. *Urology* **78**, 832-7 (2011).

74. Boleti, E. The safety and efficacy of pazopanib prior to planned nephrectomy in metastatic clear cell renal cancer. *J Clin Oncol* **30**, Suppl5, Abstr 427 (2012).

75. Rini, B.I., Campbell, S.C. & Escudier, B. Renal cell carcinoma. *Lancet* **373**, 1119-32 (2009).

76. Sennino, B. et al. Suppression of tumor invasion and metastasis by concurrent inhibition of c-Met and VEGF signaling in pancreatic neuroendocrine tumors. *Cancer Discov* **2**, 270-87 (2012).

77. Aaltomaa, S., Lipponen, P., Ala-Opas, M., Eskelinen, M. & Syrjanen, K. Prognostic value of Ki-67 expression in renal cell carcinomas. *Eur Urol* **31**, 350-5 (1997).

78. Yerushalmi, R., Woods, R., Ravdin, P.M., Hayes, M.M. & Gelmon, K.A. Ki67 in breast cancer: prognostic and predictive potential. *Lancet Oncol* **11**, 174-83 (2010).

79. Berney, D.M. et al. Ki-67 and outcome in clinically localised prostate cancer: analysis of conservatively treated prostate cancer patients from the Trans-Atlantic Prostate Group study. *Br J Cancer* **100**, 888-93 (2009).

80. Raymond, E. et al. Sunitinib malate for the treatment of pancreatic neuroendocrine tumors. *N Engl J Med* **364**, 501-13 (2011).

81. Ellis, L.M. & Hicklin, D.J. VEGF-targeted therapy: mechanisms of anti-tumour activity. *Nat Rev Cancer* **8**, 579-91 (2008).

82. Hlatky, L., Hahnfeldt, P. & Folkman, J. Clinical application of antiangiogenic therapy: microvessel density, what it does and doesn't tell us. *J Natl Cancer Inst* **94**, 883-93 (2002).

83. Wedam, S.B. et al. Antiangiogenic and antitumor effects of bevacizumab in patients with inflammatory and locally advanced breast cancer. *J Clin Oncol* **24**, 769-77 (2006).

84. Willett, C.G. et al. Direct evidence that the VEGF-specific antibody bevacizumab has antivascular effects in human rectal cancer. *Nat Med* **10**, 145-7 (2004).

85. Folkman, J. & Klagsbrun, M. Angiogenic factors. *Science* **235**, 442-7 (1987).

86. Porta, C. et al. Changes in Circulating Pro-Angiogenic Cytokines, other than VEGF, before Progression to Sunitinib Therapy in Advanced Renal Cell Carcinoma Patients. *Oncology* **84**, 115-22 (2013).

87. Presta, M. et al. Fibroblast growth factor/fibroblast growth factor receptor system in angiogenesis. *Cytokine Growth Factor Rev* **16**, 159-78 (2005).

88. Sorensen, V., Nilsen, T. & Wiedlocha, A. Functional diversity of FGF-2 isoforms by intracellular sorting. *Bioessays* **28**, 504-14 (2006).

89. Zhu, A.X. et al. Efficacy, safety, and potential biomarkers of sunitinib monotherapy in advanced hepatocellular carcinoma: a phase II study. *J Clin Oncol* **27**, 3027-35 (2009).

90. Batchelor, T.T. et al. AZD2171, a pan-VEGF receptor tyrosine kinase inhibitor, normalizes tumor vasculature and alleviates edema in glioblastoma patients. *Cancer Cell* **11**, 83-95 (2007).

91. Gerlinger, M. et al. Intratumor heterogeneity and branched evolution revealed by multiregion sequencing. *N Engl J Med* **366**, 883-92 (2012).

92. Serrels, A. et al. Identification of potential biomarkers for measuring inhibition of Src kinase activity in colon cancer cells following treatment with dasatinib. *Mol Cancer Ther* **5**, 3014-22 (2006).

93. Burnham, M.R. et al. Regulation of c-SRC activity and function by the adapter protein CAS. *Mol Cell Biol* **20**, 5865-78 (2000).

94. Montero, J.C., Seoane, S., Ocana, A. & Pandiella, A. Inhibition of SRC family kinases and receptor tyrosine kinases by dasatinib: possible combinations in solid tumors. *Clin Cancer Res* **17**, 5546-52 (2011).

95. Xu, Q. et al. Targeting Stat3 blocks both HIF-1 and VEGF expression induced by multiple oncogenic growth signaling pathways. *Oncogene* **24**, 5552-60 (2005).

96. Yang, F. et al. Sunitinib induces apoptosis and growth arrest of medulloblastoma tumor cells by inhibiting STAT3 and AKT signaling pathways. *Mol Cancer Res* **8**, 35-45 (2010).

97. Tatarov, O. et al. SRC family kinase activity is up-regulated in hormone-refractory prostate cancer. *Clin Cancer Res* **15**, 3540-9 (2009).

98. Elsberger, B. et al. Is expression or activation of Src kinase associated with cancer-specific survival in ER-, PR- and HER2-negative breast cancer patients? *Am J Pathol* **175**, 1389-97 (2009).

99. Zhang, X.H. et al. Latent bone metastasis in breast cancer tied to Src-dependent survival signals. *Cancer Cell* **16**, 67-78 (2009).

100. Nagaraj, N.S., Smith, J.J., Revetta, F., Washington, M.K. & Merchant, N.B. Targeted inhibition of SRC kinase signaling attenuates pancreatic tumorigenesis. *Mol Cancer Ther* **9**, 2322-32 (2010).

101. Park, S.I. et al. Targeting SRC family kinases inhibits growth and lymph node metastases of prostate cancer in an orthotopic nude mouse model. *Cancer Res* **68**, 3323-33 (2008).

102. Tryfonopoulos, D. et al. Src: a potential target for the treatment of triple-negative breast cancer. *Ann Oncol* **22**, 2234-40 (2011).

103. Kopetz, S. et al. Synergistic activity of the SRC family kinase inhibitor dasatinib and oxaliplatin in colon carcinoma cells is mediated by oxidative stress. *Cancer Res* **69**, 3842-9 (2009).

104. Kim, E.M., Mueller, K., Gartner, E. & Boerner, J. Dasatinib is synergistic with cetuximab and cisplatin in triple-negative breast cancer cells. *J Surg Res* **185**, 231-9 (2013).

105. Qi, H. & Ohh, M. The von Hippel-Lindau tumor suppressor protein sensitizes renal cell carcinoma cells to tumor necrosis factor-induced cytotoxicity by suppressing the nuclear factor-kappaB-dependent antiapoptotic pathway. *Cancer Res* **63**, 7076-80 (2003).

106. Roberts, A.M. et al. Suppression of hypoxia-inducible factor 2alpha restores p53 activity via Hdm2 and reverses chemoresistance of renal carcinoma cells. *Cancer Res* **69**, 9056-64 (2009).

107. Suwaki, N. et al. A HIF-regulated VHL-PTP1B-Src signaling axis identifies a therapeutic target in renal cell carcinoma. *Sci Transl Med* **3**, 85ra47 (2011).

108. Lin, C.H. et al. c-Src mediates thrombin-induced NF-kappaB activation and IL-8/CXCL8 expression in lung epithelial cells. *J Immunol* **177**, 3427-38 (2006).

109. Eum, S.Y., Rha, G.B., Hennig, B. & Toborek, M. c-Src is the primary signaling mediator of polychlorinated biphenyl-induced interleukin-8 expression in a human microvascular endothelial cell line. *Toxicol Sci* **92**, 311-20 (2006).

110. Huang, Y.H. et al. Src contributes to IL6-induced vascular endothelial growth factor-C expression in lymphatic endothelial cells. *Angiogenesis* (2013).

111. Cheranov, S.Y. et al. An essential role for SRC-activated STAT-3 in 14,15-EET-induced VEGF expression and angiogenesis. *Blood* **111**, 5581-91 (2008).

112. Chen, C.L. et al. Signal transducer and activator of transcription 3 activation is associated with bladder cancer cell growth and survival. *Mol Cancer* **7**, 78 (2008).

113. Horiguchi, A. et al. Activation of signal transducer and activator of transcription 3 in renal cell carcinoma: a study of incidence and its association with pathological features and clinical outcome. *J Urol* **168**, 762-5 (2002).

114. Ji, T. et al. Abrogation of constitutive Stat3 activity circumvents cisplatin resistant ovarian cancer. *Cancer Lett* **341**, 231-9 (2013).

115. Venkatasubbarao, K. et al. Inhibiting signal transducer and activator of transcription-3 increases response to gemcitabine and delays progression of pancreatic cancer. *Mol Cancer* **12**, 104 (2013).

116. Lopez-Lago, M.A. et al. Genomic deregulation during metastasis of renal cell carcinoma implements a myofibroblast-like program of gene expression. *Cancer Res* **70**, 9682-92 (2010).

117. Lin J, S.X., Feng B. in AACR International Symposium On Molecular Targets and Cancer Therapeutics (2010).

118. Manning, E.A. et al. A vascular endothelial growth factor receptor-2 inhibitor enhances antitumor immunity through an immune-based mechanism. *Clin Cancer Res* **13**, 3951-9 (2007).

119. Gu, Y. et al. Sunitinib impairs the proliferation and function of human peripheral T cell and prevents T-cell-mediated immune response in mice. *Clin Immunol* **135**, 55-62 (2010).

120. Florcken, A. et al. Sorafenib, but not sunitinib, induces regulatory T cells in the peripheral blood of patients with metastatic renal cell carcinoma. *Anticancer Drugs* **23**, 298-302 (2012).

121. Terme, M., Tartour, E. & Taieb, J. VEGFA/VEGFR2-targeted therapies prevent the VEGFA-induced proliferation of regulatory T cells in cancer. *Oncoimmunology* **2**, e25156 (2013).

122. Therasse, P. et al. New guidelines to evaluate the response to treatment in solid tumors. European Organization for Research and Treatment of

Cancer, National Cancer Institute of the United States, National Cancer Institute of Canada. *J Natl Cancer Inst* **92**, 205-16 (2000).

123. Sweeney, S.M. et al. Angiogenesis in collagen I requires alpha2beta1 ligation of a GFP*GER sequence and possibly p38 MAPK activation and focal adhesion disassembly. *J Biol Chem* **278**, 30516-24 (2003).

124. Feng, X., Tonnesen, M.G., Mousa, S.A. & Clark, R.A. Fibrin and collagen differentially but synergistically regulate sprout angiogenesis of human dermal microvascular endothelial cells in 3-dimensional matrix. *Int J Cell Biol* **2013**, 231279 (2013).

125. Twardowski, T., Fertala, A., Orgel, J.P. & San Antonio, J.D. Type I collagen and collagen mimetics as angiogenesis promoting superpolymers. *Curr Pharm Des* **13**, 3608-21 (2007).

126. Nerenberg, P.S., Salsas-Escat, R. & Stultz, C.M. Collagen--a necessary accomplice in the metastatic process. *Cancer Genomics Proteomics* **4**, 319-28 (2007).

127. Hall, C.L. et al. Type I collagen receptor (alpha2beta1) signaling promotes prostate cancer invasion through RhoC GTPase. *Neoplasia* **10**, 797-803 (2008).

128. Motzer, R.J. et al. Overall survival and updated results for sunitinib compared with interferon alfa in patients with metastatic renal cell carcinoma. *J Clin Oncol* **27**, 3584-90 (2009).

129. Sternberg, C.N. et al. Pazopanib in locally advanced or metastatic renal cell carcinoma: results of a randomized phase III trial. *J Clin Oncol* **28**, 1061-8 (2010).

130. Sonpavde, G. & Choueiri, T.K. Biomarkers: the next therapeutic hurdle in metastatic renal cell carcinoma. *Br J Cancer* **107**, 1009-16 (2012).

131. Motzer, R.J. et al. Efficacy of everolimus in advanced renal cell carcinoma: a double-blind, randomised, placebo-controlled phase III trial. *Lancet* **372**, 449-56 (2008).

132. Bhatt, R.S. et al. Renal cancer resistance to antiangiogenic therapy is delayed by restoration of angiostatic signaling. *Mol Cancer Ther* **9**, 2793-802 (2010).

133. Motzer, R.J. in 38th ESMO (Amsterdam, 2013).

134. Brahmer, J.R. et al. Safety and activity of anti-PD-L1 antibody in patients with advanced cancer. *N Engl J Med* **366**, 2455-65 (2012).

135. Shintani, Y., Maeda, M., Chaika, N., Johnson, K.R. & Wheelock, M.J. Collagen I promotes epithelial-to-mesenchymal transition in lung cancer cells via transforming growth factor-beta signaling. *Am J Respir Cell Mol Biol* **38**, 95-104 (2008).

136. Iwai, L.K. et al. Phosphoproteomics of collagen receptor networks reveals SHP-2 phosphorylation downstream of wild-type DDR2 and its lung cancer mutants. *Biochem J* **454**, 501-13 (2013).

137. Basile, D.P. Is angiotensin II's role in fibrosis as easy as PAI(-1)? *Kidney Int* **58**, 460-1 (2000).

138. Sweitzer, N.K. Cardiology patient page. What is an angiotensin converting enzyme inhibitor? *Circulation* **108**, e16-8 (2003).

139. Keizman, D. et al. Angiotensin system inhibitors and outcome of sunitinib treatment in patients with metastatic renal cell carcinoma: a retrospective examination. *Eur J Cancer* **47**, 1955-61 (2011).

Appendix:

Example of Patient Information and Patient Consent Form for tissue analysed in this thesis.

~ To be put on headed paper ~

PATIENT INFORMATION SHEET

A PHASE II STUDY INVESTIGATING UPFRONT PAZOPANIB IN METASTATIC CLEAR CELL RENAL CANCER (PANTHER)

VERSION 5.0 DATED 21ST DECEMBER 2011

1. Invitation paragraph

You are being invited to take part in a research study. Before you decide whether or not you want to take part, it is important for you to understand why the research is being done and what will be involved.

Please take time to read the following information carefully. Talk to others about the study if you wish. Ask your doctor if there is anything that is not clear or if you would like more information. Take time to decide whether or not you wish to take part.

2. What is the standard treatment for metastatic kidney cancer?

When kidney cancer spreads beyond the kidney it is known as metastatic kidney cancer, which is difficult to treat.

A new type of oral drug known as pazopanib, which stops the growth of cancer cells, has updated previous treatments.

At the moment, most patients with metastatic kidney cancer have surgery to remove the kidney before starting oral drug treatment. This surgery is called a nephrectomy. It is unknown whether this surgery is of any benefit in the long term, as it delays starting the drug therapy to treat cancer which has spread to other sites of the body.

So far previous research studies have looked at giving a period of another drug, sunitinib, followed by surgery. These studies are designed to hopefully make the tumour smaller, therefore making surgery easier. Published results with this approach are promising. So far there are no research studies in this area with pazopanib.

3. What is the purpose of this study?

The purpose of this study is to look at the effect of giving pazopanib for 14 weeks before surgery in metastatic kidney cancer. The drug treatment is designed to target all the cancer cells, in the kidney and other places, unlike surgery which will only treat the cancer in the kidney.

The drug used in this study is pazopanib. It is a tablet that is taken by mouth. The tablet works by stopping cancer cells from growing. It also works in kidney cancer by reducing the blood supply to cancer cells.

It is planned that approximately 95 evaluable patients across twelve UK centres, will be recruited onto this study over a 20 month period.

4. Why have I been invited to take part?

You have been invited to take part in this study because your scan suggests that you have kidney cancer which has spread to organs beyond the kidney. Your doctor feels that you may benefit from receiving pazopanib therapy. Your doctor may have discussed the possibility of surgery with you. The key to this study is to determine if 14 weeks of pazopanib prior to surgery is of benefit.

5. Do I have to take part?

No. It is up to you to decide whether or not you wish to take part. If you choose to take part you will be asked to sign the consent form. You will receive a copy of this information sheet and your signed consent form to take away.

If you do decide to take part you are free to withdraw from the study at any time and without giving a reason. A decision to withdraw or not to take part, will not affect the standard of care you receive. However, you will not be able to restart pazopanib as part of the study. You will be able to go on and receive a different agent if pazopanib fails. Your treatment will be decided by your treating doctor.

Section A: Main Compulsory Components of Study

1. What will happen to me if I take part?

Once you have decided to take part in the study and signed a consent form, your doctor will make sure that you are suitable for entry onto the study. The following tests may need to be carried out before you can start study treatment:

- full medical history (including information about other medications and illnesses)
- clinical examination
- blood tests
- pregnancy test
- Computerised Tomography (CT scan) of the chest abdomen and pelvis within 3 weeks of starting the study if this has not already taken place.

In order to confirm your diagnosis of kidney cancer, a tissue sample of the cancer in your kidney will need to be taken; this is known as a biopsy. This will take place whether or not you go into the study. For the biopsy you will need to have a local anaesthetic before a needle is passed into the kidney to remove some tissue. This tissue will be looked at further to see if there are cancer cells.

Once your study doctor is satisfied that you meet all the requirements you will then be asked to sign a consent form before you begin the study. The study drug will be prescribed for you to take orally, two tablets once a day. You will be asked to continue taking the drug without any breaks until your surgery.

You will be seen in clinic after the first 4 weeks of starting the drug to make sure you are not experiencing any side effects.

Day-to-day effects which **may** occur when taking pazopanib include a loss of appetite and nausea, changes in hair and skin colour, hair loss, rash, tiredness, bleeding (in the lungs, urine, nose and intestines), numbness in the hands and feet and an increase in blood pressure. The drug can also reduce your blood sugar levels, white blood cells, lipids and platelets in the blood and cause a change in the function of the liver. Other effects include a decrease in thyroid activity, weight loss, headache, change in taste, stroke, heart abnormalities, chest pain, abnormal amount of protein in the urine and loose stools (diarrhoea).

Appointments will then take place at 8 weeks and 12 weeks. During these visits you will have blood tests (approximately 2 teaspoons of blood will be taken), assessment of any side effects and a full physical examination if necessary. You will be allocated a research nurse who you can contact by telephone if any problems occur in between these visits.

A CT scan will take place at 6 weeks to make sure the cancer is not growing. This involves lying on a table for 5 minutes inside a machine that looks a bit like a hollow cylinder. Some dye (called contrast) will be injected into your vein and pictures will be taken of the tumour inside of your body.

You will receive between a minimum of 12 to a maximum of 16 weeks of pazopanib treatment. After this, you will have another CT scan to see whether the cancer has shrunk in size. At this point your doctors will discuss surgery with you (please see Figure 1).
Before surgery you may be required to see the surgical team and have an ultrasound scan of the heart and an ECG (electrocardiogram) to make sure you are well enough to have the surgery. An ultrasound scan of the heart checks to see if there are any cardiac problems. An

ultrasound is a harmless procedure in which your doctor will place some lubricating gel on the surface of your chest. A hand-held device which is similar to a blunt pen, will then be run over this area and pictures will be taken. An ECG is used to look at the electrical activity of the heart which can help rule out any abnormal heart rhythms. When having an ECG you will have 10 small sticky patches placed over your chest, arms and legs. These will be linked to the machine that will record the electrical activity of the heart.

You will be asked to stop taking pazopanib for at least 48 hours before the surgery and will restart taking pazopanib at least 2 weeks after surgery. A CT scan will be repeated 6 weeks after restarting pazopanib to make sure the treatment is still working. The pazopanib treatment will continue as long as the cancer appears to be responding, unless you develop severe side effects or if you wish to stop.

You may also be asked to have an MRI scan (**m**agnetic **r**esonance **i**maging) to help any biopsy procedure/ surgery. Your doctor will discuss further details about this type of scan should you require one.

If you are not able to have surgery (due to you not being well enough), you can continue on pazopanib therapy for as long as your doctor feels that it is of benefit to you. However, you may be asked to have a repeat biopsy at the time that the surgery would have taken place. The pazopanib treatment will continue as mentioned above, until there is evidence that it is no longer stopping the disease.

During the study you will be reviewed for side effects. If these occur, and are serious your doctors may advise a break in treatment until the side effects stop. Your doctor may also arrange to reduce the amount of pazopanib taken or even stop the treatment completely.

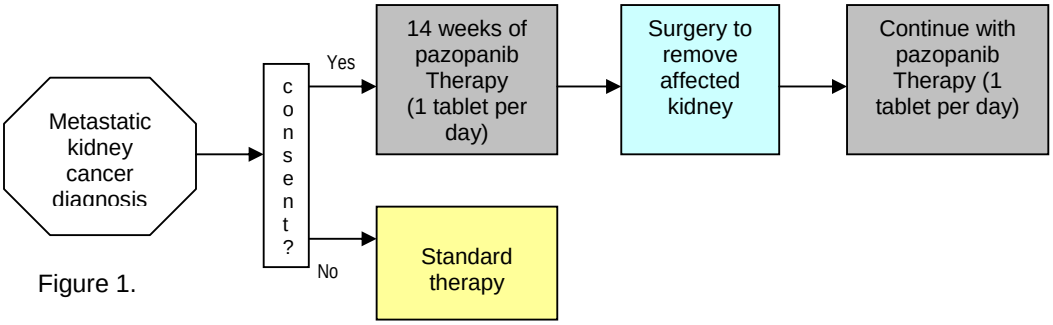

Figure 1.

2. *What will happen to any samples I give?*

A sample will be taken from your kidney, which is less than 1 gram, (approximately the weight of a paperclip) before starting treatment and will be used to confirm the type of cancer cells you have. This biopsy is part of standard treatment and you will still undergo this even if you do not take part in this research study. A sample of the affected kidney will also be removed during surgery (or for those patients not having surgery, during the repeat biopsy). We will compare the two tissue samples. This will allow us to find some areas in the tissue that may be reacting to treatment. Therefore it may be possible to use this information to predict future patients who will have a greater reaction to treatment. This will also allow us to gather new information to help patients in the future.
With your permission, any tissue remaining as a result of this project will be stored safely in a licensed tissue bank to be used for future research purposes. This could also include any

blood samples that may be taken if you go on to the main study. The tissue may be stored and used by Barts and the London NHS School of Medicine and Dentistry, and for approved research within a hospital, university, non-profit institution or a company laboratory within/outside the EU. Samples will be lawfully disposed of, when necessary. If you are willing for your tissue to be stored for future research you will be asked to sign a separate consent form.

3. What are the alternative treatments available?

Your doctor will discuss with you the alternative treatments that are available to help to manage your condition. These alternative treatments include sunitinib or immune therapy, which is widely available within the UK. Your treatment may also include surgery.

It is your decision about which treatment you wish to have and some people with this condition choose to have no further drug treatment. If you choose not to participate, your treating doctor will tell you more about all your options.

4. *What are the side effects of the study drug, pazopanib?*

Side effects that patients in other studies have experienced when taking pazopanib and the frequency of their occurrence include

Very common: (more than or equal to 1 in 10)

Common: (more than or equal to 1 in 100 and less than 1 in 10)

Uncommon (more than or equal to 1 in 1000 and less than 1 in 100)

Adverse Reaction	**Frequency**
Fatigue, weakness	Very common
Headache	Very common
Weight loss	Very common
Hair discolouration	Very common
Increased blood pressure	Very common
Diarrhoea, Nausea, Vomiting, abdominal pain	Very common
Decreased platelets, and white blood cells	Common
Reduced thyroid function	Common
Change in taste	Common
Heart abnormalities (QT prolongation, transient ischaemic attack, myocardial ischaemia)	Common
Nose bleeds, blood in urine	Common
Indigestion	Common
Liver function changes	Common
Rash, hair loss, Skin discolouration	Common
Abnormal amount of protein in the urine	Common
Chest Pain	Common
Decreased blood sugar levels	Uncommon
Stomach disorders	Uncommon
Bleeding in the lungs, intestines and brain	Uncommon
Stroke	Uncommon

Not all side effects of pazopanib are known or predicted. Many side effects go away when the study drug is stopped, but in some cases, it is possible that the side effects could be serious, long lasting, permanent (stroke, change in thyroid function skin and hair changes) or fatal (stroke, liver dysfunction and gastrointestinal perforation). You should discuss these with your doctor. In addition, there may be side effects that we cannot predict.

If during the course of this trial any new findings about pazopanib become available which may influence your decision to continue participating in this study, your study doctor will inform you.

If you do experience any unpleasant side effects or discomfort during the study you should inform your study doctor either at the next visit or sooner if you wish, by using the telephone contact number in this patient information sheet.

Pazopanib can potentially interact or interfere with a number of other drugs. For these reasons you should discuss all the drugs you take regularly or intermittently with your cancer doctor. The drugs which could be affected include specific antidepressants, erectile dysfunction drugs, specific lipid lowering drugs anticoagulants, oral diabetic drugs, specific sleeping pills, specific antihypertensives, steroids, specific antibiotics and oral contraceptives. If you are on one or more of these drugs, we may need to monitor you or change your drug before starting therapy. Your current medication should be discussed with your treating doctor.

5. What are the possible disadvantages and risks of taking part?

One of the risks of taking pazopanib is that it may not work for you.

Also we do not yet know if surgery after 14 weeks of pazopanib is the ideal time to perform the surgery. Additionally it is not yet known if this surgery is more difficult or easier after taking pazopanib.

WOMEN

There could be risks to an unborn child in this study, therefore, If you are pregnant you cannot enter the study. If you become pregnant during the study, these risks could affect you or your unborn child. You must agree to use adequate birth control during the study, which you can discuss with your study doctor. You must continue using birth control for at least 28 days after you stop taking pazopanib.

Before the study, a pregnancy test will be done for all women who are able to get pregnant. The test might not be enough to detect an early pregnancy so tests may be repeated during the study. If you think you may be pregnant, you must tell your study doctor immediately. Pregnancy will be a reason to stop study treatment. If you become pregnant, information on the outcome of your pregnancy will be requested.

MEN

If your spouse or partner thinks they are pregnant during the study, tell your study doctor immediately. The effect of pazopanib on sperm is not known, so you must agree to use adequate birth control during the study, which you can discuss with your study doctor. You must continue using birth control for at least 28 days after you discontinue the study.

6. ***What are the possible benefits of taking part?***

The medicine and surgery you receive may help you and your disease. You may not personally benefit from being in this study. However the information we gain from this study might help us to treat future patients who have metastatic kidney cancer.

7. What will happen if I don't want to carry on with the study?

You can choose to withdraw from the study at any time. Any information that has already been collected will be processed as part of the study, but no further information will be collected. A decision to withdraw at any time, or a decision not to take part, will not affect the care you receive. If you do decide to stop your treatment you will not be able to go back onto the study.

8. ***What if relevant new information becomes available?***

Sometimes during the course of a research study, new information may become available about the drug that is being studied. If this happens, your study doctor will tell you about it and discuss with you whether you want to continue in the study. If you decide to withdraw, your study doctor will make arrangements for your care to continue. If you decide to continue in the study you will be asked to sign an updated consent form to reflect any changes as a result of the new information.

Also, on receiving new information your research doctor might consider it to be in your best interests to withdraw you from the study. He/she will explain the reasons and arrange for your care to continue.

9. ***What happens when the research study stops?***

If the research study stops, you will be informed and will be offered alternative treatment.

10. What if there is a problem with the study?

We would not expect you to suffer any harm or injury because of your participation in this study. If you are harmed by taking part in this study, there is no special compensation arrangement. If you are harmed due to someone's negligence, then you may have grounds for legal action but you may have to pay your legal costs. Regardless of this, if you wish to complain or have any concerns about any aspect of the way you have been approached or treated during the course of this study, the normal National Health Service complaints mechanisms should be available to you. Participants with Personal Medical Insurance are advised to contact their companies and inform them that they intend to take part in the trial.

11. How do I make a complaint?

Please contact Patient Advisory Liaison Service (PALS) if you have any concerns regarding the care you have received, or as an initial point of contact if you have a complaint. Please

telephone ~*insert number*~, minicom ~*insert number*~, or email ~insert email address~ you can also visit PALS by asking at any hospital reception.

12. Will my taking part in the study be kept confidential?

Yes. All information which is collected about you during the course of the research will be kept strictly confidential. If you consent to take part in the research the people conducting the study will abide by the Data Protection Act 1988, and the rights you have under this Act.

If you wish to take part in this study we will ask your permission to contact your GP to let them know of your potential participation in the study. This is done so that all the doctors involved in your care are aware of the medicines you are taking. They can also tell us if there are any medical reasons why you should not take part in the study. Your hospital notes will also state that you are in the study and a label will be clearly visible on front cover of notes.

If you join the study, some parts of your medical records and the data collected for the study will be looked at by authorised personnel from your treating centre and authorised personnel from Bart's & The London NHS Trust, GlaxoSmithKline and Queen Mary University of London who are the sponsor of this study. It may also be looked at by representatives of regulatory authorities and other authorised personnel from your trust, to check that the study is being carried out correctly. All will have a duty of confidentiality to you as a research participant and nothing that could reveal your identity will be disclosed outside the research site. All data will be stored in a locked and dedicated room at the Centre for Experimental Cancer Medicine, which will only be accessible by authorised personnel.

13. What will happen to the results of the research study?

The researchers hope to publish the results of this study in a medical journal. This usually takes place months after the study has been completed. You or your relatives will be offered a summary of the study results. It will not be possible to identify you in the report/publication.

14. Who is organising and funding the research?

This is an investigator-initiated study. Dr Thomas Powles of St. Bartholomew's Hospital is the Chief Investigator. Queen Mary University of London is sponsoring the study. The doctors and other members of the clinical research teams are not being paid for participating in this study. GlaxoSmithKline is providing financial support for this study and will be providing the pazopanib for use in the study free of charge. Patients who wish to participate in the study will have their extra travel costs, (which are any additional travel costs to standard healthcare) reimbursed.

15. *Who has reviewed the study?*

This study has been through a peer review process and was given approval by Bart's & The London NHS Trust Cancer Clinical Academic Unit Review Committee. A peer review involves the examination of an author's work by other experts in the same field. These referees each return an evaluation of the work which may include suggestions of improvements if necessary.

Your local NHS trust has been given approval for the study to take place at your hospital. The study has also been given a favourable ethical opinion for conduct by the South East Research Ethics Committee. This Committee assesses the study and decides if the study will be in the best interests for the patients involved.

16. Contact Details

You can contact your local Principal Investigator or Research Nurse to discuss your concerns and/or to get help.

Name:
Address: *~insert details~*

Tel:
Fax:

Out of hours: Please contact *~insert details~* **and ask to speak to** *~insert details~ .*

If you wish to take part in the main section (A) of the Study, then Consent Form A will have o be signed.

~ to be printed on headed paper ~

CENTRE NUMBER:
STUDY NUMBER: **RC-2009-02**
PATIENT INITIALS:
DATE OF BIRTH:

PATIENT CONSENT FORM A: Main Compulsory Components of Study

STUDY TITLE: A PHASE II STUDY INVESTIGATING UPFRONT PAZOPANIB IN METASTATIC CLEAR CELL RENAL CANCER (PANTHER).

VERSION 1 [DATED 16TH NOVEMBER 2009]

Name of Researcher: ……

Please initial box

1. I confirm that I have read and understand the information sheet dated: *~insert correct version number~* for the above study. I have had the opportunity to consider the information, ask questions and have had these answered satisfactorily. ☐
2. I understand that my participation is voluntary and that I am free to withdraw at any time, without giving any reason, without my medical care or legal rights being affected. ☐
3. I understand that relevant sections of any of my medical notes and data collected during the study, may be looked at by responsible individuals from regulatory authorities or from Barts and the London/ Queen Mary University of London, where it is relevant to my taking part in this research. I give permission for these individuals to have access to my records. ☐
4. I agree to my GP being informed of my participation in the study. ☐
5. I understand that samples of my tissue will be taken from me during the study. I agree for my tissue to be used in this research project. ☐
6. I agree to take part in section A, the main components of the study. This potentially includes freezing and storage of tissue for future research ☐

_____	_____	_____
Name of Patient	Date	Signature
_____	_____	_____
Name of Person taking consent (if different from researcher)	Date	Signature
_____	_____	_____
Researcher	Date	Signature

1 for patient; 1 for researcher; 1 original to be kept with hospital notes

ORCHID
FIGHTING MALE CANCER

Barts and The London
Queen Mary's School of Medicine and Dentistry

CONSENT TO COLLECT GENITO-URINARY TISSUE AND BLOOD SAMPLES FOR RESEARCH

Patient's full name	Investigator: Dr D Berney Dr T Powles, Dr J Shamash
Date of Birth	Ethic Committee Ref: REC 09/H0704/4
Hospital name and number	Description of tissue: :
	Blood collection: Yes/No

Patient initials

I understand that tissue will be taken during my treatment/investigation and will not be used for diagnostic purposes. I agree that this tissue will be stored (-80C freezer and Liquid Nitrogen) in the Orchid Tissue Bank for current and future research. ☐

I accept that I have given my consent voluntarily to the storage of this additional tissue and that I am free to withdraw my consent at any time and the tissue will then be destroyed. ☐

I agree that the tissue may be used for future genetic research. It may not be used for research in reproductive cloning. The sample will not be tested for inherited diseases without my consent. ☐

I agree that my health records may be used by authorised members of staff who are not directly involved in my clinical care and my hospital number is written above. ☐

If blood collected:

I understand, the blood collected will not be taken for diagnostic purposes ☐

I am free to withdraw my consent at any time and the blood will then be discarded. ☐

I agree that the blood may be used for future genetic research. Blood cells will not be used for reproductive cloning and inherited disease research. ☐

_____	_____	_____
Name of Patient	Date	Signature
_____	_____	_____
Name of person taking consent	Date	Signature

1 copy for Patient, 1 copy for Investigator, 1 copy in the hospital notes
Version 2, 2nd March 2009

GENITO-URINARY TISSUE AND BLOOD SAMPLES COLLECTION
DETAILS OF RESEARCH:

The tissue samples taken routinely during your procedure are sent to the hospital laboratory. This is routine practice, essential for diagnosis and for planning further treatment. By giving your consent at the same time, excess tissue not required for diagnosis will be collected by the Orchid Tissue Bank and stored in -80C freezer and/or Liquid Nitrogen, and used for current and future research.

We are mainly collecting tissue from the bladder, prostate, testis, kidney or penis, or the peripheral blood. The most important areas of research will be to improve the methods of diagnosis and identification of the causes of cancer. This primarily involves the study of tumour markers in blood and tissue to detect and analyse proteins that are differently expressed in tumours than in normal tissue. We are also studying genes (specific sequences of DNA) and chromosomal damage that develop during tumour progression.

All staff undertaking future studies will abide by the Data Protection Act 1998, with any medical information relating to you being kept confidential. The tissue may be given to external organisations for approved research but tissue will not be sold, although costs will be recovered without any financial benefit to either you or the researcher. All tissue will be disposed of lawfully when it is no longer required.
The information obtained from our research may be published in scientific journals and discussed at scientific and medical conferences. However, all the documents relating to you will be completely anonymous.

If a blood sample is being requested, this will purely be for specific research projects and not for diagnostic purposes. The blood will not be sold and it will be disposed when it is no longer required.

IMPORTANT INFORMATION

- Your treatment will not be affected if you decline to participate.
- The work will have no direct implications for your personal health, due to the type of research involved.
- Samples may contain personal information but all such information will be anonymised when the results are published or when samples are given to external organisations.
- You can withdraw your consent at any time. Please send us a letter containing your contact details. In return, you will be informed, by courier that your tissue has been destroyed and removed from the tissue bank.

For more information:
Dr D Berney
ORCHID TISSUE BANK
Molecular Oncology & Imaging, Institute of Cancer,
Barts and The London Queen Mary's School of Medicine and Dentistry
John Vane Science Centre, Charterhouse Square
London EC1M 6BQ

Thank you for your help.

1 copy for Patient, 1 copy for Investigator, 1 copy in the hospital notes
Version 2, 2nd March 2009